

ジオスペース探査計画：ERGプロジェクト

三好由純 [1]; 篠原 育 [2]; 高島 健 [3]; 浅村 和史 [4]; 松本 晴久 [5]; 東尾 奈々 [6]; 三谷 烈史 [4]; 横田 勝一郎 [7]; 笠原 慧 [8]; 風間 洋一 [9]; Wang Shiang-Yu [10]; 平原 聖文 [11]; 笠原 禎也 [12]; 笠羽 康正 [13]; 八木谷 聡 [12]; 松岡 彩子 [14]; 小嶋 浩嗣 [15]; 加藤 雄人 [16]; 塩川 和夫 [17]; 関 華奈子 [18]; 藤本 正樹 [3]; 小野 高幸 [16]

[1] 名大 ISEE; [2] 宇宙研/宇宙機構; [3] 宇宙研; [4] 宇宙研; [5] 宇宙機構; [6] JAXA; [7] 宇宙研; [8] ISAS/JAXA; [9] 中央研究院天文・宇宙物理学研究所; [10] 中央研究院天文及天文物理研究所; [11] 名大・宇地研; [12] 金沢大; [13] 東北大・理; [14] JAXA 宇宙研; [15] 京大・生存圏; [16] 東北大・理・地球物理; [17] 名大宇地研; [18] 東大理・地球惑星科学専攻

Geospace Exploration Project:ERG

Yoshizumi Miyoshi[1]; Iku Shinohara[2]; Takeshi Takashima[3]; Kazushi Asamura[4]; Haruhisa Matsumoto[5]; Nana Higashio[6]; Takefumi Mitani[4]; Shoichiro Yokota[7]; Satoshi Kasahara[8]; Yoichi Kazama[9]; Shiang-Yu Wang[10]; Masafumi Hirahara[11]; Yoshiya Kasahara[12]; Yasumasa Kasaba[13]; Satoshi Yagitani[12]; Ayako Matsuoka[14]; Hirotsugu Kojima[15]; Yuto Katoh[16]; Kazuo Shiokawa[17]; Kanako Seki[18]; Masaki Fujimoto[3]; Takayuki Ono[16]
[1] ISEE, Nagoya Univ.; [2] ISAS/JAXA; [3] ISAS, JAXA; [4] ISAS/JAXA; [5] JAXA; [6] JAXA; [7] ISAS; [8] ISAS/JAXA; [9] Institute of Astronomy and Astrophysics, Academia Sinica, Taiwan; [10] Institute of Astronomy and Astrophysics, Academia Sinica, Taiwan; [11] ISEE, Nagoya Univ.; [12] Kanazawa Univ.; [13] Tohoku Univ.; [14] ISAS/JAXA; [15] RISH, Kyoto Univ.; [16] Dept. Geophys., Grad. Sch. Sci., Tohoku Univ.; [17] ISEE, Nagoya Univ.; [18] Dept. Earth & Planetary Sci., Science, Univ. Tokyo

The ERG (Exploration of energization and Radiation in Geospace) is a geospace exploration project in Japan. The project focuses on dynamics of Geospace and accelerations of radiation belt electrons in the context of the cross-energy coupling. The project consists of the satellite observation team, the ground-based network observation team, and integrated-data analysis/simulation team. The ERG satellite will be launched in this fiscal year. The satellite apogee and perigee altitudes are 5.2 Re and 300 km, respectively, and the orbital period is about 8 hour. Comprehensive instruments for plasma/particles, and field/waves are installed in the ERG satellite. Two ion instruments (LEP-i/MEP-i) measure ions from 10 eV/q to 180 keV/q with mass discrimination. Four electron instruments (LEP-e/MEP-e/HEP/XEP) measure electron from 12 eV to 20 MeV. LEP-i/MEP-i and LEP-e/MEP-e/HEP can measure three-dimensional distribution functions. The plasma wave instrument (PWE) measures electric fields as well as plasma waves in the frequency range from DC to 10 MHz (electric field) and 100 kHz (magnetic field). The fluxgate magnetometer (MGF) measures DC and low frequency magnetic field. Newly developed wave-particle interaction analyzer (S-WPIA) is installed in the satellite, which measure directly the energy transfer process between electrons and plasma waves. S-WPIA will provide definitive evidence on wave-particle interactions in space plasma, which is essential to understand elementary process of electron accelerations.

Several ground-network teams join; magnetometer networks, radar networks including SuperDARN and EISCAT, VLF antenna network, optical imager networks, riometer network, standard radio wave observation network, which provide a global view of geospace and complementary observation with the ERG satellite observation. Japanese STP community has prepared the ground-based observation facilities and networks to collaborate with the ERG satellite over the years. The new big project for the ground-network observations PWING and PsA have just started in this year. Moreover, the modeling/simulations play an important role for the quantitative understanding. Besides research teams in the project, the science center has been operated. All science data from the project have been archived in the ERG-Science Center. The science center has also developed integrated data analysis software that is a plug-in for SPEDAS in cooperation with the THEMIS mission. These data and softwares are available via the ERG-Science Webpage (<http://ergsc.isee.nagoya-u.ac.jp>).

In this presentation, we will talk about an overview of the ERG project and discuss a plan for the initial observation after the ERG launch. The international collaborations with Van Allen Probes, MMS, THEMIS, Cluster, etc and ground network observations under the flame work of Heliosphere/Geospace (H/GSO) system observatory are also discussed.

ジオスペース探査衛星 ERG 搭載磁場観測器 (MGF) の最終性能と観測計画

松岡 彩子 [1]; 寺本 万里子 [2]; 野村 麗子 [3]; 三好 由純 [4]; 能勢 正仁 [5]; 藤本 晶子 [6]; 田中 良昌 [7]; 篠原 学 [8]; 長妻 努 [9]; 塩川 和夫 [10]

[1] JAXA 宇宙研; [2] JAXA, 宇宙研; [3] ISAS; [4] 名大 ISEE; [5] 京大・理 地磁気センター; [6] 九大・ICSWSE; [7] 極地研; [8] 鹿児島高専; [9] NICT; [10] 名大宇地研

The design, performance and observation plan of magnetometer (MGF) for the ERG mission

Ayako Matsuoka[1]; Mariko Teramoto[2]; Reiko Nomura[3]; Yoshizumi Miyoshi[4]; Masahito Nose[5]; Akiko Fujimoto[6]; Yoshimasa Tanaka[7]; Manabu Shinohara[8]; Tsutomu Nagatsuma[9]; Kazuo Shiokawa[10]

[1] ISAS/JAXA; [2] JAXA, ISAS; [3] ISAS; [4] ISEE, Nagoya Univ.; [5] DACGSM, Kyoto Univ.; [6] ICSWSE, Kyushu Univ.; [7] NIPR; [8] Kagoshima National College of Technology; [9] NICT; [10] ISEE, Nagoya Univ.

The acceleration process of the charged particles in the inner magnetosphere is considered to be closely related to the deformation and perturbation of the magnetic field. Accurate measurement of the magnetic field is required for the understanding of the acceleration mechanism of the charged particles, which is one of the major scientific objectives of the ERG mission. We designed a fluxgate magnetometer which is optimized to investigate following topics;

(1) accurate measurement of the background magnetic field - the deformation of the magnetic field and its relationship with the particle acceleration.

(2) MHD waves - measurement of the ULF electromagnetic waves of frequencies about 1mHz (Pc4-5), and investigation of the radiation-belt electrons radially diffused by the resonance with the ULF waves.

(3) EMIC waves - measurement of the electromagnetic ion-cyclotron waves of frequencies about 1Hz, and investigation of the ring-current ions and radiation-belt electrons dissipated by the interaction with the EMIC waves.

A fluxgate magnetometer (MGF) was built for the ERG satellite to measure DC and low-frequency magnetic field. The design is based on MGF-I, one of the magnetometers for MMO, Mercury orbiter, which would also suffer high radiation on the Mercury orbit.

The requirements to the magnetic field measurements by ERG was defined as (1) accuracy of the absolute field intensity is within 5 nT (2) angular accuracy of the field direction is within 1 degree (3) measurement frequency range is from DC to 60Hz or wider.

We tested the characteristics of MGF and confirmed that its performance satisfies these requirements.

ジオスペース探査衛星 ERG は、放射線帯の相対論的電子加速メカニズムと、ジオスペースストームの解明を目的とし、2016 年度の打ち上げを目指して準備が進められている。

ERG に搭載される磁場観測器 (MGF) は、(1) 粒子の異方性、プラズマ波動の特性など、あらゆるプラズマ観測の基準となる背景磁場観測 (2) 放射線帯粒子の磁力線を横切る輸送とそれに伴う加速を担う、磁気流体波動観測 (3) 放射線帯の相対論的電子や、環電流のイオンのピッチ角散乱による消失を引き起こす EMIC 波動観測 等において主要な機器である。ERG 衛星は厳しい放射線環境が予想されるため、同じく厳しい放射線環境用に開発された、水星探査機 BepiColombo MMO 搭載磁場観測器 MGF-I を基本にして設計した、フラックスゲート方式磁力計である。

ERG ミッション目的達成のために、8000nT と 60000nT の 2 つのダイナミックレンジを持ち、最大 256Hz でベクトル磁場を測定する。また、5nT 精度の絶対磁場、1 度精度の磁場方向の測定を可能とするように、MGF の設計、試験、校正および、衛星と伸展物のアライメント計測、衛星システムの EMC 対策を行った。

MGF フライトモデルの最終性能の試験と評価を行った結果を報告し、打ち上げ後の観測計画に関する発表を行う。

アナログ・デジタル混載ワンチップ小型プラズマ波動受信器

頭師 孝拓 [1]; 小嶋 浩嗣 [1]; 笠原 禎也 [2]; 高橋 翼 [2]; 尾崎 光紀 [3]; 八木谷 聡 [2]; 徳永 祐也 [2]
[1] 京大・生存圏; [2] 金沢大; [3] 金沢大・理工・電情

Development of the one-chip mixed-signal plasma wave receiver

Takahiro Zushi[1]; Hirotsugu Kojima[1]; Yoshiya Kasahara[2]; Tsubasa Takahashi[2]; Mitsunori Ozaki[3]; Satoshi Yagitani[2]; Yuya Tokunaga[2]
[1] RISH, Kyoto Univ.; [2] Kanazawa Univ.; [3] Electrical and Computer Eng., Kanazawa Univ.

The plasma wave receiver is an essential scientific instrument for plasma observations in space. In spaceborne instrument design, reductions in the resources are critical issues. We have been studying the miniaturization of plasma wave receiver by using the analog ASIC (Application Specific Integrated Circuit) technology. We have already developed the analogue ASIC chips for the waveform and the spectrum type receivers.

Recent plasma receivers require an onboard digital signal processing. The digital signal processing is realized by using an FPGA or CPU in conventional receivers. The spectrum receivers require a digital signal processing unit to calculate the frequency spectrum, and the waveform receivers require a digital processing unit to compress huge waveform data.

We are developing a one-chip plasma observation system as a mixed-signal ASIC by integrating digital signal processing units. The mixed-signal ASIC chip includes analog circuit for both the spectrum and the waveform receivers, the analog to digital converters (ADC), and logic circuits for the fast Fourier transform and for the wave compression. The mixed-signal ASIC chip leads to the drastic miniaturization of the receiver and decreases development costs because the ASIC has the advantage of easy mass-production. We have already finished designing ADC. In the present paper, we will introduce the detailed design of the mixed-signal one-chip waveform receiver.

プラズマ波動受信器はプラズマ波動観測に不可欠な観測機器であり、これまでに様々な理学ミッションにおいてプラズマ波動受信器を利用した観測が行われてきた。しかしながら、これまでのプラズマ波動受信器においてはそのサイズが問題となっていた。そこで我々は、特定用途向け集積回路 (ASIC) を利用して、プラズマ波動受信器の中で大きな体積を占めていたアナログ回路を小型集積化することによる観測器の小型化を行ってきた。これまでに、波形捕捉型、スペクトル型両方の受信器を ASIC により小型で実現することに成功している。

近年のプラズマ波動受信器では、アナログ回路による信号処理に加えてデジタル信号処理が必要とされている。波形捕捉受信器においては観測した波形データを効率よく地上へ伝送するための波形圧縮処理に、スペクトル受信器ではスペクトル計算のための高速フーリエ変換 (FFT) にそれぞれデジタル信号処理が用いられている。これまでの受信器では、このようなデジタル信号処理は FPGA や CPU を利用して実現していた。

我々は、このようなデジタル信号処理ユニットをアナログ回路実装が実現した ASIC 内に組み込むことにより、アナログ・デジタル混載ワンチップ小型プラズマ波動受信器の実現を目指している。この受信器は大部分がアナログ・デジタル混載 ASIC チップで構成され、その中には波形捕捉受信器・スペクトル受信器用のアナログ回路、A/D コンバーター、波形圧縮用デジタル信号処理ユニット、FFT 用デジタル信号処理ユニットが含まれる。これによりプラズマ波動受信器の大幅な小型化が可能となり、また受信器全体をワンチップで実現することにより製作コストを大幅に下げることができる。現在 A/D コンバーターの設計が完了しており、現在は FPGA 上で実現されていた波形圧縮用デジタル信号処理ユニットの移植を行っている。発表においては特に波形捕捉型受信器を中心にアナログ・デジタル混載ワンチップ小型プラズマ波動受信器設計の詳細について述べる。

かぐやによる単一および両伝搬モードのオーロラキロメートル波の観測

橋本 弘藏 [1]; 後藤 由貴 [2]; 笠原 禎也 [2]; 澤田 佳大 [2]
[1] 京都大学; [2] 金沢大

Single and both propagation modes of auroral kilometric radiation (AKR) observed by KAGUYA

Kozo Hashimoto[1]; Yoshitaka Goto[2]; Yoshiya Kasahara[2]; Keita Sawada[2]
[1] Kyoto Univ.; [2] Kanazawa Univ.

In the KAGUYA (SELENE) LRS instrument [1], WFC-H [2] observes wave spectra in 1kHz-1,000kHz and various plasma waves like Auroral Kilometric Radiation (AKR), electron plasma waves, and broadband electrostatic waves have been observed. This system can observe wave polarizations by two pairs of dipole antennas. We have analyzed the AKR polarizations.

The propagation mode of AKR has become possible from the polarization measurement of WFC-H using lunar occultations [3]. This method is applied to other examples. For examples, the propagation mode can be decided since the source hemisphere can be decided clearly, both polarizations are observed while both hemispheres can be seen, and the other mode is observed after an occultation. Their propagation modes can be estimated based on their source hemispheres. The results will be compared with ray tracing studies.

References

[1] T. Ono, A. Kumamoto, Y. Kasahara, Y. Yamaguchi, A. Yamaji, T. Kobayashi, S. Oshigami, H. Nakagawa, Y. Goto, K. Hashimoto, Y. Omura, T. Imacahi, H. Matsumoto, and H. Oya, The Lunar Radar Sounder (LRS) Onboard the KAGUYA (SELENE) Spacecraft, The Kaguya Mission to the Moon (Guest Editors: A. Matsuoka, C.T. Russell), Space Science Reviews, 154, Nos. 1-4, 145-192, DOI:10.1007/s11214-010-9673-8, 2010

[2] Y. Kasahara, Y. Goto, K. Hashimoto, T. Imachi, A. Kumamoto, T. Ono, and H. Matsumoto, Plasma Wave Observation Using Waveform Capture in the Lunar Radar Sounder on board the SELENE Spacecraft, Earth, Planets and Space, 60, 341-351, 2008.

[3] K. Hashimoto, Y. Goto, Y. Kasahara, H. Matsumoto, and R. R. Anderson, Auroral Kilometric Radiation: Polarization and Spectra Observed far from the Earth, "Auroral Dynamics and Space Weather", (eds. by Y. Zhang, L. Paxton), AGU Geophysical Monograph Series, Wiley, 255-273.

月周回衛星「かぐや (SELENE)」搭載 LRS[1] の WFC-H 波動観測装置 [2] では、1-1,000kHz の波動のスペクトルを観測でき、オーロラキロメートル波 (AKR)、電子プラズマ波、広帯域静電波などが観測され、周辺プラズマ環境のモニターにもなっている。本装置は二対のダイポールアンテナを用いた偏波観測が可能であり、AKR の偏波解析を行ってきた。

AKR の偏波観測に月による掩蔽を用いて、プラズマ波動で言う磁場方向に対する偏波の同定が可能となった [3]。この手法を他の例にも広げていく。例えば、単一の伝搬モードが、掩蔽で源半球が識別できる例や、両半球可視時に両偏波が受かった例、掩蔽後に別のモードが見えた例。これらの源半球の決定しそれに基づく伝搬モードを推定する。レイトレーシングとの比較による検討も行う。

References

[1] T. Ono, A. Kumamoto, Y. Kasahara, Y. Yamaguchi, A. Yamaji, T. Kobayashi, S. Oshigami, H. Nakagawa, Y. Goto, K. Hashimoto, Y. Omura, T. Imacahi, H. Matsumoto, and H. Oya, The Lunar Radar Sounder (LRS) Onboard the KAGUYA (SELENE) Spacecraft, The Kaguya Mission to the Moon (Guest Editors: A. Matsuoka, C.T. Russell), Space Science Reviews, 154, Nos. 1-4, 145-192, DOI:10.1007/s11214-010-9673-8, 2010

[2] Y. Kasahara, Y. Goto, K. Hashimoto, T. Imachi, A. Kumamoto, T. Ono, and H. Matsumoto, Plasma Wave Observation Using Waveform Capture in the Lunar Radar Sounder on board the SELENE Spacecraft, Earth, Planets and Space, 60, 341-351, 2008.

[3] K. Hashimoto, Y. Goto, Y. Kasahara, H. Matsumoto, and R. R. Anderson, Auroral Kilometric Radiation: Polarization and Spectra Observed far from the Earth, "Auroral Dynamics and Space Weather", (eds. by Y. Zhang, L. Paxton), AGU Geophysical Monograph Series, Wiley, 255-273.

かぐや衛星で観測したオーロラキロメートル放射の伝搬モードの緯度分布の解析

澤田 佳大 [1]; 後藤 由貴 [1]; 笠原 禎也 [1]; 橋本 弘藏 [2]
[1] 金沢大; [2] 京都大学

Statistical analyses of AKR polarization in lunar orbits using KAGUYA wave data

Keita Sawada[1]; Yoshitaka Goto[1]; Yoshiya Kasahara[1]; Kozo Hashimoto[2]
[1] Kanazawa Univ.; [2] Kyoto Univ.

Auroral kilometric radiation (AKR) is one of the plasma waves that KAGUYA observed from lunar orbits. It is radiated from polar regions of the Earth in a frequency range from 50 kHz to 700 kHz. An important feature of AKR is its propagation mode; left-handed ordinary mode (L-O) and right-handed extraordinary mode (R-X). According to past satellite observations, L-O mode AKR propagates to both high and low latitudes while R-X mode does only to high latitudes [ex. Hashimoto et al., 1984, 1998, 2015]. AKR observations from KAGUYA make it possible to study latitudinal distribution of the propagation mode statistically.

Because the propagation mode of AKR is defined by wave polarization for external magnetic field directions at sources, it is necessary to find source hemisphere to determine the mode. For that purpose, we used occultation of the Moon. There are short periods when only one polar region can be seen from the satellite along its orbit. During those periods, intensity variations are based on diffraction theory. Since the diffraction effects are different depending on source locations, we determined the source hemisphere by comparing the observed intensity variation with theoretical ones.

From statistical analysis of the AKR mode observed by KAGUYA, it is found that there is a clear dependence of observation probability of each mode on Earth's magnetic latitude. The number of R-X mode waves decreases when the latitude gets lower. On the other hand, the number of L-O mode waves increases when the latitude gets higher in the opposite hemisphere to the source. Because intensity of R-X mode is much larger than that of L-O mode, R-X mode and L-O mode waves were dominantly observed in the same and opposite hemisphere, respectively

地球の極起源のオーロラキロメートル放射 (AKR) は強い強度をもつ電磁波で、地球から 60 Re 離れた月軌道上のかぐや衛星においても高頻度で観測されている。かぐや衛星に搭載された波形捕捉受信器 WFC は、2 本の直交ダイポールアンテナで観測した電界の位相差からアンテナ面内における偏波を測定することができる。AKR には波源において地球の磁力線に対して右回り偏波をもつ R-X モードと左回りの偏波をもつ L-O モードの 2 種類がある。過去の衛星観測および理論解析より、L-O モードは波源から高緯度および低緯度の両方向へ伝搬するが、R-X モードはプラズマ圏の密度勾配の影響で高緯度方向へのみ伝搬することが知られている [例 Hashimoto et al., 1984, 1998, 2015, Calvert, 1990]。本研究では、かぐやのデータを解析することで、各伝搬モードが観測される緯度分布とプラズマ圏の密度分布との関係を調べた。

伝搬モードを特定するには、観測された偏波に加え、その波が南北半球のどちらから伝搬してきたかを決める必要がある。本研究では、この波源半球の特定のために月の掩蔽を利用した。月の極軌道を周回するかぐや衛星において、地球の北または南半球の片方の波源が見え始める (隠れ始める) 時間が存在する。そうした時間において波の強度は回折の影響を大きく受ける。そこで、実際に観測された AKR の強度変化と、ある波源を仮定した回折に基づく強度変化を比較することから波源半球を推定した。

伝搬モードの統計解析の結果、高緯度側では、北及び南半球の両側において同半球へ伝搬する R-X モードの数が多く、低緯度へいくにつれて数が減少していくことが明らかになった。一方、L-O モードは波源と逆半球側で観測されるものが多く、逆半球の高緯度ほど数が多くなった。具体的には、R-X モードについて同半球に伝搬する割合は 99%、逆半球に伝搬する割合は 1%であった。L-O モードは同半球への伝搬が 4%、逆半球への伝搬が 96%となった。R-X モードは L-O モードよりも強度が非常に大きいため、R-X、L-O の両モードが存在した場合に R-X により L-O が見えなくなる。このため、本解析結果はレイトレイシングによる理論解析と大きな矛盾はないといえる。ただし、逆半球側へ達する R-X モードも少数であるが確認されており、R-X モードが高緯度方向にのみ伝搬する訳ではないことが分かった。

太陽風動圧変化に伴う放射線帯外帯電子の加速

林 昌広 [1]; 三好 由純 [1]; 齊藤 慎司 [2]; 松本 洋介 [3]; 桂華 邦裕 [1]; 堀 智昭 [1]; 天野 孝伸 [4]; 関 華奈子 [5]; 町田 忍 [6]
[1] 名大 ISEE; [2] 名大理; [3] 千葉大理; [4] 東大・理; [5] 東大理・地球惑星科学専攻; [6] 名大・ISEE

Rapid acceleration of outer radiation belt electrons associated with solar wind pressure pulse

Masahiro Hayashi[1]; Yoshizumi Miyoshi[1]; Shinji Saito[2]; Yosuke Matsumoto[3]; Kunihiro Keika[1]; Tomoaki Hori[1];
Takanobu Amano[4]; Kanako Seki[5]; Shinobu Machida[6]

[1] ISEE, Nagoya Univ.; [2] Nagoya Univ.; [3] Chiba University; [4] University of Tokyo; [5] Dept. Earth & Planetary Sci.,
Science, Univ. Tokyo; [6] ISEE, Nagoya Univ.

Relativistic electron fluxes of the outer radiation belt dynamically change in response to solar wind variations. There are several time scales for the particle acceleration in MeV energy range. One of the shortest acceleration processes is wave-particle interactions between drifting electrons and fast-mode waves induced by compression of the dayside magnetopause through interplanetary shocks (e.g., Li et al., 1993). In order to investigate how relativistic electrons are accelerated by fast-mode waves induced by solar wind pressure pulse, we perform a code-coupling simulation using the GEMSIS-RB test particle simulation (Saito et al., 2010) and the GEMSIS-GM global MHD magnetosphere simulation (Matsumoto et al., 2010). As a case study, the interplanetary pressure pulse with a dynamic pressure of ~ 5 nPa is used as an up-stream condition. In the magnetosphere, the fast mode waves with the azimuthal electric field (negative E_{ϕ} : $|E_{\phi}| \sim 10$ mV/m) is launched around the subsolar point and then extends to the entire dayside magnetosphere from 0600 to 1800 MLT. The azimuthal mode number at each MLT and L-shell is derived using the Hilbert transformation, and waves due to the pressure pulse with small mode number ($m \sim 2$) are observed. Using the electric/magnetic fields simulated by the GEMSIS-GM, we calculate electron motion with different initial conditions (energy, L value and pitch angle). As a result, some of electrons are accelerated through the resonance with the negative E_{ϕ} . We find that electrons whose initial energy is higher than a critical energy are strongly accelerated by seeing negative E_{ϕ} spread from 0600 to 1800MLT along the electron drift orbits. We also derive theoretically the critical energy for the possible acceleration due to the earthward propagation of the fast mode waves, and confirm that this acceleration condition is consistent with the simulation results. It has been suggested by the previous studies that electrons are selectively accelerated at the resonance energy through the drift-resonance. In contrast, the present result indicates that wide energy electrons can be accelerated through the interactions with propagating fast mode waves.

放射線帯外帯の電子は、太陽風の変化に伴って大きく変動する。様々な時間スケールで電子の加速が起きているが、その中でも最も短い時間スケールで起きる加速機構に、惑星間空間衝撃波による昼間側磁気圏の圧縮に伴う fast モード波と電子の波動粒子相互作用がある (e.g., Li et al., 1993)。本研究では、テスト粒子シミュレーションである GEMSIS-RB(Saito et al., 2010) とグローバル MHD シミュレーションである GEMSIS-GM(Matsumoto et al., 2010) を連成し、fast モード波によってどのように電子が加速されるかを調べた。5 nPa の振幅の太陽風動圧を 100 秒間、印加させたときの計算を実施したところ、10mV/m 程度の振幅を持つ西向きの電場が発生し、昼間側磁気圏に広く分布し、その後、夜側に向かって伝播していく様子が観測された。また、ヒルベルト変換を用いて、誘導電場の各 MLT、L 値における経度方向のモード数を求めたところ、モード数およそ 2 の波が卓越していることが明らかになった。この GEMSIS-GM の計算にもとづく電場、磁場のデータを用い、GEMSIS-RB によって様々な初期条件 (エネルギー、L 値、ピッチ角) を与えて粒子の運動についてのシミュレーションを行った。その結果、電子の効率的な加速がおこる際にある閾値となるエネルギーが存在し、その閾値よりも高いエネルギーを持ち、なおかつ電場を長距離にわたって感じることで MLT に位置した電子が効率的に加速されることが明らかとなった。また、理論的な検討から閾値となるエネルギーを導出し、シミュレーションで加速を受けている電子のエネルギー分布と比較を行ったところ、良い一致を示した。本結果は、これまで考えられてきたドリフト共鳴条件にもとづいて特定のエネルギーの電子が加速される条件とは異なり、電子の加速が広いエネルギー範囲において起きる可能性を示すものである。

サブパケット構造を伴ったコーラス放射による相対論的電子加速

大村 善治 [1]; 久保田 結子 [2]
[1] 京大・生存圏; [2] 京大・工・電気

Relativistic electron acceleration by chorus emissions with sub-packet structures

Yoshiharu Omura[1]; Yuko Kubota[2]
[1] RISH, Kyoto Univ.; [2] RISH, Electric engineering, Kyoto Univ.

We perform test particle simulations of relativistic acceleration processes of energetic electrons interacting with chorus emissions with sub-packet structures. Recent analyses of whistler-mode chorus emissions observed by spacecraft show that a wave packet of a rising-tone chorus element consists of many sub-packets with gradually increasing frequencies. The strong modulation of the wave amplitude affects dynamics of resonant electrons, making them detrapped from the wave potential or entrapped into it. We set up two wave models, i.e., a chorus element with and without subpacket structures. We compare the acceleration efficiencies in the two different wave models by tracing the formation processes through many interactions with the wave packets of chorus emissions based on the Green's function method [1]. In both cases, resonant electrons undergoing the cyclotron resonance with the waves are efficiently accelerated by nonlinear wave trapping. In the case of the wave model with the subpacket structure, a larger number of electrons are entrapped into the wave potentials, while the acceleration efficiency in energy is decreased due to shorter interaction. In the case of the wave model without the subpackets, the acceleration efficiency in energy is much higher while the number of electrons undergoing the acceleration is decreased. Eventually the total acceleration efficiencies in forming the relativistic electron flux are not much different in the two different wave models. In both cases, we find formation of butterfly distributions of MeV electrons.

Reference

[1] Omura, Y., Y. Miyashita, M. Yoshikawa, D. Summers, M. Hikishima, Y. Ebihara, and Y. Kubota (2015), Formation process of relativistic electron flux through interaction with chorus emissions in the Earth's inner magnetosphere, *J. Geophys. Res. Space Physics*, 120, 9545-8211;9562, doi:10.1002/2015JA021563.

カナダ、フィンランド、昭和基地の同時観測に基づく磁気圏 ELF/VLF 波動の経度スケールの研究

米津 佑亮 [1]; 塩川 和夫 [2]; Connors Martin[3]; 尾崎 光紀 [4]; Manninen Jryki[5]; 山岸 久雄 [6]; 岡田 雅樹 [7]
[1] 名大 ISEE; [2] 名大宇地研; [3] Centre for Science, Athabasca Univ.; [4] 金沢大・理工・電情; [5] SGO; [6] 極地研; [7] 極地研

Longitudinal extent of magnetospheric ELF/VLF emissions observed at Athabasca, Kannuslehto, and Syowa stations

Yusuke Yonezu[1]; Kazuo Shiokawa[2]; Martin Connors[3]; Mitsunori Ozaki[4]; Jryki Manninen[5]; Hisao Yamagishi[6]; Masaki Okada[7]

[1] ISEE, Nagoya Univ.; [2] ISEE, Nagoya Univ.; [3] Centre for Science, Athabasca Univ.; [4] Electrical and Computer Eng., Kanazawa Univ.; [5] SGO; [6] National Inst. Polar Res.; [7] NIPR

We report on the longitudinal spatial extent of whistler mode wave emissions in the ELF/VLF range at multiple ground-based stations. We used the wave data obtained at 3 longitudinally-separated stations at auroral and subauroral latitudes, i.e., Athabasca (ATH), Canada (54.7N, 113.3W, magnetic latitude (MLAT): 61.3N), Kannuslehto (KAN), Finland (67.7N, 26.3E MLAT: 64.4N) and Syowa Station (SYO), Antarctica (69.0S, 39.6E, MLAT: 70.5S). Simultaneous observation data at these stations are available for total 48 days during December 10-14, 2012, January 9-19 and January 29-February 5, 2013, and February 26-March 21, 2014. MLT differences are about 3 hours for SYO-KAN, 8 hours for SYO-ATH, and 11 hours for KAN-ATH.

We analyzed the probability of the ELF/VLF emissions being simultaneously observed at 2 stations when the ELF/VLF emission is observed at one station. For the KAN-SYO pair (3-h MLT difference), the probability of simultaneous wave occurrence is 36.8 % of all the intervals when the emissions are observed at KAN, and, 38.5 % of all the intervals when the emission are observed at SYO. These results indicate that the spatial extent of the emissions is about 37 % with the 3-h MLT differences. However, for SYO-ATH (8 h), they drop down up to 31.5 % (ATH) and 9.9 % (SYO) and, for ATH-KAN (11 h), they are 30.4 % (ATH) and 11.9 % (KAN). These numbers clearly indicate that the probability of simultaneous wave occurrence decreased with increasing MLT differences. We also found that the simultaneous wave occurrence rate at 2 stations is higher when 2 stations are on the dayside sector.

Hybrid simulation of EMIC falling tone emission

Masafumi Shoji[1]; Yoshiharu Omura[2]
[1] ISEE, Nagoya Univ.; [2] RISH, Kyoto Univ.

Theoretical study suggest the existence of electromagnetic ion cyclotron (EMIC) falling tone emissions, as well as the EMIC rising tone emissions. We develop self-consistent hybrid simulation code with parabolic ambient magnetic field with longitudinal electric field. We successfully reproduce a helium band falling tone EMIC emission in the simulation space. In upstream region of the wave propagation, we find electromagnetic proton hill predicted in the nonlinear wave growth theory. The proton hill results in nonlinear resonant current causing falling frequency in the upstream region. Cold ion density modulation is induced by forward and backward propagating oxygen band EMIC waves. The linear growth of the helium band EMIC wave is also enhanced due to the spatial inhomogeneous density distributions, and then helium band waves are modulated in density modulation scale. The strong trapping takes place due to the packeted waves. The trapped particle guided by the increasing resonance velocity in the upstream region, the proton hill appears in the distribution function.

Van Allen Probes 衛星が観測した、fast magnetosonic waves の性質

山本 和弘 [1]; 能勢 正仁 [2]

[1] 京大・理・地物・電磁気; [2] 京大・理 地磁気センター

Properties of the fast magnetosonic waves observed by Van Allen Probes

Kazuhiro Yamamoto[1]; Masahito Nose[2]

[1] Geophysics, Kyoto Univ.; [2] DACGSM, Kyoto Univ.

In this study, we report two topics: the relation between fast magnetosonic waves and thermal protons, and the radial propagation of fast magnetosonic waves.

Fast magnetosonic waves are sometimes called as equatorial noise or ion Bernstein mode waves and are frequently observed in magnetic equatorial region in the inner magnetosphere. These waves are typically compressional and have peaks in the spectra of electric and magnetic fields at the harmonics of ion cyclotron frequency.

Many theoretical studies and observations show that the energetic proton ring/shell distributions (~ 10 keV) are the source of these waves [Perraut *et al.*, 1982; Denton *et al.*, 2010; Gray *et al.*, 2010; Zhou *et al.*, 2014, Maldonado *et al.*, 2016]. The influence of thermal protons ($1\sim 100$ eV) is also mentioned in some theoretical studies. Horne *et al.* [2000] demonstrate the proton heating through the Doppler-shifted cyclotron resonance between thermal protons and fast magnetosonic waves by performing ray-tracings. Min and Liu [2015] perform linear dispersion analysis and show that the waves become electrostatic when the ratio of a Maxwellian thermal component to an isotropic shell velocity component decreases. However, there are few observations on the relation between fast magnetosonic waves and thermal protons.

The other topic is the wave propagation. Perraut *et al.* [1982] propose that we can estimate the radial propagation direction of fast magnetosonic waves from the harmonic frequency because it relates to the magnitude of the magnetic field where the waves are generated. Wave propagation may explain the harmonic structures that deviate from the local proton cyclotron frequency.

Here we investigate fast magnetosonic waves and their associated enhancements of thermal proton flux observed by Van Allen Probes. On February 6, 2014, Probe B observed two fast magnetosonic wave events in the equatorial region ($L = 5.8$ and 5.4 , $MLT = 12.8$ and 13.5 , and $MLAT = 0.2$ and 1.4) at 1700 and 1800 UT. The compressional waves appeared above 10 Hz in magnetic field. We also found electric harmonic structure below 10 Hz. Small disturbance ($Dst \sim -30$ nT) occurred on the day. There was a sudden increase of proton density of solar wind at 1750 UT (from $2/cc$ to $3/cc$), but around 1700 UT the condition of solar wind was stable. AE index slowly changed from 200 nT to 100 nT. At the same time, proton flux increased at the energy of 10-100 eV and had peaks around 1700 and 1800 UT. Such a simultaneous increase of thermal proton flux can be also found on March 06, 2013. We attribute the increase the flux to fast magnetosonic waves, and discuss the relation between them from the two points of view: wave-particle interaction and regime transition of fast magnetosonic waves.

In addition, we show simultaneous observation of fast magnetosonic waves by probe A and B on March 1, 2014. The radial distance between probe A and B was ~ 0.5 Re and probe A was nearer the earth than probe B. Probe A observed harmonics of the local proton cyclotron frequency (5 Hz, 10 Hz, ...). The harmonic structure was observed by probe B about 2 minutes after the observation of probe A. The structure had peaks at same frequency as probe A and deviated from harmonics of the local proton cyclotron frequency (4 Hz, 8 Hz, ...). We consider these spectral features as results of wave propagation in radially outward direction from the strong magnetic field region (at probe A) to the weak magnetic field region (at probe B). From the time difference between two observations, we estimate the radial component of the group velocity of the fast magnetosonic waves (v_g^{rad}) and the result is $v_g^{rad} \sim 20$ km/s.

Investigation of ion components in the plasmasphere using plasma wave observations from Van Allen Probes observations

Koji Nomura[1]; Yoshizumi Miyoshi[1]; Satoshi Kurita[1]; Shoya Matsuda[1]; Kunihiro Keika[1]; Masafumi Shoji[1]; Shinobu Machida[2]; Yoshiya Kasahara[3]; Naritoshi Kitamura[4]; Ondrej Santolik[5]; Craig A. Kletzing[6]; Scott Boardsen[7]
[1] ISEE, Nagoya Univ.; [2] ISEE, Nagoya Univ.; [3] Kanazawa Univ.; [4] ISAS/JAXA; [5] The Czech Academy of Sciences; [6] Department of Physics and Astronomy, UoI; [7] NASA/GSFC

Magnetosonic waves (MSWs) (or equatorial noise) are electromagnetic emissions whose properties can be described by the cold plasma extraordinary mode. MSWs are typically observed between the proton cyclotron frequency and the lower hybrid resonant frequency generated by the ring distributions of energetic protons. Our previous studies indicated that MSWs becomes left-handed (LH) polarized inside the plasmasphere when the wave frequency becomes lower than the cross-over frequency. Since the local cross-over frequency depends on the local ion composition, it is possible to investigate the local ion compositions by estimating the frequency at which polarization reversal of MSWs takes place. Taking into consideration of this point, we estimate the local ion compositions by estimating both the cross-over frequency and the $L=0$ cut off frequency that also depends on the local ion compositions. We use both EFW and EMFISIS data from Van Allen Probes to study the frequency spectrum of MSWs. In this study, $M/Q = 2$ ion is identified as have reported by Matsuda et al. [2016]. We also find that the ion composition depends on the radial distance from the Earth at relatively low altitude. We will report this result and the spatial distribution of the ion composition from the statistical survey of the Van Allen Probe observations.

Measurement and Modeling of the Plasmasphere during the St. Patrick's Day 2013 and 2015 Geomagnetic Storms

Yuki Obana[1]; Naomi Maruyama[2]

[1] Engineering Science, Osaka Electro-Communication Univ.; [2] CU/CIRES, NOAA/SWPC

The plasmasphere is a region of cold plasma trapped in the inner magnetosphere by closed geomagnetic field lines. The comprising electrons and ions diffusively come from the underlying ionosphere. Thus, the properties of the plasmasphere are controlled by the dynamics of the magnetosphere, ionosphere, and thermosphere. The plasmasphere is typically eroded during a storm, with a time scale of hours, and refills during quiet times with a time scale of days.

Using cross-phase analysis of geomagnetic data from the CRUX magnetometer array in New Zealand, we determined the equatorial plasma mass density during the two St. Patrick's Day geomagnetic storms: March 2013 and 2015. Its trends during the 2013 storm present typical erosion and subsequent refilling features. On the other hand, during the 2015 storm, Plasma mass density values kept pre storm level throughout the storm time. Apparently, no erosion has happened.

Comparing these experimental results to model results from the Global three-dimensional ionosphere-plasmasphere-electrodynamics (IPE) model, we will discuss the plasmasphere dynamics and its coupling to the ionosphere-thermosphere system.

SuperDARN 北海道-陸別第一・第二 HF レーダーによる低緯度オーロラ発生時における電離圏対流の観測

西谷 望 [1]; 堀 智昭 [1]; 片岡 龍峰 [2]; 海老原 祐輔 [3]; 塩川 和夫 [4]; 大塚 雄一 [4]; 鈴木 秀彦 [5]; 吉川 顕正 [6]
[1] 名大 ISEE; [2] 極地研; [3] 京大生存圏; [4] 名大宇地研; [5] 明治大; [6] なし

SuperDARN HOP radars observation of ionospheric convection associated with low-latitude aurora events at Hokkaido, Japan

Nozomu Nishitani[1]; Tomoaki Hori[1]; Ryuho Kataoka[2]; Yusuke Ebihara[3]; Kazuo Shiokawa[4]; Yuichi Otsuka[4]; Hidehiko Suzuki[5]; Akimasa Yoshikawa[6]
[1] ISEE, Nagoya Univ.; [2] NIPR; [3] RISH, Kyoto Univ.; [4] ISEE, Nagoya Univ.; [5] Meiji Univ.; [6] ICSWSE/Kyushu Univ.

The SuperDARN HOKkaido Pair of (HOP) radars, consisting of the Hokkaido East (2006-) and West (2014-) radars, are the SuperDARN radars located at the lowest geomagnetic latitude (36.5 degrees), and have been continuously measuring ionospheric convection at high to subauroral and middle latitudes with high temporal resolutions (≤ 1 to 2 mins). These radars enable us to study the two-dimensional evolution of ionospheric convection ever 1 or 2 minutes.

In this paper we study two low latitude aurora events observed in Hokkaido, Japan from 15 to 19 UT on March 17, 2015 and from 1900 to 2030 UT on December 20, 2015, identified using optical instruments such as all-sky CCD camera, wide field of view digital camera and meridian scanning photometer. Both events occurred during the main phase of the relatively large geomagnetic storms with minimum Dst of -223 nT and -170 nT respectively. The ionospheric convection at mid-latitude regions associated with the low-latitude auroral emission is characterized by (1) transient equatorward flows up to about 500 m/s in the initial phase of the emission (the geomagnetic field data at Paratunka, Far East Russia show corresponding negative excursions in the D component), and (2) sheared flow structure consisting of westward flow (about 500 m/s) equatorward of eastward flow (1000 m/s), with the equatorward boundary of auroral emission embedded in the westward flow region which expanded up to below 50 deg geomagnetic latitude. These observations imply that the electric field / convection distribution plays important roles in continuously generating the low latitude auroral emission. In particular the observation of the equatorward flow (dawn-dusk electric field) up to as low as about 50 deg geomagnetic latitude is the direct evidence for the presence of electric field to drive ring current particles into the plasmaspheric regions.

SuperDARN 北海道-陸別第一・第二 HF レーダーは現存の SuperDARN レーダーの中で最も低い磁気緯度 (36.5 度) に位置しており、特に大磁気嵐等の地磁気擾乱時における 1-2 分以内の高時間分解能を持つ電離圏対流の観測に威力を発揮する。

本講演においては、2015 年 3 月および 2015 年 12 月にそれぞれ発生した大磁気嵐 (minimum Dst がそれぞれ -223 nT, -170 nT) 時に報告された低緯度オーロラ (観測期間はそれぞれ 2015/3/17 15-19 UT、2015/12/20 1900-2030 UT) に関連した中緯度-サブオーロラ帯における電離圏対流変動の特性について報告する。両方のイベントについて共通した以下の特徴が観測された。1) オーロラ発生初期段階において低緯度方向の対流 (最速で 500~1000 m/s 程度) が磁気緯度 50 度以下の領域までわたって卓越する (地磁気緯度約 45 度の Paratunka における磁場もこの対流強化に伴って西向きの変動を示している)。2) その後のオーロラ発光が続いている時間帯においては、低緯度側に西向き (約 500 m/s)、高緯度側に東向き (約 1000 m/s) のフローシア構造が形成され、オーロラ発光の低緯度側境界は低緯度側西向きフローの中に位置している。この観測から、前者の対流は磁気嵐に伴う dawn-dusk 電場が磁気圏内部 ($L < 2.4$) まで侵入し、リングカレント荷電粒子がプラズマ圏の位置まで輸送されてその低エネルギー荷電粒子と相互作用を起こして低緯度オーロラが発生したと解釈できる。後者については詳細なメカニズムはまだ検討中であるが、オーロラ発光を維持するために対流のシア構造を作り出す電場分布が何らかの役割を果たしていると示唆される。重要な点は二つの磁気嵐中の低緯度オーロラ発生時刻において類似した対流の特徴が同定された点であり、今後より詳細な検討を進める予定である。

Spherical Elementary Current を用いた SC 極電流の解析 — 2013/2015 年 St. Patrick Day の SC

Marsal S[1]; Segarra Antonio[1]; Torta J. M.[1]; # 荒木 徹 [2]
[1] OE; [2] 京大理

Use of Spherical Elementary Currents for Analysis of SCs observed on 2013 and 2015 St. Patrick's Day storms

s Marsal[1]; Antonio Segarra[1]; J.M. Torta[1]; # Tohru Araki[2]
[1] OE; [2] none

Araki's model of geomagnetic sudden commencements (SCs) proposes a successive appearance of the DPpi- and DPmi-current system. By applying the Spherical Elementary Current Systems (SECS) to SC data from more than 100 ground stations we confirmed the existence of the proposed current systems for two fairly large SCs occurred on 2013 and 2015 St. Patrick's Day. The DPpi current system is converted to DPmi-current system reversing polarity during the first couple of minutes of the SC. It is the first time that SECS have been used for this purpose.

SC のモデル (Araki,1994) は, DPpi と DPmi の二つの電流系が引き続いて現れることを提起している. ここでは, SECS(Spherical Elementary Current System) と 100 以上の地上観測点データを用いて, この二つの電流系の生起を確かめた. それらは電場方向を逆転させながら連続して生じている. SECS を SC の解析に用いたのは, これが初めてである.

Global evolution and propagation of electric fields during sudden commencements based on multi-point observations

Naoko Takahashi[1]; Yasumasa Kasaba[1]; Yukitoshi Nishimura[2]; Atsuki Shinbori[3]; Takashi Kikuchi[4]; Tomoaki Hori[5]; Nozomu Nishitani[5]

[1] Tohoku Univ.; [2] UCLA; [3] RISH, Kyoto Univ.; [4] ISEE, Nagoya Univ.; [5] ISEE, Nagoya Univ.

Sudden commencements (SCs) are triggered by an abrupt compression of the dayside magnetopause, which causes a fast mode wave propagating toward the Earth in the equatorial magnetosphere across the magnetic field line. The sudden compression also induces the Alfvén wave propagation toward the polar ionosphere along magnetic field lines. The latter causes the global transmission of ionospheric electric field at speed of light, and can propagate the influence back to the inner and/or night-side magnetosphere. These general propagation processes have been demonstrated in previous papers using direct observations.

Motivated by these issues, we investigate global evolution and propagation of electric fields using in-situ satellites and ionospheric radars. In order to clarify the magnetospheric response, we obtain the magnetospheric electric and magnetic field data from THEMIS (5 probes) and Van Allen Probes (RBSP, 2 probes). Magnetospheric magnetic field data obtained from GOES 13 and 15 are also referred to. We identify the ionospheric response using the C/NOFS satellite and SuperDARN radar. The event selection criteria are set as follows: (1) SCs occurred from January 2013 to December 2014. (2) The amplitude of the SYM-H is more than 10 nT, and its rise time is less than 5 min. One hundred and thirty events satisfied these criteria.

An event study on 17 March 2013 shows that the magnetospheric electric field is propagated from dayside to nightside magnetosphere. At the onset time, the magnetospheric magnetic field starts to increase, which indicates that the detected electric field is associated with the compression of the magnetosphere. In the ionosphere, C/NOFS satellite and SuperDARN radar detect the dusk-to-dawn electric field about 1 min after the onset in the magnetosphere. Poynting fluxes evaluated from THEMIS and RBSP data are directed toward the ionosphere along magnetic field lines in both dayside and nightside, which indicates that the Alfvén wave launches toward the polar ionosphere at the onset. We statistically derive the spatial evolution of magnetospheric electric fields. This result can be interpreted as follows: First, the fast mode wave propagates from dayside to nightside magnetosphere, and ~105-120 s after the onset, the magnetospheric convection becomes stronger. We also find that the spatial distribution of the response time is asymmetric between dawn and dusk, which can be explained by the asymmetry of the plasmapause location.

大規模沿磁力線電流による磁気シア効果を取り入れた磁気圏—電離圏結合の理論解析

渡邊 智彦 [1]; 三輪 有輝 [2]; 前山 伸也 [2]
[1] 名大; [2] 名大・理・物理

Theoretical analysis of the M-I coupling including magnetic shear effect due to the large-scale field-aligned currents

Tomo-Hiko Watanabe[1]; Yuki Miwa[2]; Shinya Maeyama[2]
[1] Nagoya Univ.; [2] Dept. Physics, Nagoya Univ.

It has been considered that auroral arc formation and its spontaneous growth originate from physical processes intrinsic to the magnetosphere-ionosphere coupling. The feedback instability is one of the most plausible mechanism. Theoretical analyses of the feedback instability have been limited to the simple geometries such as the straight field line or the dipole configurations. In the present study, we have extended our analysis with including the magnetic shear effects due to the large-scale field-aligned currents (FACs).

For simplicity, we consider a model with straight field lines with a constant shear, where the east-west components of the magnetic field due to the FACs are taken into account. Then, we could derive the linear dispersion relation of the feedback instability in presence of the finite magnetic shear.

In this study, we have found (1) a frequency upshift of the Alfvén resonance, and (2) enhancement of the feedback instability due to the magnetic shear. The result (1) is confirmed by an analytical solution under the weak shear approximation. The obtained results are the first demonstration that the fine-scale auroral dynamics can be influenced by the large-scale current structure in the magnetosphere. More detailed results including roles of dissipation will also be discussed.

地磁気静穏時におけるオーロラ・アーク構造の自発的形成とその成長は、磁気圏—電離圏結合系に元来備わった固有の物理機構に起因すると考えられる。対流電場が閾値を超えた時、それをエネルギー源として成長する Alfvén 波の不安定性、すなわちフィードバック不安定性は、その有力な候補の一つであり、これまでに線形・非線形解析を用いた様々な理論・シミュレーション研究が行われてきた。しかし、従来の解析では、簡単な直線磁場モデルや双極子磁場を仮定する 경우가ほとんどであった。本研究では、オーロラ領域における大規模沿磁力線電流に着目し、そこで生じる磁気シアがフィードバック不安定性に及ぼす影響について理論解析を行った。

ここでは理論の簡潔さのために、定常な直線磁場が一定のシアをもつ局所モデルを考察する。大規模沿磁力線電流がつくる東西成分の磁場は、その磁気シア成分として取り扱われる。磁力線に沿った一般座標を用いることで、簡略化磁気流体方程式から、シア磁場下での線形分散関係式を導出することができる。

これまでに、沿磁力線電流の向きに応じてその符号を変える磁気シアに依存して、(1) Alfvén 共鳴周波数の変化がおきること、(2) これにともなってフィードバック不安定性の成長率が影響されること、が確認できた。磁気シアが十分弱い場合、(1) の共鳴周波数の変化は近似方程式による解析解とよく一致することが確かめられた。これらは、磁気圏中の大規模電流構造が、微細なオーロラ・アークの発達に影響し得ることを理論的に示した初めての結果である。今後、散逸効果の影響などを含めたより詳細な解析を進める予定である。

MI結合のドライバーとしてはたらく電離層

#坂翁介 [1]
[1] オフィス ジオ

Ionosphere as a driver of substorm MI-coupling

Osuke Saka,[1]
[1] Office Geophysik

Dynamic properties of the terrestrial ionosphere and the magnetosphere are coupled electrically and magnetically through the field-aligned current closure. The driver of the Alfvén waves in the magnetosphere, often represented by the perpendicular gradients of plasma pressure at right angles to the field gradient in the equatorial plane, is a source of field-aligned currents (FAC) in the MI coupling.

Meanwhile, the ionosphere may act as the driver of the FAC. Knowing that the expansion of the flux tube cross-section leads to the reduction of the magnetic field intensity in the ionosphere, we can assume that the inductive fields (fast mode) are set up in the auroral zone ionosphere at substorm onset. The Hall conductance of the ionosphere generates the static fields (Alfvén mode) in the auroral zone ionosphere by the mode coupling. The upward and downward FAC from the static field regions may form a current closure themselves through the Hall currents. The auroral zone ionosphere in northern and southern hemispheres individually serves as the source of the FAC at substorm dipolarization.

Initial statistical study of FACs simultaneously observed along the same field line by MAGDAS on the ground and by QZS in space

Hideaki Kawano[1]; Osamu Ogushi[2]; Yuta Abematsu[3]; Nana Higashio[4]; Haruhisa Matsumoto[5]; Alexey Moiseev[6]; Dmitry Baishev[6]; Teiji Uozumi[7]; Shuji Abe[8]; Akimasa Yoshikawa[9]; Akimasa Yoshikawa MAGDAS/CPMN Group[10]
[1] Earth and Planetary Sci., Kyushu Univ.; [2] Earth and Planetary Sciences, Kyushu University; [3] Dept. Earth Planet. Sci., Kyushu Univ.; [4] JAXA; [5] JAXA; [6] IKFIA, SB, RAS; [7] ICSWSE, Kyushu Univ.; [8] ICSWSE, Kyushu Univ.; [9] ICSWSE/Kyushu Univ.; [10] -

The QZS satellite of JAXA has an orbit whose geocentric distance is almost the same as those of geosynchronous satellites but whose orbital plane makes an angle of about 45 degrees from the equatorial plane. The footpoint of the magnetic field line running through QZS keeps staying very close to the Siberian MAGDAS ground magnetometer stations KTN, TIK, and CHD. Thus, they can simultaneously and continuously monitor the same FAC at high-latitudes in space and on the ground, for the first time in history. This enables us to study the detailed spatial structure and motion of the current circuit consisting of the FAC and the ionospheric current. At present we have data from QZS and Siberian MAGDAS for the same five years, and we can study them on a statistical basis. So far we have made an overview-type analysis of one-year data, and the following is the features of the FACs simultaneously identified both in space and on the ground along the same field line. (1) The majority of them was observed on the nightside. (2) The majority of them flowed into (away from) the ionosphere in the postmidnight (premidnight) sector. (3) They tended to move away from the midnight meridian in the east-west direction. (4) They tended to move away from the equatorial plane in the north-south direction. (5) Their current intensities had a positive correlation with the AE index.

Generalization of Ionospheric polarization and Magnetospheric Field-Resonance

Akimasa Yoshikawa[1]
[1] ICSWSE/Kyushu Univ.

Generalized wave equations for the three-dimensional magnetosphere-ionosphere coupling are derived. This formulation unifies two types of mode conversion between shear Alfvén wave and compressional wave, that is, one by the inhomogeneity of the Alfvén velocity in the magnetosphere and the other by the multi-step inductive Hall effect in the ionosphere. Wave generation by the magnetospheric dynamo in the source region of the magnetosphere and by the polarization effect in the loading region of the ionosphere can also be described by the same equation. The resultant horizontal propagation of ionospheric electrostatic potential field accompanied by the formation process of Birkeland current system could be explained by this formulation.

In this talk, we will discuss the formation process of Birkeland current system from viewpoint of the three-dimensional magnetosphere-ionosphere coupling.

低高度衛星によって観測された磁場変動の磁気圏赤道面への投影

横山 佳弘 [1]; 家森 俊彦 [2]; 青山 忠司 [3]

[1] 京大・理・地惑; [2] 京大・理・地磁気センター; [3] 京大・理

Mapping the magnetic fluctuations observed by LEO satellites onto the equatorial plane of magnetosphere

Yoshihiro Yokoyama[1]; Toshihiko Iyemori[2]; Tadashi Aoyama[3]

[1] SPEL, Kyoto Univ.; [2] WDC for Geomagnetism, Kyoto Univ.; [3] Graduate School of Science, Kyoto Univ.

In the regions of high-beta plasma such as the plasma sheet or the boundary layer in the magnetosphere, it can be expected that the plasma behaves as turbulence due to the effects of various plasma instabilities, non-linear development of Alfvén waves, and so on. Satellites in the plasmasheet also have observed the fluctuations in velocity and magnetic field that have the characteristics of fluid turbulence (Borovsky et al. 1997). If the plasmas usually behave as turbulence, the spectrum and their distribution are important for understanding phenomena in the magnetosphere. However, it is almost impossible to have sufficient simultaneous satellite observations that cover the huge magnetospheric domain.

On the other hand, we confirmed that the magnetic fluctuations having period longer than 2s observed by low Earth orbit (LEO) satellites can be regarded as the manifestation of the spatial structure of the field-aligned currents by using the magnetic data obtained by Swarm satellites during December, 2013 when the satellites flew on nearly the same orbits with slight time separations. In addition, the LEO satellites fly through wide range of magnetic latitudes in a short period of time, so, by projecting their orbits into the magnetosphere, they can scan wide range on the equatorial plane of the magnetosphere. therefore, by projecting these fluctuations onto the equatorial plane of the magnetosphere, i.e., the source regions of field-aligned currents, we try to estimate the distribution of turbulent region and their characteristics there.

We made statical maps of the amplitude of magnetic fluctuations for both quiet ($AE < 50\text{nT}$) and disturbed ($AE > 50\text{nT}$) conditions. We also made spectral analysis of magnetic fluctuations by MEM and found that there are many peaks in wide frequency range in every spectrum regardless of the geomagnetic conditions, MLTs, and so on.

This result suggests that the magnetospheric plasmas usually behave as turbulence.

In this paper, in addition to the result above, we also discuss the wave-number spectrum in the magnetosphere.

プラズマシートや磁気圏境界層など高 β プラズマ領域では、様々なプラズマの不安定性やアルフベン波の非線形発展などによって、プラズマが乱流的に振る舞っていると考えられる。実際、磁気圏観測衛星はプラズマシート中において、プラズマの速度や磁場が流体乱流の特性を持っていることを観測している (Borovsky et al. 1997)。仮にプラズマが乱流的に振る舞うのであれば、そのスペクトルや分布は磁気圏内の現象を理解するために重要である。しかし、広大な磁気圏領域を包括する衛星による十分な同時観測はほぼ不可能である。

一方で、我々は SWARM 衛星の初期軌道と磁場観測データを解析することで、低高度衛星によって観測される周期 2 秒以上の磁場変動の大部分が沿磁力線電流の空間構造の表れであることを確かめた。加えて、低高度衛星は短時間で広い磁気緯度幅を通り抜けるため、衛星の軌道を磁気圏へ投影することで磁気圏赤道面の広大な領域を網羅することができる。それゆえ、これらの変動を磁気圏赤道面、つまり沿磁力線電流生成領域に投影し、乱流領域の分布やそれらの特性を見積もることを試みた。

我々は、磁気圏赤道面における磁場変動の振幅についての統計分布図を磁気静穏時 ($AE < 50\text{nT}$) と磁気擾乱時 ($AE > 50\text{nT}$) について作成した。また、MEM 方を用いてスペクトル解析も行い、磁気緯度や MLT などによらず全てのスペクトルが広い周波数帯に多くのピークを持つことを確認した。

このことは磁気圏プラズマが一般に乱流的に振る舞うことを示唆している。

本発表では、上記の結果に加え、磁気圏における波数スペクトルについても議論する。

General properties in the ion composition and energy in the plasma sheet observed during March to July in 2016 by the MMS mission

Masafumi Hirahara[1]; Naritoshi Kitamura[2]; Karlheinz Trattner[3]; Stephen Fuselier[4]

[1] ISEE, Nagoya Univ.; [2] ISAS/JAXA; [3] LASP, Univ. Colorado; [4] Space Science and Engineering Division, SwRI

We survey for the recent high-quality data obtained in the near- and mid-distant plasma sheet by the HPCA (Hot Plasma Composition Analyzer) on the MMS (Magnetospheric Multiscale) mission of NASA. The MMS mission is the most recent mission in the Solar-Terrestrial physics for studying magnetic reconnection processes in the terrestrial magnetosphere with four identical spacecraft (Burch and Torbert, SSR, 2016; Burch et al., SSR, 2016; Fuselier et al., SSR, 2016), and the HPCA is the ion energy-mass spectrometer consisting of a top-hat electrostatic energy analyzer and a time-of-flight mass spectrometer, covering the energy range from 10 eV to 40 keV for typical ion species in the magnetosphere (Young et al., SSR, 2016). We report the general properties of hot and beam components of the ions and their dependence on the mass composition. Most of the observational periods used in our survey from March to June of 2016 were in the southern plasma sheet and the boundary adjacent to the lobe because of the orbital elements of MMS. According to our quick survey of the energy-time (E-t) spectrograms of the HPCA data, the hot O⁺ component intensities in the keV range in the plasma are strongly correlated with the geomagnetically disturbed times while the beam-like O⁺ signatures at lower-energies could be seen even under mid and low active conditions. It should also be noted that the low-energy beam-like H⁺ signatures could be seen inside and vicinity of the plasma sheet also during the quiet times, and the intensity ratios of H⁺ to O⁺ are clearly anti-correlated with geomagnetic activity. The other types of H⁺ signatures, e.g., the very low-energy H⁺ population at less than 100 eV and the energy-dispersive band-like H⁺ structures whose energies monotonically decreases with the distance from the Earth, were often observed in the near-Earth orbits, particularly under quiet conditions. These facts indicate that the energization mechanisms acting on the outflowing and plasma sheet heavier ions may be more effective with increase of geomagnetic activity while some processes driving the outflows of the ionospheric ions were always engaged more and less. The beam-like O⁺ energy distributions found in the E-t spectrograms tend to have slower variations particularly in and near the plasma sheet boundary layer, than those of H⁺. These slower variations could be a consequence of the mass-dependent energization processes. Also in our presentation, we discuss how similar and different the mass-resolved signatures in the hot/beam components are among the four MMS satellite measurements.

MMS 衛星データを用いた磁気リコネクション過程の解明：2流体モデルの適用

町田 忍 [1]; 宮下 幸長 [2]; 家田 章正 [3]; 桂華 邦裕 [2]; 三好 由純 [2]; 齋藤 義文 [4]
[1] 名大・ISEE; [2] 名大 ISEE; [3] 名大宇宙地球研; [4] 宇宙研

Investigation of the magnetic reconnection process with MMS data: Application of the two-fluid model

Shinobu Machida[1]; Yukinaga Miyashita[2]; Akimasa Ieda[3]; Kunihiro Keika[2]; Yoshizumi Miyoshi[2]; Yoshifumi Saito[4]

[1] ISEE, Nagoya Univ.; [2] ISEE, Nagoya Univ.; [3] ISEE, Nagoya Univ.; [4] ISAS

<http://www.isee.nagoya-u.ac.jp/>

It is known that the magnetic reconnection is one of the most significant processes for understanding the structure of the magnetosphere and the mass and energy transport in the Earth's magnetosphere. The MMS (Magnetospheric Multi-Scale) mission which consists of four spacecraft was planned to study microscopic processes involved in the magnetic reconnection. Each spacecraft conducts fast electron and ion measurements as never done before with time resolution of 30 msec and 150 msec, respectively, as well as DC/AC magnetic field, DC/AC electric field measurements. If we adopt a set of two-fluid equations to the data obtained by four MMS spacecraft with spatial separations of 50-400 km, it is possible to conduct the following studies all essential to understand the magnetic reconnection:

- (1) Direct derivation of the anomalous resistivity
- (2) Determination of the physical mechanism to merge the magnetic field lines
- (3) Examination of the frozen-in relation for ions and electrons to the magnetic field
- (4) Verification of the causality relationship of plasma dynamics, i.e., Clarification the mechanism that causes the motion of plasma, and heats/accelerates ions and electrons

Those are completely evaluated and verified with the use of the data from MMS spacecraft whose primary subject is to clarify the physical process of the magnetic reconnection.

The method proposed in this study can be applicable not only to the magnetic reconnection but also to the other processes such as discontinuities or shocks, thus it may become a useful tool to investigate various fundamental processes in the magnetosphere.

磁気リコネクションは磁気圏の構造や質量・エネルギーの輸送を考える上で、最も重要な物理過程の一つである。その現象の微視的構造を実証的に解明すべく、MMS (Magnetospheric Multi-Scale) 衛星が打ち上げられた。この衛星では、電子 30msec、イオン 150msec といった、これまでにない極めて高い時間分解能のプラズマ観測が行われ、また同時に、DC (直流) 磁場と DC 電場およびそれらの波動成分の観測が実施されている。意外なことに、4機の衛星同士の距離を 50~400km に保って上記の観測を実施する MMS 衛星の特性を生かしつつ、単純な 2 流体方程式を用いると、磁気リコネクションの基礎過程について、これまでできなかった以下のような研究を実施することが可能である。

- (1) 異常抵抗テンソル各成分の値
- (2) 磁気中性線で磁場を融合させる物理過程の決定
- (3) 電子、イオンのそれぞれについて磁場の凍結則が成立しているかの確認
- (4) プラズマのダイナミクスにおける因果律の解明、すなわち、何が原因でプラズマの運動が発生し、プラズマ粒子が加速、加熱されるかの解明

これらはいずれも衛星データを直接計算して求めたり、確認することができる。MMS 衛星が主目的にしている磁気リコネクション、特に、磁気中性線周辺の構造の解明と磁場を融合させるメカニズムの同定とリコネクションジェット生成のメカニズムの解明を進めることが可能である。本研究で提唱する手法は、磁気リコネクション以外にも、不連続面や衝撃波の研究に極めて有効であり、磁気圏物理学の実証的研究にブレークスルーをもたらすことが期待される。講演においては、本手法の詳細について報告を行う。

Geotail 衛星のデータを用いた昼側磁気リコネクションのホール磁場構造に関する研究

田中 瑠 [1]; 町田 忍 [2]; 内野 宏俊 [3]; 今田 晋亮 [2]; 三好 由純 [1]; 関 華奈子 [4]; 家田 章正 [5]; 宮下 幸長 [1]; 桂華 邦裕 [1]; 齋藤 義文 [6]

[1] 名大 ISEE; [2] 名大・ISEE; [3] 京大・理・地惑; [4] 東大理・地球惑星科学専攻; [5] 名大宇宙地球研; [6] 宇宙研

Structures of the Hall magnetic field in the dayside magnetic reconnection inferred from Geotail data

Ryu Tanaka[1]; Shinobu Machida[2]; Hirotochi Uchino[3]; Shinsuke Imada[2]; Yoshizumi Miyoshi[1]; Kanako Seki[4]; Akimasa Ieda[5]; Yukinaga Miyashita[1]; Kunihiro Keika[1]; Yoshifumi Saito[6]

[1] ISEE, Nagoya Univ.; [2] ISEE, Nagoya Univ.; [3] SPEL, Kyoto Univ.; [4] Dept. Earth & Planetary Sci., Science, Univ. Tokyo; [5] ISEE, Nagoya Univ.; [6] ISAS

Using Geotail data, we have investigated relationships between Hall-field structures and physical parameters in magnetic reconnection at the dayside magnetopause. In the magnetotail, symmetric reconnection generally occurs, since upstream conditions of magnetic field and plasmas are almost the same between the northern and southern sides. On the other hand, at the dayside magnetopause, asymmetric reconnection tends to occur, because properties of magnetospheric and solar wind plasmas that contribute to the dayside magnetopause reconnection are quite different. In addition, while magnetotail reconnection has a quadrupole structure of the magnetic field due to the Hall effect, dayside reconnection has basically a dipole structure. In the present study, we used simultaneous sign reversals of the ion outflow velocity and the magnetic field observed by Geotail from year 1994 to 2014 as criteria to select reconnection events, and selected 26 dayside reconnection events where Geotail crossed the neutral line of the reconnection. We find that the reconnection events have either quadrupole or dipole structure in the duskward magnetic field component (B_y). We further investigated the magnetic field structure near the neutral line by analyzing changes in the ion density and magnetic field when Geotail passed near the neutral line. In the quadrupole-structure cases, the average ratio of the ion density in the magnetosheath to that at the magnetopause is 7.5, and the average ratio of B_z at the magnetopause to $|B_z|$ in the magnetosheath is 1.5. On the other hand, in the dipole-structure cases, the average ion density ratio is 36.1, and the average magnetic field intensity ratio is 2.7. These values are greater than those for the quadrupole structure. These results indicate that dayside reconnection has the dipole structure in the Hall magnetic field when density asymmetry is large and the electron flux from the magnetosheath is much larger than that from the dayside magnetosphere. Under the condition, Hall currents due to magnetosheath electrons moving from the magnetosheath to the magnetosphere along the separatrix can form the dipole magnetic field structure.

本研究グループでは、Geotail 衛星のデータを用いて、昼側磁気圏界面の磁気リコネクションにおける Hall 磁場構造と、特徴的な物理量の関係性を調べている。磁気圏尾部では、電流層の北側と南側それぞれの上流のプラズマと磁場の性質が同じであるため、対称な磁気リコネクションが起これと考えられている。一方、昼側磁気圏界面では、性質の異なる磁気圏プラズマと太陽風プラズマがリコネクションに寄与し、非対称なリコネクションを生じさせると考えられている。また、磁気圏尾部のリコネクションでは Hall 効果に起因する四重極磁場構造がみられるのに対し、昼側リコネクションでは基本的に双極子磁場構造がみられる。本研究では、リコネクションイベントの判定基準として、Geotail 衛星の観測データのイオンのアウトフローの速度と磁場の同時符号反転を用いた。これにより、1994 年から 2014 年の期間において、Geotail 衛星がリコネクションの中性線付近を通過する 26 例のイベントを選定した。それぞれのイベントの朝夕方向の磁場成分 (B_y) には四重極構造あるいは双極子構造のいずれかがみられた。選定したイベントにおいて、Geotail 衛星の磁気中性線通過前後のイオンの密度や磁場の大きさの変化量等を調べることで、中性線付近の磁場構造について詳細に解析した。その結果、四重極構造がみられたイベントでは、磁気中性線通過前後のイオンの密度比 (磁気圏中の密度に対するシース中の密度) の平均値は 7.5、磁場 B_z 成分の絶対値の比 (シース中の B_z の絶対値に対する磁気圏中の B_z) の平均値は 1.5 と小さかったのに対し、双極子構造がみられたイベントではイオンの密度比の平均値は 36.1、磁場強度比の平均値は 2.7 と大きかった。これらの結果は、昼側磁気リコネクションにおいて密度の非対称性が強く、シース側からの電子フラックスが磁気圏側からのものに比べて大きい時に、Hall 磁場構造は双極子構造を持つことを示している。そのような状況下では、拡散領域を経由してシース側から磁気圏側に、セパトトリクスに沿って流れるシース電子による Hall 電流が双極子磁場構造を形成することが示唆される。

動く red line カスポオーロラの水平プロファイル

田口 聡 [1]; 細川 敬祐 [2]; 小川 泰信 [3]
[1] 京大理; [2] 電通大; [3] 極地研

Horizontal profile of a moving red line cusp aurora

Satoshi Taguchi[1]; Keisuke Hosokawa[2]; Yasunobu Ogawa[3]
[1] Grad school of Science, Kyoto Univ.; [2] UEC; [3] NIPR

Auroral emission at a wavelength of 630.0 nm (red-line) has a long radiative time. We have shown how this long radiative time controls the horizontal extent of a moving mesoscale aurora, which is typical of the cusp. Using high time resolution (4 s) observations by an all-sky imager at Longyearbyen, Svalbard, and observations by the EISCAT Svalbard Radar (ESR) pointing along the magnetic field direction, we examined the auroral emission enhancements obtained in the cusp during the interval of southward IMF on November 27, 2011. Simultaneous observations from the all-sky imager and ESR clearly show how auroral emission regions passed through the radar's field-of-view. When the front edge of the moving auroral structure intersected the radar's field-of-view, the ESR electron temperature was enhanced. A few minutes later, the ESR electron temperature dropped to the background level, indicating that the mesoscale electron precipitation region shifted away from the radar's field-of-view. At this time, the auroral emission in the radar's field-of-view decreased, but still had adequate intensities. These results provide evidence demonstrating that the moving cusp auroral emission occurs behind the electron precipitation region as well as inside that region. We have interpreted this feature semi-quantitatively using the equation of continuity of the density of the excited atomic oxygen. Our model indicates that the maximum intensity in the moving auroral structure occurs at a point along the trailing edge of the electron precipitation region, and that the velocity of that region is important for determining how the 630-nm aurora emissions extend horizontally.

MHD シミュレーションで得られた南 IMF 時の昼間の magnetopause 構造

藤田 茂 [1]; 田中 高史 [2]; 渡辺 正和 [3]
[1] 気象大; [2] 九大・宙空センター; [3] 九大・理・地惑

Simulation study of the dayside magnetopause in the southward IMF condition

Shigeru Fujita[1]; Takashi Tanaka[2]; Masakazu Watanabe[3]
[1] Meteorological College; [2] SERC, Kyushu Univ.; [3] Earth & planetary Sci., Kyushu Univ.

The dayside magnetopause is usually determined as a boundary interface where the magnetic pressure in the magnetosphere and the thermal pressure in the magnetosheath are balanced [Hughes, 1995]. Consequently, a thin diamagnetic current sheet flows along the magnetopause. This current produces a sharp deflection of a magnetic field vector tangential to the current sheet in the magnetopause. Indeed, the satellite observations identify the magnetopause as a sharp deflection of the magnetic field [i.e., Paschmann et al., 1979]. Finally, one might think that the magnetopause determined from the force balance relation corresponds to the magnetopause identified from a sharp deflection of the magnetic field. However, this speculation is not confirmed in the solar wind-magnetosphere interface with the magnetic field configuration regulated by the null-separator structure. Here, we investigate the two magnetopauses by using the simulation results.

From the global simulation, it is obtained that the two magnetopauses are located in the place different places. The magnetosphere determined from the force balance appears in the lowermost boundary between the magnetosheath and the magnetosphere. The plasma flow momentum can be ignored in this region. We call this region as the boundary region. On the other hand, the sharp deflection appears in the region next to the boundary region. The plasmas in this region are accelerated by the magnetic tension force because the magnetic field exhibits a kink. We call this region as the acceleration region. The kinked field lines may remind us occurrence of the reconnection in this region.

The electric current flowing in the boundary region is the Chapman-Ferraro current because this current invokes the Lorentz force against the pressure-gradient force. This eastward current connects the load in the boundary region and the dynamo in the lobe region. It is also obtained from analysis of the Poynting flux that the magnetic energy is transported from the lobe region. Next, we need to identify the source of the current causing the magnetic tension in the acceleration region. The simulation indicates that the current flowing eastward in the acceleration region comes from the dynamo in the bow shock. So, we call this current as the bow shock current. At the same time, the simulation indicates that the magnetic energy is transported from the bow shock. As a result, we find that the two magnetopauses correspond to two different current systems. Physical significance of the bow shock current is not so clear yet. In order to understand the significance, we need to investigate the global magnetic field configuration. This issue will be presented in the talk.

Hughes, W. J. (1995), in *Introduction to Space Physics*, pp. 227-287, ed. by M. Kivelson and C. T. Russell, Cambridge.

Paschmann, G., B. U. O. Sonnerup, I. Papamastorakis, N. Sckopke, G. Haerendel, S. J. Bame, J. R. Asbridge, J. T. Gosling, C. T. Russell, and R. C. Elphic (1979), *Nature*, 282, 243-246; doi:10.1038/282243a0.

地球磁気圏を X 線で可視化する GEO-X 衛星の検討現状

江副 祐一郎 [1]; 三好 由純 [2]; 笠原 慧 [3]; 木村 智樹 [4]; 石川 久美 [4]; 藤本 正樹 [5]; 山崎 敦 [6]; 長谷川 洋 [6]; 沼澤 正樹 [7]

[1] 首都大・理工・物理; [2] 名大 ISEE; [3] ISAS/JAXA; [4] 理研; [5] 宇宙研; [6] JAXA・宇宙研; [7] 首都大・理工・物理

GEO-X : Future Japanese Geospace X-ray Imager

Yuichiro Ezoe[1]; Yoshizumi Miyoshi[2]; Satoshi Kasahara[3]; Tomoki Kimura[4]; Kumi Ishikawa[4]; Masaki Fujimoto[5]; Atsushi Yamazaki[6]; Hiroshi Hasegawa[6]; Masaki Numazawa[7]

[1] Tokyo Metropolitan University; [2] ISEE, Nagoya Univ.; [3] ISAS/JAXA; [4] RIKEN; [5] ISAS, JAXA; [6] ISAS/JAXA; [7] Physics, Tokyo Metropolitan Univ.

We present the latest update and progress on the future Japanese X-ray micro satellite mission GEO-X (GEOspace X-ray imager). X-rays from the Earth's magnetosphere have

been established in X-ray astronomy observations (e.g., Snowden et al. 1994 ApJ, Ezoe et al. 2009 PASJ). GEO-X aims at demonstration of X-ray global imaging of the Earth's magnetosphere, especially structures of the dayside boundary such as cusps and magnetosheath. We have been sophisticating the design of the satellite and the instrument to achieve high spatial and time resolution imaging with a compact X-ray imaging spectrometer composed of micromachined light-weight X-ray telescope(s) and a high-speed semiconductor active pixel sensor. The results would have impacts on our understanding of how the solar wind interacts with the magnetosphere.

我々は高解像度、高時間分解能の磁気圏昼側境界面の撮像を目指す GEO-X 計画の検討を行っている。太陽風の酸素などの多価イオンは、ジオコロナと呼ばれる 10 地球半径以上に広がる地球の超高層大気の水素原子などと電荷交換反応を生じ、X 線輝線を放射することが分かってきた (Snowden et al. 1994 ApJ, Ezoe et al. 2009 PASJ など)。

これら地球周回の X 線天文衛星の観測や、MHD シミュレーションとジオコロナの空間分布を用いた理論予測によって、地球磁気圏の特に昼側境界面 (カスプやシース) は、イオン密度が高く、またジオコロナ密度も高いため、X 線が強く放射されると予想される。すなわち、X 線を用いることで昼側境界面に発生する Flux Transfer Event や、Kelvin Helmholtz 渦といった構造を可視化できる可能性がある。しかしながら、従来の X 線観測は地球周回の天文衛星の観測が中心であり、X 線放射の全貌はよく分かっていない。

我々は、太陽風と地球磁気圏の相互作用を知るために不可欠な昼側境界層の形状や変動を、高解像度 (~ 0.1 地球半径)、高時間分解能 (~ 1 時間以下) で像として捉える新しい GEO-X 計画の検討を進めて来た。従来の「その場」観測と相補的でありつつ、撮像によって低コストで磁気圏の全貌を知るための手段となりうる。サイエンスおよび装置の実証として、我々はまず 50-100kg クラスの超小型衛星を検討している。独自の超軽量 X 線望遠鏡とピクセル型半導体イメージャーを組み合わせ、視野直径 ~ 5 deg、角度分解能 9 分角以下、エネルギー 0.3-2 keV の実現を目指す。本講演では、計画の概要と現状について報告する。

オメガバンドオーロラの統計的特性

佐藤 夏雄 [1]; 行松 彰 [2]; 田中 良昌 [1]; 堀 智昭 [3]
[1] 極地研; [2] 国立極地研究所/総研大; [3] 名大 ISEE

Statistical signature of omega band auroras

Natsuo Sato[1]; Akira Sessai Yukimatu[2]; Yoshimasa Tanaka[1]; Tomoaki Hori[3]
[1] NIPR; [2] NIPR/SOKENDAI; [3] ISEE, Nagoya Univ.

We examined statistical characteristics of Omega band auroras using the THEMIS ground-based all-sky imager network data for 8 years from January 2007 to December 2014. We could pick up ~330 events of Omega band type auroras. In this study we examined statistical features for the following characteristics when Omega aurora observed: 1) Magnetic local time (MLT), 2) Seasonal and annual variations, 3) Duration and recurrence period of the aurora, 4) Drift speed of the aurora, 5) Kp, AE, and SYM-H dependence, 6) Solar wind speed and pressure, 7) IMF By and Bz dependence.

THEMIS 全天オーロラ画像ネットワークで観測されたデータを用いてオメガバンドオーロラの統計的な特性を調べた。データ期間は 2007 年 1 月から 2014 年 12 月までの 8 年間であり、その中から約 330 イベントを抽出した。そのイベントデータを用いてオメガバンドオーロラの発生に関して、下記の統計解析を行った。オメガバンドオーロラ発生時の 1) 地磁気地方時 (MLT)、2) 季節変化、3) 年変化、4) 観測点、5) Kp、6) AE、7) SYM-H。そして、太陽風パラメータとの比較として、8) IMF Bz、9) IMF By、10) 太陽風速度、11) 太陽風動圧。また、可視オーロラの画像解析から求めた、12) オメガオーロラのタイプ別発生頻度、13) オーロラのドリフト速度、14) オーロラの存続時間、15) 繰り返し出現間隔、などである。明らかになった顕著な特性としては、発生時間帯が主に 01-03 MLT であり、2 月と 3 月に多く、Kp 指数が 3~4、AE が 300~700nT、SYM-H がマイナス 10~40nT であった。IMF との関係では Bz がマイナスの時と By がプラスの時に、太陽風速度が 300~600km/sec の時に発生頻度が高かった。オーロラのドリフト速度は東向きに 300~500m/sec、視野内の存続時間が 15~25sec、そして、出現の繰り返し間隔が 10~30sec であるイベントが多かった。

フリッカリングオーロラの発生特性

福田 陽子 [1]; 片岡 龍峰 [2]; 内田 ヘルベルト陽仁 [3]; 三好 由純 [4]; 加藤 雄人 [5]; 塩川 和夫 [6]; 海老原 祐輔 [7]; Hampton Donald[8]; 岩上 直幹 [9]; 関 華奈子 [10]
[1] 東大・理・地惑; [2] 極地研; [3] 総研大; [4] 名大 ISEE; [5] 東北大・理・地球物理; [6] 名大宇地研; [7] 京大生存圏; [8] アラスカ大学フェアバンクス校; [9] なし; [10] 東大理・地球惑星科学専攻

Occurrence property of flickering aurora

Yoko Fukuda[1]; Ryuho Kataoka[2]; Herbert Akihito Uchida[3]; Yoshizumi Miyoshi[4]; Yuto Katoh[5]; Kazuo Shiokawa[6]; Yusuke Ebihara[7]; Donald Hampton[8]; Naomoto Iwagami[9]; Kanako Seki[10]
[1] Dept. Earth & Planet. Sci, Univ. Tokyo; [2] NIPR; [3] SOKENDAI; [4] ISEE, Nagoya Univ.; [5] Dept. Geophys., Grad. Sch. Sci., Tohoku Univ.; [6] ISEE, Nagoya Univ.; [7] RISH, Kyoto Univ.; [8] GI, Univ. of Alaska Fairbanks; [9] none; [10] Dept. Earth & Planetary Sci., Science, Univ. Tokyo

Flickering auroras typically appears within active and bright auroral arcs just prior to and during auroral breakup, and their typical frequencies are 3-15 Hz which correspond to oxygen ion cyclotron frequency at altitudes of 3000-10000 km. The flickering aurora has been considered to be generated by Landau resonance between electrons and electromagnetic ion cyclotron (EMIC) waves. The necessary condition of their appearance remains unsolved due to lack of continuous observations. We have conducted 50-320 fps sCMOS camera observations at Poker Flat Research Range, Alaska for more than 3 winter seasons to elucidate the occurrence property and to reconsider the generation mechanism.

We report statistical results of the correlations between the occurrence of the flickering aurora and magnitudes of AE index, non-flickering background auroral intensities, and microscale (1-10 km) flow speeds in the non-flickering background aurora, which appeared at the same time of the flickering aurora, based on 50 fps data obtained for the 2014 winter season. It is found that the flickering aurora was likely to occur in case of the high AE index and the bright background aurora with the fast microscale flow speeds. These results indicate that the occurrence of the flickering aurora is likely to be affected by the intense parallel potential drop of the auroral acceleration region because the EMIC waves are considered to be excited by the electron beams. In comparison with the background auroral intensity and the microscale flow speed, it is also found that the former largely contributed to generate the flickering aurora. We also report the first evidence of the fastest flickering of >60 Hz from new data obtained during the winter of 2015, which is possibly generated by the proton-band EMIC waves.

フリッカリングオーロラは、主にブレイクアップやその直前に、活発で明るいアークの中に出現する。その典型的な振動数は 3-15 Hz で、これは高度 3000-10000 km における酸素イオンのサイクロトロン振動数に相当することが知られている。フリッカリングオーロラを形成するメカニズムとして、電子と電磁イオンサイクロトロン (EMIC) 波によるランダウ共鳴が考えられているが、フリッカリングオーロラの発生に必要な条件は連続観測が不十分なために未解決のままである。これまで我々は、フリッカリングオーロラの出現特性を明らかにし、発生メカニズムを再考するために、アラスカ・ポーカーフラットで3年間以上、sCMOS カメラを用いた高速撮像 (50-320 fps) を行ってきた。

本研究では、2014 年度の冬に取得した 50 fps のデータを用いて、フリッカリングオーロラの発生と、AE インデックス、フリッカリングしていない背景オーロラの明るさやその内部のミクロスケール (1-10 km) のフロースピードの相関関係を統計的に調べた。その結果、AE インデックスが高く、明るい背景オーロラの内部でミクロスケールのフローが速いほど、フリッカリングオーロラが発生しやすい傾向があることが分かった。EMIC 波は電子ビームによって励起されると考えられるため、この結果は、フリッカリングオーロラの発生は強いオーロラ加速電場による影響を受けやすいことを示唆する。また、背景オーロラの明るさとミクロスケールのフローの速さを比較すると、背景オーロラの明るさの方がフリッカリングオーロラの発生頻度に寄与しているという事も分かった。さらに、発表では 2015 年度に観測した最新データの中から、プロトンバンド EMIC 波によって形成された可能性のある 60 Hz 以上の最速のフリッカリングオーロラについても報告する。

画像処理を用いたオーロラ特徴抽出に基づく自動解析手法の検討

吉浪 遼 [1]; 才田 聡子 [1]; 田中 良昌 [2]; 佐藤 由佳 [2]
[1] 北九州高専; [2] 極地研

Aurora automatic analysis based on aurora features extraction with image processing

Ryou Yoshinami[1]; Satoko Saita[1]; Yoshimasa Tanaka[2]; Yuka Sato[2]
[1] NITkit; [2] NIPR

In the recent years, owing to the resolution improvement of the all-sky camera images and the information transmission technology, the number of all-sky camera images for analysis of the auroral dynamics has increased explosively. Thus there is a need for technology which automatically analyzes the moving image and assists manual analysis of these images by using a computer. The automatically analysis enable us to verify a relevance between environmental conditions and Auroral phenomena by comparing various moving image data in the same conditions. Therefore, automatic determination of auroral shapes, movements, and changes in auroral forms can effectively select moving images under the same conditions for the analysis of auroral dynamics.

This study aims to provide a computer program for determination of aurora features using image processing.

To recognize objects and features in the image, we need some preprocessing to the image data and then extracting features. Currently, some research is conducting on feature representation to recognize, such as human and road signs using a technology such as HOG (Histograms of Oriented Gradients) feature, SIFT (Scale-Invariant Feature Transform) feature, and any more.

Research example of feature extraction using the SIFT feature for aurora exists but yet optimal feature extraction approach for automatic identification has not been established. Therefore, in this research to verify some of the feature extraction way to aurora and comparing the effect.

As a result, expression of aurora features with HOG features were found to be effective against a light aurora luminance value. In addition, it was found that the luminance value histogram can be expected to be applied to the aurora position and movement tracking. However, to use a luminance value histogram as a feature, it was also found that it is necessary to devise for region segmentation of an image of interest.

The results of creating background subtraction by the code book method, it was possible to clearly extract only Aurora region.

However, when extracting the Aurora by the background subtraction, it has also been found that it is necessary to devise, such as removing the aurora thin point.

In conclusion, the approach to some extent by extracting features of aurora, practicality expectations for a number of determination using that approaches.

However, there are issues corresponding to the above-stated approach, and we have to select appropriate preprocessings in accordance with the required types of aurora for proper use.

近年のオーロラ観測機器の精度の向上や情報通信技術の高度化によって膨大な量のオーロラ動画像データが生産されつつある。この現状に対し、コンピュータを用いて動画像を自動的に解析し、人間のオーロラ解析を演算速度によって補助する手法が必要である。解析を行う際、同一条件の複数の動画像データを比較することで、オーロラの条件と現象の関連性の検証が可能である。従って、オーロラの形状や移動、及びその変化を自動的に判別することで、同一条件の動画像を効率的に選択し、その解析へとスムーズに移行できる。

本研究ではこれをプログラムによって実現するため、画像処理技術を用いてオーロラ特徴を判定することを目的とする。

画像中の物体や特徴を認識するためには、その画像データに何らかの処理を行い、特徴を抽出することが必要である。

現在、人間や道路標識などを認識するための特徴表現として、HOG(Histograms of Oriented Gradients)特徴量やSIFT(Scale-Invariant Feature Transform)特徴量などの手法を用いて研究が行われている。オーロラについてもSIFT特徴量を用いた特徴抽出に関する研究例が存在するが、未だ自動識別のための最適な特徴抽出手法は確立していない。

そこで、本研究ではオーロラに対していくつかの特徴抽出手法を検証し、その効果を比較する。今回は、前述のHOG特徴量を用いた特徴抽出のほかに、輝度値ヒストグラムを用いた特徴抽出、コードブック法を用いた差分画像作成による特徴抽出をそれぞれ検証し、比較を行う。

その結果、HOG特徴量を用いたオーロラ特徴の表現は、輝度値の明るいオーロラに対して有効であることがわかった。また、輝度値ヒストグラムがオーロラの位置及びオーロラの移動追跡への応用が期待できることがわかった。しかし、輝度値ヒストグラムを特徴として用いるためには、対象となる画像の領域分割についての工夫が必要であることも明らかになった。そして、コードブック法によって背景差分を作成したところ、オーロラの領域のみを鮮明に抽出することができた。しかし、背景差分によってオーロラを抽出する際は、オーロラの薄い箇所を取り除くような工夫が必要となることも明らかになった。

以上のように、各手法はある程度オーロラの特徴を抽出し、それを用いたいくつかの判定への実用性が期待できる。

しかし、それぞれの手法に対応すべき問題点が存在し、対象となるオーロラに応じた使い分けや前処理などの工夫が必要である。

多点イメージャとEISCATレーダーで得られたオーロラ放射及び電子密度プロファイルの定量的比較

田中 良昌 [1]; 小川 泰信 [1]; 門倉 昭 [1]; 宮岡 宏 [1]
[1] 極地研

Quantitative comparison of auroral emission and electron density profiles obtained by multiple imagers and the EISCAT radar

Yoshimasa Tanaka[1]; Yasunobu Ogawa[1]; Akira Kadokura[1]; Hiroshi Miyaoka[1]
[1] NIPR

We have studied the magnetosphere - ionosphere coupling process in the auroral region by using data obtained from ground-based optical, radar, and magnetic measurements. We analyzed monochromatic (427.8nm) images taken at a sampling interval of 10 seconds simultaneously at seven stations in Northern Europe and the ionospheric data along the magnetic zenith obtained by the EISCAT UHF radar at Tromso, Norway, during 22-24 UT on March 14, 2015. During this interval, wave/vortex structures along discrete arcs were observed and followed by auroral breakup, poleward expansion, and pulsating auroras.

For some auroral wave/vortex events, we applied the tomographic inversion technique to the auroral images to reconstruct 3D distribution of the 427.8nm emission and quantitatively compared it with height profile of the ionospheric electron density observed by the EISCAT radar. The results indicated that the height profiles are very similar between the 427.8nm emission and the electron density. In addition, the electron density profiles estimated from the auroral images by modeling the auroral emission and ionization processes due to the electron precipitation were smaller than the actually-observed one by a factor of about 2. Such a small difference of the electron density obtained by two methods indicates that the auroral tomography analysis is promising to derive the spatial distribution of the ionospheric electron density and conductivity. In the presentation, we will further show results from statistical analysis and the generalized auroral tomography method, which combines both the imager and radar data for the 3D reconstruction.

サブストーム開始前の磁気圏尾部および地上における Pi2 脈動の THEMIS による事例研究

宮下 幸長 [1]; Angelopoulos Vassilis[2]; 平木 康隆 [3]; 家田 章正 [4]; 町田 忍 [5]
[1] 名大 ISEE; [2] UCLA; [3] 電通大; [4] 名大宇宙地球研; [5] 名大・ISEE

A THEMIS case study of Pi2 pulsations in the magnetotail and on the ground before a substorm onset

Yukinaga Miyashita[1]; Vassilis Angelopoulos[2]; Yasutaka Hiraki[3]; Akimasa Ieda[4]; Shinobu Machida[5]
[1] ISEE, Nagoya Univ.; [2] UCLA; [3] UEC; [4] ISEE, Nagoya Univ.; [5] ISEE, Nagoya Univ.

Using THEMIS spacecraft and ground data, we studied low-frequency Pi2 pulsations in the magnetotail and on the ground just before a substorm onset. A case study shows that a new compressional Pi2 pulsation was observed in the plasma sheet just earthward of the near-Earth reconnection site 4 min before initial auroral brightening or 2 min before auroral fading. The ion and magnetic pressure perturbations appeared to be partly in phase at the beginning, indicating that the wave had fast mode. A similar wave was observed also tailward of the near-Earth reconnection site, although it occurred 4 min later. These waves may have been generated at the near-Earth reconnection site. On the ground, Pi2 pulsations were observed widely in the polar cap and at the auroral oval before initial auroral brightening and auroral fading, although the amplitudes were small, compared to those associated with auroral poleward expansion. There was a tendency that the waves were observed first in the polar cap near the initial auroral brightening site and then in the surrounding regions. Ionospheric convection began to be enhanced gradually 1 or 2 min after the Pi2 onsets. We discuss the causal relationship between the Pi2 pulsations in the magnetotail and on the ground as well as their role in substorm triggering.

Poleward boundary intensification に伴う Pi2 型地磁気脈動の地上-衛星連携観測

今城 峻 [1]; 西村 幸敏 [2]; 吉川 顕正 [3]; 魚住 禎司 [4]; Ohtani Shinichi[5]; 中溝 葵 [6]; Angelopoulos Vassilis[7]; Mende Stephen[8]; MAGDAS/CPMN グループ 吉川 顕正 [9]
[1] 九大・理・地惑; [2] カリフォルニア大学ロサンゼルス校; [3] なし; [4] 九大・イクセイ; [5] なし; [6] NICT; [7] UCLA; [8] カリフォルニア大・パークレー; [9] -

Satellite-ground coordinated observations of Pi2 pulsations associated with poleward boundary intensification

Shun Imajo[1]; Yukitoshi Nishimura[2]; Akimasa Yoshikawa[3]; Teiji Uozumi[4]; Shinichi Ohtani[5]; Aoi Nakamizo[6]; Vassilis Angelopoulos[7]; Stephen Mende[8]; Akimasa Yoshikawa MAGDAS/CPMN Group[9]
[1] Earth and Planetary Sci., Kyushu Univ.; [2] UCLA; [3] ICSWSE/Kyushu Univ.; [4] ICSWSE, Kyushu Univ.; [5] The Johns Hopkins University Applied Physics Laboratory; [6] NICT; [7] UCLA; [8] UCB; [9] -

Pi2 pulsations are irregular geomagnetic oscillations that occur with various auroral phenomena, such as substorms, pseudo breakups, and poleward boundary intensifications (PBI). Pi2s are believed to be generated by plasmaspheric resonances and/or oscillations of bursty bulk flows that involve oscillating substorm current wedge (SCW). SCW oscillations are often associated with middle-latitude and auroral region Pi2, but it is not clear whether the substorm current system (DC current component) is necessary for the generation of the oscillating current system. The purpose of this study is to determine if a Pi2-related oscillating current system associated with PBI can occur in an absence of a significant CD component current system. We examined spatial and temporal relations between PBI aurora, which corresponds to an upward field-aligned current, observed by the THEMIS all-sky imagers and Pi2 magnetic oscillations observed globally by ground-based magnetometers and satellites.

We found several cases where east-west elongated auroral arcs quasi-periodically intensified near the brightest region of PBI, and each emission propagated both eastward and westward, corresponding to each Pi2 pulse. We focus on two consecutive Pi2 events associated with quasiperiodic PBI auroras around 2013-02-06 07:00 UT. In these events, Z-component magnetic field oscillations reversed with respect to the PBI latitude (GMLat. ~ 72 degrees), indicating that oscillating auroral electrojet drives Pi2s near the PBI. Spatial distribution of horizontal magnetic field in the nightside region lower latitude than PBI latitude is consistent with ground magnetic field produced by oscillating upward and downward FACs located near the PBI location, and the magnetic field did not show substantial positive or negative bays. These observations suggest that a wedge-shaped oscillating current system was generated by PBI-related phenomena without a substorm DC current system. Dayside Pi2s showed a very similar waveform to nightside Pi2 and an amplitude enhancement at the magnetic equator, indicating that dayside ionospheric current was driven by electric field transmitted from the oscillating FAC almost instantaneously. The RBSP-B satellite at $\sim 3R_E$ radial distance observed Pi2s with a similar waveform to ground Pi2 with no significant time delay. On the other hand, RBSP-A at $\sim 6R_E$ radial distance observed a Pi2 that preceded ground Pi2 onset by ~ 45 s, and its waveform was somewhat different from ground Pi2. The delay time is almost of the same order as the travel time of fast mode waves from the satellite to the ground, and the reason for a different waveform may be some resonance process or a localized disturbance.

Ground-based observations suggest that PBI-related phenomena without a substorm DC current system can be a cause of a wedge-shaped oscillating current system. We will investigate whether the resonance features of Pi2s in the magnetosphere can be coexistent with such an oscillating current system or not, using relation of electric and magnetic fields observed by the THEMIS satellites.

サブストームオンセットの詳細構造：CWの誤り

田中 高史 [1]
[1] 九大・宙空センター

Reproduction of detailed signatures of the onset from the high-resolution global simulation

Takashi Tanaka[1]
[1] SERC, Kyushu Univ.

We have developed a global simulation code with very high resolution. The substorm solution that is calculated from this simulation code can reproduce the detailed features of the substorm onset in the ionosphere. It can reproduce the onset that starts from the equatorward side of the oval, and the westward traveling surge (WTS) that starts two minutes after the onset, in the same way as observations. Then, we investigated magnetospheric structure corresponding to each variation in the ionosphere. The onset is caused by the near-earth dynamo. The near-earth dynamo is driven by the pressure increase due to the squeezing, combined with equatorward field-perpendicular flow due to the effect of the near earth neutral line (NENL). Pressure increase is caused by the effect of field-parallel flow. The onset starts before the arrival of flow from the NENL to the equatorial plane of the inner magnetosphere. Flow reach two minutes after the onset, when it is around the start timing of the WTS. The expansion phase is further developed by the arrival of flow. Looking at the result that the solution of the near-earth dynamo very realistically reproduces the details of the onset signature in the ionosphere, we cannot avoid to conclude that the current wedge (CW) is a misleading concept.

解像度の極めて高いグローバルシミュレーションを開発した。これにより計算したサブストームシミュレーションの解は、電離圏でサブストームオンセットの詳細を再現する。オーバルの赤道側から始まるオンセット、その2分後に始まる westward traveling surge (WTS) などを、観測と同じように再現できる。次に、電離圏の各変動に対応する磁気圏変動を明らかにした。オンセットは地球近傍ダイナモにより起こる。地球近傍ダイナモは、squeezing による圧力上昇と、near earth neutral line (NENL) の影響による南北方向の磁場垂直流により、駆動される。圧力上昇は沿磁力線フローの効果である。オンセット開始は、NENL からのフローが、内部磁気圏の赤道面に到達する前である。フローが到達するのは、オンセットから2分後、WTS が開始するところである。これによって拡大相がさらに発展する。地球近傍ダイナモの解がオンセットの詳細を極めて忠実に再現することを見れば、current wedge (CW) は誤りであると結論せざるを得ない。

THEMIS データによるサブストームと疑似サブストームに伴う磁気圏尾部変動の統計解析

福井 健人 [1]; 町田 忍 [2]; 宮下 幸長 [1]; 家田 章正 [3]; 三好 由純 [1]; Angelopoulos Vassilis[4]
[1] 名大 ISEE; [2] 名大・ISEE; [3] 名大宇宙地球研; [4] UCLA

A THEMIS statistical study of near-Earth magnetotail changes during substorms and pseudosubstorms

Kento Fukui[1]; Shinobu Machida[2]; Yukinaga Miyashita[1]; Akimasa Ieda[3]; Yoshizumi Miyoshi[1]; Vassilis Angelopoulos[4]
[1] ISEE, Nagoya Univ.; [2] ISEE, Nagoya Univ.; [3] ISEE, Nagoya Univ.; [4] UCLA

Substorms and pseudosubstorms (pseudobreakups) are very similar phenomena. In terms of auroral morphology, pseudosubstorms are generally more localized and more short-lived, compared with substorms, and are not accompanied by poleward expansion. We examined auroral development for events from November 2007 through April 2010, using data from THEMIS all-sky imagers. We defined events accompanied and not accompanied by poleward expansion as substorms and pseudosubstorms, respectively. To understand the cause of auroral development, we investigated temporal and spatial development of the near-Earth magnetotail during substorms and pseudosubstorms, based on superposed epoch analysis of THEMIS data. We find that B_z begins to increase at $-9.5 > X(\text{GSM}) > -11.5 \text{ Re}$ around onset for both substorms and pseudosubstorms. The amount and rate of B_z change are larger for substorms than for pseudosubstorms. In the earthward ($-7.5 > X > -9.5 \text{ Re}$) and tailward ($-11.5 > X > -15.5 \text{ Re}$) regions, B_z increases substantially for substorms, whereas it does not increase very much for pseudosubstorms. These results indicate that dipolarization is weaker for pseudosubstorms than for substorms, and the dipolarization region does not spread extensively for pseudosubstorms. We, therefore, suggest that current disruption related to dipolarization does not develop tailward and hence auroral poleward expansion does not occur for pseudosubstorms. Meanwhile, the plasma and magnetic pressures increase at $-6.5 > X > -7.5 \text{ Re}$ after onset in association with dipolarization, particularly for substorms. The total pressure (the sum of the plasma and magnetic pressures) prior to the onset is about 1.3 times larger there for substorms than for pseudosubstorms. At $-7.5 > X > -9.5 \text{ Re}$ the total pressure hardly differ between substorms and pseudosubstorms. Thus we conclude that the spatial gradient of the total pressure is a factor that determines whether the current disruption region develops tailward, that is, whether initial activation develops into a substorm or subsides into a pseudosubstorm.

サブストームと疑似サブストーム (疑似ブレイクアップ) はともによく似た現象である。オーロラの発生という観点において、一般に後者は前者と比べ小規模で継続時間が短く、極方向の拡大 (Poleward expansion) がないものを指す。本研究では 2007 年 11 月から 2010 年 4 月までのイベントについて、THEMIS の全天カメラのデータから極方向の拡大の有無を調べ、極方向の拡大が見られたものをサブストーム、見られなかったものを疑似サブストームとした。サブストームと疑似サブストームの発達の違いの要因の手掛かりを得るため、それぞれについて THEMIS 衛星データを用いて、オンセット前後の磁気圏尾部プラズマシートにおけるプラズマ速度、磁場、圧力の時間変化を時間重畳法 (Superposed Epoch Analysis) により調べた。その結果、 $-9.5 > X(\text{GSM}) > -11.5 \text{ Re}$ の領域ではサブストーム、疑似サブストームともにオンセット付近で B_z の増大がみられ、サブストームの方が変化量と変化率が大きかった。それよりも地球側 ($-7.5 > X > -9.5 \text{ Re}$) と尾部側 ($-11.5 > X > -15.5 \text{ Re}$) の領域では、疑似サブストームでは B_z はあまり変化しなかった。このことから、疑似ブレイクアップではサブストームに比べ磁気双極子化の度合いが弱く、また広範囲で起こらないことが示唆される。つまり、磁気双極子化に伴う Current Disruption が尾部方向に発展せず、オーロラの極方向の拡大が発生しないと考えられる。一方、圧力について、 $-6.5 > X > -7.5 \text{ Re}$ の領域では、プラズマ圧と磁気圧がともにオンセット後に磁気双極子化に伴って増大し、特にサブストームの場合にその傾向が著しかった。また、サブストームの場合は、オンセット前の磁気圧とプラズマ圧の和 (全圧) が疑似ブレイクアップの場合に比べて、およそ 1.3 倍であった。 $-7.5 > X > -9.5 \text{ Re}$ においてサブストームと疑似サブストームでほとんど全圧に差がないことを考え合わせると、 -8 Re 付近での圧力の空間勾配の大きさが Current Disruption 領域が尾部方向に広がる要因、すなわちサブストームに発展するか、疑似サブストームに留まるかを決定する要因であることが結論付けられる。

Solar wind-substorm intensity connection revisited

Akira Morioka[1]; Yoshizumi Miyoshi[2]; Masahito Nose[3]

[1] PPARC, Tohoku Univ.; [2] ISEE, Nagoya Univ.; [3] DACGSM, Kyoto Univ.

While the intensity distribution of substorms is an essential issue in space physics, it had not been studied due to difficulties in identifying every substorm for a long period with reliable and definite criteria. In 2016, we made a database of substorm onsets and intensities for 10 years from 2005 to 2014 using the favorable wave and planetary (Wp) index to identify almost all of the substorm onset events and AL index for substorm intensity determination. Then, the distribution of substorm intensity ($|AL|$ index at substorm) was statistically studied. The results showed that substorm intensities consist of two groups with log-normal distribution: small substorms termed group-S substorms with an intensity peak around 100 nT and larger substorms termed group-L substorms with an intensity peak around 250 nT (Morioka et al., JpGU Meeting 2016). In this presentation, we revisit a problem, what determines the intensity of substorms. Our statistical study showed that the empirical magnetopause distance r_0 is highly correlated with the intensities of group-L and storm-time substorms, as well as the solar wind electric field E_m . Both the solar wind pressure (P_d and P_m) and erosion of the earth's magnetic field by IMF B_z constrain the magnetosphere, determine the magnetopause location, and compress the plasma sheet. Thus, r_0 can reflect the tail current intensity. Under these considerations, we statistically re-examine the relationship of r_0 and E_m with the substorm intensity to discuss the problem what determines the substorm intensity.

オーロラ爆発の衛星画像と全天画像による同時観測

家田 章正 [1]; 西村 幸敏 [2]; 宮下 幸長 [3]; 町田 忍 [4]; 川嶋 貴大 [1]; 三浦 翼 [3]
[1] 名大宇宙地球研; [2] カリフォルニア大学ロサンゼルス校; [3] 名大 ISEE; [4] 名大・ISEE

Auroral substorm onset in satellite global images and all-sky images

Akimasa Ieda[1]; Yukitoshi Nishimura[2]; Yukinaga Miyashita[3]; Shinobu Machida[4]; Takahiro Kawashima[1]; Tsubasa Miura[3]

[1] ISEE, Nagoya Univ.; [2] UCLA; [3] ISEE, Nagoya Univ.; [4] ISEE, Nagoya Univ.

Optical substorm onset signatures in Polar satellite global images and ground all-sky images in Finland were compared. Substorm onset has been identified using ground all-sky images to have two stages (initial brightening and auroral breakup), which are separated by a few minutes. In contrast, such two stages are usually unclear in satellite global images, presumably due to limited temporal and spatial resolutions of observations.

In this study, we used high time resolution (37 seconds) ultraviolet (170 nm) global images taken by the Polar satellite. The 20-second resolution green line (557 nm) all-sky images in Finland were also used. We first identified an auroral breakup in global images and then searched for substorm onset signatures in all-sky images. As a result, the auroral breakup was observed simultaneously within a minute between global and all-sky images. In contrast, the initial brightening was not observed in global images but in all-sky images two minutes before the breakup. This result implies that the substorm onset identified in global images can be delayed from the Akasofu-type substorm onset by a few minutes, possibly when the initial brightening is relatively faint.

オーロラサブストームの開始過程を明らかにするために、衛星グローバル画像と、地上全天画像を比較した。全天画像でのサブストームの開始（オンセット）は、経度方向に長い「initial brightening」と、その数分後に始まる、極側に拡大する「オーロラ爆発」との二つのステージを持つと考えられている。一方、衛星グローバル画像では、時空間分解能の制限のために、両者を区別することは通常困難である。このために、これまで衛星画像で同定されてきたオンセットと、二つのステージとの関係は不明瞭であった。

本研究では、Polar 衛星がフィルタを固定した高時間分解観測（37 秒毎）を行っていた期間を調べることで、衛星画像と全天画像の比較を行った。全天画像は、20 秒毎のフィンランドにおけるグリーンライン観測を用いた。事例解析の結果、オーロラ爆発は衛星画像と全天画像で同時に観測されていたが、その 2 分前に開始した initial brightening は全天画像でのみ観測されていた。本研究では高時間分解の衛星画像を用いたため、衛星画像で initial brightening が観測されなかった原因は空間分解能にあると考えられる。

サブストーム拡大相オンセットの力学

海老原 祐輔 [1]; 田中 高史 [2]
[1] 京大生存圏; [2] 九大・宙空センター

Mechanics of substorm expansion onset: An update

Yusuke Ebihara[1]; Takashi Tanaka[2]
[1] RISH, Kyoto Univ.; [2] SERC, Kyushu Univ.

Auroral breakup is a long-standing unsolved issue in the magnetospheric physics, despite many theories and models have been developed. Abrupt intensification of upward field-aligned current (FAC) is central to this issue because the upward FAC is responsible for accelerating electrons downward and emitting bright aurora. The purpose of this presentation is to update and refine the mechanisms that were suggested by Ebihara and Tanaka [2015, JGR, doi:10.1002/2015JA021516] by reanalyzing the result of the global magnetohydrodynamics (MHD) simulation. We obtained the following results: (1) When a near-Earth neutral line (NENL) forms, plasma originating in the lobe starts to be accelerated toward the equatorial plane. The plasma within 10 R_e then traverses the separatrix, or a last-closed field line at off-equator, and enters the inner magnetosphere. (2) Near the separatrix, magnetic field is intensified by perpendicular motion of plasma (compression and advection), resulting in the intensification of the Lorentz force pointing toward the equatorial plane. (3) Successively, the trajectory of plasma turns to the east and west directions by pressure gradient force associated with field-aligned pressure increase by compression. (4) The directional change of the flow at off-equator generates (matches with) the upward FAC that is responsible to auroral breakup. In short, the abrupt intensification of upward FAC is a result of the formation of the NENL and the subsequent magnetospheric reconfiguration that takes place three-dimensionally. In the course of the three-dimensional reconfiguration, the changes in the magnetic field and the plasma pressure result in turning of plasma motion that generates onset-associated upward FAC. The most important and relevant flow of plasma lies at off-equator.

Moving Transpolar Arc 消失時に発生するオーロラオーバルの部分的増光

小原 隆博 [1]

[1] 東北大・惑星プラズマセンター

Disappearance of moving transpolar arc and its relation to the intensification of oval activity

Takahiro Obara[1]

[1] PPARC, Tohoku University

In the northern polar cap region, the transpolar arc was detached from the morning (evening) side oval and moves dusk ward (dawn ward), corresponding to IMF B_y change from negative to positive (positive to negative) during northward IMF condition. In the past work by Obara et al. (1988), it was demonstrated that oval intensification has been taking place when the transpolar arc was diminishing its intensity.

Based on the IMAGE FUV data, we have examined the location of intensification in the night side oval. Though the number of moving transpolar arcs was small, it seems likely that the intensification of the night side oval occurs dusk ward (dawn ward) of the transpolar arc with respect to local time during positive IMF B_y (negative IMF B_y) condition in the northern hemisphere.

Tanaka et al. (2004) demonstrated that a movement of transpolar arc is caused by the growth of new merging cell. Open field lines in the new merging cell in the polar cap may reconnect, and newly formed closed lines result in the blocking of the return path of closed field lines generated in the old merging cell. Losing their return path, closed field lines which have been generated in the old merging cell accumulate on the night side, resulting in the transpolar arc.

Merging of field lines in the new merging cell in the night side could accumulate magnetic fluxes. Some changes of IMF B_z polarity; positive to negative for instance, could trigger oval intensification.

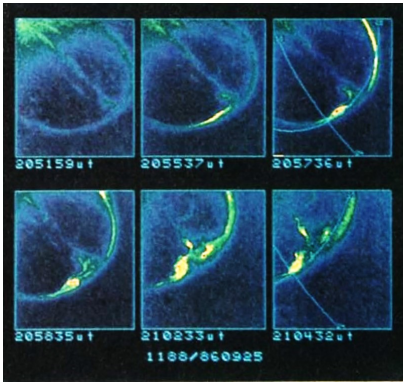
In the presentation, we like to demonstrate the examples of the events and will discuss the location of the oval intensification with respect to the transpolar arc location and consider the onset of the oval intensification.

北向き IMF 時に於いて、IMF B_y の polarity の反転によって、アークがオーロラオーバルから分離し、極冠域に張り出して行く事が、多くの論文によって指摘されている。IMF B_y の反転は、Transpolar Arc が生成される一つの原因と考えられているが、小原他 (GRL,1988) では、移動している Arc が消失する少し前のタイミングから、Transpolar Arc の付け根付近のオーバルが増光する事例が紹介されている。

IMAGE 衛星のデータの中に、数十例の Transpolar Arc が識別されたが、その中の数例が朝夕方向に移動していた。この Transpolar Arc の動きは IMF B_y の変化と関係しており、北半球における観測では、IMF B_y がプラスになると夕方側に向かって動き、IMF B_y がマイナスになると朝側に向かって移動していた。そして、その後、暫くして、夜側のオーバルの一部に増光が見られたが、増光は、アークの運動の向きにかかわらず、移動方向の後方のオーバルで起こっていた。

田中他 (2004) による Transpolar Arc の MHD シミュレーションでは、IMF B_y の反転がプラズマシートの傾斜を逆転させ、その結果、プラズマシートの折れ曲がり構造が作られた。そして、この過程で、昼夜を結ぶ子午面に対して、古いマーキング領域と反対側に出来た新しいマーキング領域で、開いた磁力線が新しく生成され、これら磁力線は新しいマーキングセルを形成するべく、極冠域に侵入して行く。古いマーキングセルの夜側にあるオーバルの領域では、両半球から移動して来た開いた磁力線がマーキングを起こし閉じた磁力線になる。古いマーキングセルのオーバル領域に作られた閉じた磁力線は、通常であれば、昼側に戻って行くが、新しいマーキングセルで新たに生成された閉じた磁力線によって、昼側に戻る運動が阻止される。これは、新マーキングセルのオーバル領域で作られた閉じた磁力線は、古いセルの閉じた磁力線と逆方向に進む事が、求められているからである。そして、行き場を失いオーバルに蓄積された閉じた磁力線群は、オーバルからはみ出す形で、高緯度の極冠域に進出して行き、Transpolar Arc が形成されるとしている。

新しいマーキングセルでは、継続して閉じた磁力線が生成されている。これは、プラズマシートにプラズマとエネルギーが供給され続けていると捉える事が出来る。そして、IMF B_z が南向きに転じると、昼側磁気圏から更に多くの磁気フラックスが極冠域を経由し、プラズマシートに供給され、程なく、サブストームを発生させる事になる。IMAGE 衛星が見たオーロラオーバルの増光は、以上のシナリオで説明できそうである。



未解決の問題・新しい課題

西田 篤弘 [1]
[1] 宇宙研

Unsolved Issues and New Challenges

Atsuhiko Nishida[1]
[1] ISAS

- (1) Connecting magnetic fields between IMF flux ropes and their solar sources
- (2) Role of non-linear process in auroral breakup
- (3) Thermodynamics of the radiation belt
- (4) Origin of the Magnetospheric Period Oscillation on Saturn
- (5) Generation mechanism of MSTID in high latitudes

磁気圏の活動は IMF の極性に強く依存しているから、IMF 極性を太陽表面の磁場構造と結びつけることは宇宙空間天気予報の重要な要素である。擾乱源として特に重要な CME の場合、観測される IMF は太陽面活動域の arcade 状磁力線が引き延ばされて形成される flux rope の構造と多くの場合に一致する (Marubashi et al., 2015)。しかし、太陽面磁場の構造がより複雑である場合には、CME の伝搬方向がかならずしも radial ではないとか、CME が発生後に周辺からの影響で変形するとか、更に長時間のスケールでは背景をなす磁場構造が変化する (Bisoi et al., 2016) ことも考えられ、これらの状況における IMF の予測は今後の課題である。

(2) オーロラ・ブレイクアップにおける非線形過程の役割

サブストームは、「太陽風のエネルギーが昼側磁気圏境界面におけるリコネクションによって磁気圏尾部に流入し、蓄積される」 Growth phase から、「このエネルギーが尾部の磁気中性面に発生するリコネクションによって解放される」 Expansion phase へと進行する。この過程は確立されているが、オーロラで Expansion phase の開始を告げるものとされる Breakup のメカニズムについてはまだ謎が残されている。南北共役点における発生時間が必ずしも同時でないことから見て、Breakup は尾部と夜側の磁気圏で進行する大規模なプロセスそのものではなく、そのプロセスの中で局所的に発生する非線形的なプロセスに起因しているのではないだろうか (Sato et al., 1998; Morioka et al., 2013)。その場合には沿磁力線電流と電離層のカプリングが重要であろう。また、Breakup のエネルギーが供給されるのは尾部からではなく、昼間のカスプ領域からである、という simulation 結果 (Ebihara and Tanaka, 2015) も考慮する必要がある。

(3) 放射線帯の熱力学

放射線帯電子の加速機構として、keV 域の電子から発生する波動が一部の電子を共鳴的に加速して MeV 域に押し上げる、という機構 (Omura et al., 2007) が有力視されている。電子のエネルギーが自動的に高まるという過程は、一見、熱力学第 2 法則に抵触するようである。しかし、Debye sphere 内の全粒子が電場によって結ばれているとか、波動粒子相互作用の際には共鳴粒子が集団的に振る舞うという性格を持つプラズマにおいては、エントロピーが Gibbs-Boltzmann の古典的な定義によるものではなく、多項式で表現されるという理論が提起されている (Tsallis, 1988; Livadiotis and McComas, 2009)。高エネルギー電子の速度分布関数は冪型になるということである。放射線帯電子の観測データにこの理論を適用し、熱力学的な裏付けを確認することが望ましい。

(4) 土星磁気圏内に発生する准双極子磁場 (Magnetospheric Period Oscillation) の起源

土星の磁気圏には大規模な電流系が存在し、自転軸 (= 主磁場の磁軸) と直交する磁気双極子を作っている (Andrews et al., 2010)。この電流系は南半球と北半球のそれぞれにあり、回転周期が異なる、磁気圏の形状にも影響を及ぼす、などの形態は明らかにされているものの、成因についての研究は未だ乏しい。高緯度の熱圏大気中に渦運動があり、そのダイナモ作用によって発生する電流に起因するという説 (Jia et al., 2012) は興味深い。渦の発生機構をはじめ基本的な点が説明されていない。このような准双極子磁場は地球・水星はもとより木星磁気圏でも知られておらず、極めて興味深い現象である。

(5) 中規模伝搬性電離層擾乱 (MSTID) の発生機構

MSTID の伝搬は詳細に調べられているが、高緯度における発生機構に関する研究論文は意外に少ない。大気の擾乱に起因するのか、あるいはオーロラとその関連現象によって励起されるのか。最近の論文 (Frissell et al., 2016) によれば MSTID の観測頻度は成層圏大気の極渦が強い時期に高く、極渦が弱まる (同心円状の流線が崩れる) と低下する。より直接的には、周極風が東向き of 時期に高く西向き of 時期に低い。この事実は発生条件そのものであるのか、あるいは大気重力波の成層圏から電離圏への伝搬条件を表すのか。基本的な課題が残されている。

地上多点ネットワーク観測による内部磁気圏の粒子・波動の変動メカニズムの研究：PWINGプロジェクト

塩川 和夫 [1]; 大塚 雄一 [1]; 大山 伸一郎 [2]; 三好 由純 [3]; 西谷 望 [3]; 尾崎 光紀 [4]; 片岡 龍峰 [5]; 能勢 正仁 [6]; 関 華奈子 [7]; 篠原 育 [8]; 長妻 努 [9]; 田中 良昌 [5]; 坂野 井 健 [10]; 土屋 史紀 [11]; 尾花 由紀 [12]; 鈴木 臣 [13]
 [1] 名大宇地研; [2] 名大・宇地研; [3] 名大 ISEE; [4] 金沢大・理工・電情; [5] 極地研; [6] 京大・理 地磁気センター; [7] 東大理・地球惑星科学専攻; [8] 宇宙研/宇宙機構; [9] NICT; [10] 東北大・理; [11] 東北大・理・惑星プラズマ大気; [12] 大阪電通大・工・基礎理工; [13] 愛知大学

Study of dynamical variation of particles and waves in the inner magnetosphere using ground-based network - PWING Project

Kazuo Shiokawa[1]; Yuichi Otsuka[1]; Shin-ichiro Oyama[2]; Yoshizumi Miyoshi[3]; Nozomu Nishitani[3]; Mitsunori Ozaki[4]; Ryuho Kataoka[5]; Masahito Nose[6]; Kanako Seki[7]; Iku Shinohara[8]; Tsutomu Nagatsuma[9]; Yoshimasa Tanaka[5]; Takeshi Sakanoi[10]; Fuminori Tsuchiya[11]; Yuki Obana[12]; Shin Suzuki[13]
 [1] ISEE, Nagoya Univ.; [2] ISEE, Nagoya Univ.; [3] ISEE, Nagoya Univ.; [4] Electrical and Computer Eng., Kanazawa Univ.; [5] NIPR; [6] DACGSM, Kyoto Univ.; [7] Dept. Earth & Planetary Sci., Science, Univ. Tokyo; [8] ISAS/JAXA; [9] NICT; [10] Grad. School of Science, Tohoku Univ.; [11] Planet. Plasma Atmos. Res. Cent., Tohoku Univ.; [12] Engineering Science, Osaka Electro-Communication Univ.; [13] Aichi Univ.

http://www.isee.nagoya-u.ac.jp/dimr/PWING/PWING_web.j.htm

Dynamical variation of particles and waves in the inner magnetosphere is one of the most important research topics in recent space physics. The inner magnetosphere contains plasmas in wide energy ranges from below electron volts to Mega-electron volts. These plasmas (electrons and ions) interact with ULF/ELF/VLF waves at frequencies of 0.1 Hz to 10 kHz to cause their energization in the equatorial plane of the magnetosphere and loss into the ionosphere. In order to provide global distribution and quantitative evaluation of the dynamical variation of plasmas and waves in the inner magnetosphere, we have started PWING Project (study of dynamical variation of Particles and Waves in the INner magnetosphere using Ground-based network observations, http://www.isee.nagoya-u.ac.jp/dimr/PWING/PWING_web.e.htm), which will last for 5 years from April 2016, as a Grant-in-Aid for Specially Promoted Research of the Japan Society for the Promotion of Science (JSPS).

In the PWING project, we plan to construct a longitudinal observation network at 8 ground-based stations at subauroral latitudes (magnetic latitudes: ~60 degree) to monitor 2-dimensional images of particle precipitation and ULF/ELF/VLF waves at frequencies from 0.1Hz to 10 kHz. We combine these longitudinal network observations with the ERG satellite, which will be launched in fiscal year 2016, and global modeling. Using these comprehensive observations and modeling, we provide global distribution and quantitative evaluation of the dynamical variation of plasmas and waves in the inner magnetosphere at $L \sim 4$ Re near the plasmapause.

The MeV-energy electrons in the inner magnetosphere forms the radiation belts around the Earth, which are continuous thread for space vehicles and human bodies in space. The outcome from the PWING Project will increase the accuracy of forecasting the variations of radiation belt particles in the inner magnetosphere and contribute to the safe operation of human activities in space. The results of the PWING Project are applicable to any astronomical bodies which have dipole magnetic field and atmosphere, and will increase the basic understanding of physical processes on the energization and loss of plasmas in space.

地球周辺の宇宙空間のうち、特に地球半径の4倍付近を中心とした内部磁気圏は、磁気圏の最高エネルギーであるMeVエネルギーのプラズマで構成される放射線帯から、1eV以下の低エネルギーのプラズマで構成されるプラズマ圏まで、6桁以上の広いエネルギー範囲のプラズマ粒子(電子・イオン)が混在し、周波数が0.1Hz - 10kHzのULF/ELF/VLF帯の電磁波動と相互作用しながら、粒子の加速・消失が起きている興味深い領域である。内部磁気圏では、地球磁場の勾配と曲率のために、プラズマ粒子は数十分から数時間の周期で地球周辺を経度方向に回りながら加速・消失していく。このため、特定の経度だけに偏在する変動場を地球規模でグローバルに把握していくことが、粒子・電磁場変動の定量的な理解には必須である。私たちは、2016-2020年に日本学術振興会の科学研究費補助金(特別推進研究)として、PWINGプロジェクト「地上多点ネットワーク観測による内部磁気圏の粒子・波動の変動メカニズムの研究」(http://www.isee.nagoya-u.ac.jp/dimr/PWING/PWING_web.j.htm)を開始した。本プロジェクトでは、この内部磁気圏におけるプラズマ粒子と電磁波動の変動過程をグローバルに把握するとともに、その変動機構を定量的に明らかにすることを目的としている。

このために、本研究では、磁気緯度(地磁気の極を90度とした緯度)で60度付近の緯度帯(サブオーロラ帯)に、北半球で地球を一周するように経度方向に8カ所の観測点を国際協力によって開設し、地球周辺の宇宙空間で地球のまわりを経度方向に周回しているプラズマ粒子の地球大気への降り込みや、これと相互作用する周波数が0.1Hz-10kHzの電磁波動を観測する。これらの観測を、新しい人工衛星による宇宙空間での粒子・波動の直接観測や波動粒子相互作用

のモデリングと組み合わせて、内部磁気圏におけるプラズマ粒子と電磁波動の変動過程をグローバルに把握するとともに、その変動のメカニズムを定量的に明らかにしていく。

本研究では、連続した定常観測が可能な地上観測点を地球規模で経度方向に戦略的に配置して、プラズマ変動や波動のグローバルな状況を24時間モニターすることを可能にする。この地上ネットワーク観測と、2016年度に打ちあがる我が国の新しいERG衛星による磁気圏の直接観測、さらにモデリングを組み合わせて、内部磁気圏におけるプラズマ粒子と電磁場の変動のメカニズムの定量的な評価を与えることができる。放射線帯粒子を含めた内部磁気圏の高エネルギープラズマは、人工衛星の内部帯電やメモリー反転、太陽電池パネルの劣化や衛星-地上間通信の障害などの問題を引き起こすことが知られている。本研究によって得られる成果は、これらの衛星機器の障害の予測や評価にも活用される予定である。

Imaging observation for the Earth's plasmasphere from Lunar orbit by nano-spacecraft

Kazuo Yoshioka[1]; Masaki Kuwabara[2]; Reina Hikida[3]; Fumiharu Suzuki[4]; Go Murakami[5]; Ichiro Yoshikawa[6]
[1] The Univ. of Tokyo; [2] The Univ. of Tokyo; [3] Frontier Sciences, Tokyo Univ.; [4] Earth and planetary science,
Univ.Tokyo; [5] ISAS/JAXA; [6] EPS, Univ. of Tokyo

The nano-spacecraft mission named EQUULEUS is now under development. It will be launched in 2018 as one of the secondary payloads of SLS (Space Launch System) mission of NASA. EQUULEUS will fly to a libration orbit around the Earth-Moon L2 point and demonstrate trajectory control techniques within the Sun-Earth-Moon region (e.g. low-energy transfers using weak stability regions) for the first time by a nano-spacecraft. A small telescope in extreme ultraviolet named PHOENIX will be boarded on EQUULEUS. It consists of multilayer-coated entrance mirror (diameter of 6 cm) and photon counting device (microchannel plate and resistive anode), and electronics parts. The reflectance of mirror is optimized for the emission line of ionic helium (wavelength of 30.4 nm) which is the important component of the plasmasphere of the Earth. By flying far from the Earth, the entire image of plasmasphere can be obtained. Our observation will complement and enhance the geospace in-situ plasma measurements conducted by the ERG (JAXA) and Van Allen probe (NASA) missions. As a result, we can understand natures of geospace and radiation belt, which we have to understand to realize future manned space exploration. In this presentation, the mission concept and the design of the telescope will be shown. The status of the development will also be shown.

人工飛翔体搭載用 熱的・超熱的イオン分析器の開発

須藤 雄志 [1]; 浅村 和史 [2]; 齋藤 義文 [3]
[1] 東大・理・地惑; [2] 宇宙研; [3] 宇宙研

Development of a Thermal and Supra-thermal ion Analyzer for Space-borne Experiments

Yushi Suto[1]; Kazushi Asamura[2]; Yoshifumi Saito[3]
[1] Earth and Planetary Science, Univ of Tokyo; [2] ISAS/JAXA; [3] ISAS

In the terrestrial magnetosphere, plasma particles with a wide energy range from $<1\text{eV}$ to MeV exist simultaneously. These particles are generated and/or transported via interactions with plasma waves. For example, in-situ particle observations have revealed that the inner magnetosphere contains significant fraction of low-energy plasma particles originated from the ionosphere. Their typical energy is a few tens of eV in contrast to much lower energies in the ionosphere. However, acceleration and transport processes of these particles are still unknown. This is mainly due to lack of observations of thermal and supra-thermal ions. It is known that satellite potential reaches about 5-30 V in the inner magnetosphere. Because of this, a measurement of plasma particles with energies less than a few tens of eV is easily affected by spacecraft potential. One of the solutions to suppress this effect is to mount the instrument on top of an extendable boom. The effects of the spacecraft potential are suppressed by controlling the chassis potential of the instrument. In this study, we are developing a thermal and supra-thermal ion mass spectrometer which is light enough to be mountable on top of the boom.

Our instrument consists of a top-hat type electrostatic energy analyzer which have a full-field of planar view and a time-of-flight type mass analyzer. We miniaturized these structures based on numerical simulations in which trajectories of incoming charged particles are traced inside the sensor structure. Diameter of the analyzer becomes less than 10 cm in the current design. The sensitivity and resolution of the instrument is enough to observe the ionospheric ions. In addition, we applied a photon trap inside the analyzer to reduce UV photons reaching the detector area.

We are developing this instrument as a payload of SS-520-3 sounding rocket. In the presentation, we will show the instrument design and its development status.

地球磁気圏には数 eV 程度の熱的・超熱的と呼ばれる低エネルギー粒子から数 MeV を超える高エネルギー粒子まで、幅広いエネルギー帯のプラズマ粒子が同時に存在している。これらの粒子は電磁場を介して相互作用し、加速や輸送を経て生成・消滅することで多様なプラズマ環境を形成している。例えば、内部磁気圏には電離圏起源のプラズマが存在することが知られており、磁力線に沿って電離圏プラズマが磁気圏へと流出する現象「polar wind」が衛星観測によっても確認されている。このとき、電離圏では 1eV ほどであった粒子が高高度では数十 eV ほどにまで加速されている。しかし、その加速機構は未だ解明されていない。この理由の一つとして、数十 eV 以下の熱的・超熱的イオンの直接観測を行う場合、衛星の帯電電位が粒子軌道に影響を与えてしまい、観測自体が容易でないという問題が挙げられる。

内部磁気圏において人工衛星は約 5~10V ほどに帯電することが知られている。このとき衛星は熱的・超熱的イオン (0.1-10 eV) の加速電位と同等以上の電位を持っているため、それらを衛星周辺で観測することは非常に難しい。したがってこれらの影響を抑制するために、観測器を衛星から伸展したブーム上に設置し、観測器の筐体電位を制御する方法が考えられる。この場合、観測器は小型軽量である必要がある。そのため我々は、小型化を重視した熱的・超熱的イオン分析器の開発を行っている。

一般的なイオン分析器はエネルギー分析部と質量分析部の 2 つの部分から構成される。本機器のエネルギー分析部には、360 度の平面状視野を持ち各粒子のエネルギー・飛来方向が同定可能なトップハット型静電分析器の構造を採用した。本機器はスピン衛星に搭載することで分析器周辺の全視野を網羅することが可能である。したがって、本機器によって得られたデータを解析することでイオン粒子の 3 次元速度分布を取得することができる。一方、質量分析部には Kaguya などに搭載実績を持つ飛行時間分析型質量分析器を採用した。我々は、入射イオンの軌道シミュレーションをもとにこれらの構造を小型化することで、アナライザ部の大きさが $100\ \phi \times 60\ \text{mm}$ 程の熱的・超熱的イオン分析器を設計した。粒子シミュレーション結果から、本機器は電離圏イオン観測に十分な感度や分解能を持つことが分かっている。また、本機器で使用する検出器は紫外線に対する感度も持つため、イオンの入射口や静電分析部には紫外線への対策加工も施されている。

本機器は技術実証試験を兼ねて極域観測ロケット SS-520 3 号機への搭載が予定されており、その打ち上げに向けた開発が進められている。現在は上記の基本設計をもとに内部機構の詳細設計が完了し、実機の開発を行っている。今後は性能試験およびキャリブレーションを実施する予定である。

本発表では、熱的・超熱的イオン分析器の詳細な設計および現在の開発状況について述べる。

Low-energy particle instruments (LEPe and LEPi) to be onboard ERG spacecraft

Kazushi Asamura[1]; Yoichi Kazama[2]; B.-J. Wang[3]; Yushi Suto[4]; Shiang-Yu Wang[5]; Shoichiro Yokota[6]; Satoshi Kasahara[7]

[1] ISAS/JAXA; [2] Institute of Astronomy and Astrophysics, Academia Sinica, Taiwan; [3] ASIAA, Taiwan; [4] Earth and Planetary Science, Univ of Tokyo; [5] Institute of Astronomy and Astrophysics, Academia Sinica, Taiwan; [6] ISAS; [7] ISAS/JAXA

ERG spacecraft, which explores terrestrial inner magnetosphere, is planned to be launched in fiscal year 2016. We have developed LEPe (Low-energy electron energy spectrum analyzer) and LEPi (Low-energy ion energy mass spectrometer) instruments to be onboard ERG. They cover particle energies 19-19000eV (LEPe) and 10-25000eV/q (LEPi). Three dimensional distribution functions of electrons and ions in these energy ranges are believed to play significant roles on excitation of plasma waves such as Whistler waves, EMIC waves, and magnetosonic waves. These waves are considered to be closely related to acceleration and loss mechanisms of high-energy electrons in the inner magnetosphere. We will present performance and planned observation modes of the instruments.

Data products of Medium Energy Particle analysers (MEPs) onboard ERG

Satoshi Kasahara[1]; Shoichiro Yokota[2]; Takefumi Mitani[3]; Kazushi Asamura[3]; Masafumi Hirahara[4]; Takeshi Takashima[5]; Kazuhiro Yamamoto[6]

[1] ISAS/JAXA; [2] ISAS; [3] ISAS/JAXA; [4] ISEE, Nagoya Univ.; [5] ISAS, JAXA; [6] Geophysics, Kyoto Univ.

ERG (Exploration of energization and Radiation in Geospace) is the geospace exploration spacecraft, which is planned to be launched in FY2016. The mission goal is to unveil the physics behind the drastic radiation belt variability during space storms. One of key observations is the measurement of ions and electrons in the medium-energy range (10-200 keV), since these particles excite EMIC, magnetosonic, and whistler waves, which are theoretically suggested to play significant roles in the relativistic electron acceleration and loss. In previous space missions, however, the medium energy range has been the missing region due to the limitation of conventional particle instruments. We introduce these instruments in terms of specifications, observation modes, and data products.

Preflight performance and expected data products of “High energy Electron exPeriment (HEP)” onboard the ERG satellite

Takefumi Mitani[1]; Satoshi Kasahara[2]; Takeshi Takashima[3]; Masafumi Hirahara[4]; Wataru Miyake[5]
[1] ISAS/JAXA; [2] ISAS/JAXA; [3] ISAS, JAXA; [4] ISEE, Nagoya Univ.; [5] none

The Exploration of energization and Radiation in Geospace (ERG) project will explore how relativistic electrons in the radiation belts are generated during space storms. “High energy Electron exPeriment (HEP)” on board ERG satellite will observe 70 keV -2 MeV electrons, which covers energy range of electrons to be accelerated and accelerated electrons, and play an important role to understand electron acceleration.

HEP provide three-dimensional velocity distribution of electrons every spacecraft spin period. Electrons are observed by two types of camera designs, HEP-L and HEP-H, with regard to geometrical factor and energy range. HEP-L observes 0.1 - 1 MeV electrons and its geometrical factor is $\sim 10^{-3}$ cm² str, and HEP-H observes 0.7 - 2 MeV and g-factor is $\sim 10^{-2}$ cm² str. HEP-L and HEP-H each consist of three pin-hole type cameras, and each camera consist of mechanical collimator, stacked silicon semiconductor detectors and readout ASICs. HEP-H has larger opening angle of the collimator and more silicon detectors to observe higher energy electrons than HEP-L.

In this presentation we introduce the HEP instrument and report the results of performance tests of the flight model. We also describe data products from HEP observation in orbit.

ERG 衛星搭載超高エネルギー電子観測装置 (XEP-e)

東尾 奈々[1]; 松本 晴久 [2]
[1] JAXA; [2] 宇宙機構

The extremely high-energy particle sensor for electron (XEP-e)

Nana Higashio[1]; Haruhisa Matsumoto[2]
[1] JAXA; [2] JAXA

It is well known that satellites are always in danger in space and especially high-energy radiation damages them. One of the sources that cause them is the radiation belt (the Van Allen belt). It was thought to be static, but in the 1990s it rediscovered the radiation belt fluctuates greatly. There are some reasons to occur this phenomenon, but we have not understood a clear reason of this yet. On the other hand, it is well known that the energetic particle flux vary during geomagnetic disturbances and the relativistic electrons in the other radiation belt change with solar wind speed.

The Exploration of energization and Radiation in Geospace (ERG) will try to reveal this mechanism. The ERG satellite is the small space science platform for rapid investigation and test satellite of JAXA/ISAS. This satellite will be lunched in 2016. Our group is developing the instrument (The eXtremely high-Energy Particle sensor for electron (XEP)) to detect a high-energy electron (400keV-20MeV). The XEP-e has 5 SSDs (Solid-State Silicon Detectors), one GSO single crystal scintillator and an anti-scintillator. It has one-way conic sight.

In this presentation we introduce the XEP-e and report the results of performace tests of the flight model.

将来惑星探査に向けた超小型軽量磁場観測器の開発研究

野村 麗子 [1]; 松岡 彩子 [2]; 池田 博一 [3]; 小嶋 浩嗣 [4]
[1] ISAS; [2] JAXA 宇宙研; [3] JAXA・宇宙研; [4] 京大・生存圏

Development of ultraslim magnetometers for future interplanetary explore missions

Reiko Nomura[1]; Ayako Matsuoka[2]; Hirokazu Ikeda[3]; Hirotsugu Kojima[4]
[1] ISAS; [2] ISAS/JAXA; [3] ISAS, JAXA; [4] RISH, Kyoto Univ.

Since the single spacecraft observation cannot distinguish between temporal and spatial variations, for example, the wave vector and the dispersion relation cannot be determined to find a wave mode of the plasma turbulence in the solar wind for energy dissipations.

In order to find the wavenumber by deploying four magnetometers at edges of the large thin film solar cell (~50m each) of the Solar Sail (Trojan asteroid exploration mission), we are developing an ultra-slim and light magnetometer integrated with signal processing circuits of low power and noises. One of the problems for installing our magnetometers is that the signal process circuits are too large and heavy to deploying into the solar cell. Therefore we developed the 5mm-chip (ASIC; Application Specific Integrated Circuit) for the analog parts of our signal process circuits to achieve both weight saving and downsizing. This magnetometer is planed to perform a flight proof by SS-520-3 sounding rocket experiment.

In our presentation, we will show the simulation results and the performance evaluations of the developed circuits of ASIC. Also, we will show the attitude analysis results and the performance evaluation of a new method on digital data processing of S-520-29 DFG for preparing the flight proof by SS-520-3.

これまでの惑星間空間での観測的研究は単機衛星によるものであったため、時間・空間変化を分離することができず、例えば、太陽風中のプラズマ乱流については、エネルギー散逸に寄与する波動決定に必要な波数ベクトルと分散関係の導出が難しい。

本研究では、ソーラーセイルミッション（木星トロヤ群小惑星探査）の大規模な（一辺~50m）薄膜太陽電池パネルの4隅に磁力計を搭載し、波数を計測することを目指して、センサ部と信号処理部一体型の超小型・軽量、省電力かつ低ノイズの磁場観測器を開発している。大型薄膜太陽電池パネルに搭載するためには、従来の磁場観測器のままでは信号処理回路部が大きく重すぎるのが問題とのひとつとなる。そこで、センサ部と信号処理回路で構成されているフラックスゲート磁力計のうち、信号処理回路のアナログ回路部全体を5mm角の集積回路(ASIC; Application Specific Integrated Circuit)に納めることにより軽量化及び1/3以下に小型化をおこなった。この磁場観測器は、2017年冬季に欧州より打ち上げ予定のSS-520-3号機観測ロケット実験において、フライト実証を実施する予定である。

本発表では、回路の各機能部分における性能について、シミュレーション結果との比較とともに、ASICを組み込んだ回路の評価を報告する。また、SS-520-3号機でのフライト実証に向け、S-520-29号機観測ロケット実験におけるデジタル方式フラックスゲート磁力計データを用いた姿勢解析結果、及び新方式デジタル処理の性能評価を報告する。

SS-520-2号機による低高度昼側カスプ領域のDC電場観測

加納 康裕 [1]; 石坂 圭吾 [2]; 三宅 壮聡 [3]; 小嶋 浩嗣 [4]; 田中 真 [5]
[1] 富山県立大; [2] 富山県大・工; [3] 富山県大; [4] 京大・生存圏; [5] 東海大・情教セ

DC electric field measurement in the low altitude dayside cusp region by SS-520-2 sounding rocket

yasuihiro kano[1]; Keigo Ishisaka[2]; Taketoshi Miyake[3]; Hirotsugu Kojima[4]; Makoto Tanaka[5]
[1] Toyama Pref. Univ.; [2] Toyama Pref. Univ.; [3] Toyama Pref. Univ.; [4] RISH, Kyoto Univ.; [5] Tokai Univ.

SS-520-2 sounding rocket experiment was carried out at the Svalbard rocket range in the Norwegian Spitsbergen Ny-Olesund at 9:16 on 4 December, 2000. The purpose of this experiment is launch a rocket to the region where occurred the ion heating at low altitude dayside cusp region, and it is to investigate the physical mechanism of the ion heating. SS-520-2 sounding rocket reached to an altitude 1100 km to about 600 seconds after launch, and observed of 1147 seconds. The SS-520-2 sounding rocket payload was equipped with Electric Filed Detector (EFD). EFD is one of the sub-system of Plasma Wave Analyzer (PWA) on the rocket, and it is a receiver to observe the DC electric field and the low-frequency wave (0-50 Hz). PWA is using four Wire antenna (WANT) as a sensor. The WANT placed two by two on diagonally line, and called the two sets of 10 m tip-to-tip dipole antenna WANT-X and WANT-Y. Observed x and y components were extended to operate without problems since are 90deg out of phase. We analyze the EFD data analysis during the period from 184 seconds to 1109 seconds after launch. Further, the waveform observed by the EFD contains distortion of the pulse-like waveform. The distortion of this waveform is thought to influence by photoelectron emission surrounding the rocket. This paper analyzes the DC electric field is considered to be involved in the heating behavior of ions at low altitude dayside cusp region using an EFD data, and performs the derivation of the DC electric field vector. In particular, we explain the removing method of the pulse noise by photoelectron emission.

SS-520-2 観測ロケット実験は、2000年12月4日午前9時16分にノルウェーのスピッツベルゲン島ニューオルスンにあるスバルバード・ロケット実験場で行われた。この実験の目的は、低高度昼側カスプ領域におけるイオンの加熱が起きている現場にロケットを打ち上げ、その物理機構を調査することである。SS-520-2 観測ロケットは発射後約600秒後に高度1100kmに到達し、1147秒の観測を行った。SS-520-2 観測ロケットは電界観測装置 Electric Filed Detector (EFD) を搭載している。EFDは、ロケットに搭載されたプラズマ波動観測装置 Plasma Wave Analyzer(PWA) のサブシステムの一つであり、直流電場と低周波波動(0-50Hz)を観測する受信機である。PWAは、センサとしてワイヤアンテナ Wire antenna(WANT)を4機用いている。このWANTを2機ずつ対角線上に配置し、2組の10m tip-to-tipのダイポールアンテナ WANT-X、WANT-Yとして機能させる。観測されたx成分とy成分は、90deg位相がずれているので問題なく伸展し動作したことが確認された。解析には打ち上げ後184秒から1109秒のEFDデータを用いた。また、観測されたEFDの波形は、パルス状の波形の歪みを含んでいる。この波形の歪みは、光電子放出による影響だと考えられる。本論では、EFDデータを用いて低高度昼側カスプ領域でのイオンの加熱現象に関与していると考えられるDC電場の解析を行い、DC電場ベクトルの導出を行う。特に、観測データに含まれる光電子放出に関するノイズの除去方法について説明する。

SS-520-3/LFAS 搭載用デジタル処理部の FPGA モジュールの設計

高橋 翼 [1]; 笠原 禎也 [1]; 小嶋 浩嗣 [2]; 頭師 孝拓 [2]; 太田 守 [1]; 尾崎 光紀 [3]; 八木谷 聡 [1]; 石坂 圭吾 [4]; 後藤 由貴 [1]

[1] 金沢大; [2] 京大・生存圏; [3] 金沢大・理工・電情; [4] 富山県大・工

Design of FPGA modules for digital processing part in the SS-520/LFAS

Tsubasa Takahashi[1]; Yoshiya Kasahara[1]; Hirotsugu Kojima[2]; Takahiro Zushi[2]; Mamoru Ota[1]; Mitsunori Ozaki[3]; Satoshi Yagitani[1]; Keigo Ishisaka[4]; Yoshitaka Goto[1]

[1] Kanazawa Univ.; [2] RISH, Kyoto Univ.; [3] Electrical and Computer Eng., Kanazawa Univ.; [4] Toyama Pref. Univ.

The rocket SS-520-3 experiment will be performed in the next fiscal year. LFAS (Low Frequency Analyzer System), TSA (Thermal Ion Spectrum Analyzer) and IMS (Ion Mass Spectrometer) will be mounted on the SS-520-3 rocket. Energy exchange process between plasma waves and plasma particles via wave particle interaction is planned to be evaluated directly and quantitatively by SWPIA (Software-type Wave Particle Interaction Analyzer). We are responsible for the development of the digital data processing module for LFAS mounted in the SS-520-3 rocket.

LFAS contains two pairs of dipole antenna, and two receivers named EFD (Electric Field Detector) and WFC (Waveform Capture). The EFD measures electric wave field in the frequency range from DC to 400 Hz and the data will be sent by analogue telemetry, while WFC covers electric field measurements in the VLF range below 10 kHz and generate digital data which consist of one channel of spectrum and two channels of waveform.

Two FPGAs will be installed in the LFAS. One FPGA is supplied to the WFC digital part and another one is used for a common digital part of LFAS. WFC digital part performs data compression of waveforms and generation of spectrum data. Two channels of waveform data will be sampled at 30 kHz and digitized into 16 bits/sample, and fed into the first FPGA. In addition, as a counter to secure the synchronousness between waveforms and particles, SWPIA counter is generated in the FPGA. In the waveform compression module, subband compression is carried out every 1,024 points. In the spectrum generation module one set of 512 points of FFT followed by two combinations of 1/8 decimation and 512 points of FFT are performed in parallel, and the logarithm amplitude is finally calculated. It observes spectrums of three frequency bands, that is, 1 kHz - 10 kHz, 100 Hz - 1 kHz and below 100 Hz. Both the compressed waveform and spectrum data are transmitted to another FPGA which is responsible for a common digital part of LFAS. It performs telemetry transmission processing afterwards.

We have already developed a baseline of waveform compression as well as spectrum processing, and inspected that these modules work fast enough to process these data within real-time. We also confirmed that the total amount of generation data is within telemetry transmission capacity. As a next step, it is necessary to decide the details of the I/F with the peripheral circuits including the data entry part from ADC and the data output part after the processing.

In the presentation, we report further detailed signal processing section and the I/F with peripheral circuits, observation sequence.

2000年12月4日に観測ロケット SS520-2号機を用いて、極域カスプ領域における重イオンの加速・加熱の解明を目的としたロケット実験が行われた。SS-520-2号機にはイオンの加速・加熱機構に大きく寄与していると考えられているプラズマ波動を観測するためにプラズマ受信機 (Plasma Wave Analyzer : PWA) が搭載され、PWAにはDSPを用いて日本初のオンボードリアルタイム波形圧縮処理機能が実装された。同様の観測目標を達成するための後継実験として、来年度にSS-520-3号機による北欧ロケット実験が予定されている。SS-520-3号機には低周波波動解析システム (Low Frequency Analyzer System : LFAS), 熱的イオン分析器 (Thermal Ion Spectrum Analyzer : TSA) や低エネルギーイオン質量分析器 (Ion Mass Spectrometer : IMS) などが搭載される。また、「ソフトウェア型波動粒子相互作用解析装置 (Software-type Wave Particle Interaction Analyzer : WPIA)」により取得したデータから波動粒子相互作用によるプラズマ粒子とプラズマ波動間のエネルギー交換過程を直接かつ定量的に評価する予定である。本研究ではこのSS-520-3観測ロケット搭載のLFASのデジタル処理部の開発を行う。

LFASは2組のダイポールアンテナと電場観測器 (Electric Field Detector : EFD), 波形捕捉受信器 (Waveform Capture : WFC) と呼ばれる2種類の受信器を搭載している。EFDではDCから400 Hzの電界を計測しそれをアナログテレメトリで送信する。また、WFCでは電場2成分 (CH1, CH2) の10 kHz以下の低周波信号を計測し、地上へは1チャンネルのスペクトルデータと圧縮処理を施した2チャンネルの波形データを伝送する。

WFCデジタル部の詳細について述べる。それには単体のFPGAが供給される。これは、前回のSS-520-2号機では波形圧縮などの信号処理をDSP上でソフトウェア処理をしていたものをFPGAに変更することで高速化・小型化を図るのが目的である。このFPGA上で波形データの圧縮処理とスペクトル観測を行う。ここで、WFCデジタル部にはサンプリング周波数30 kHzでADCから量子化ビット数16 bitの2chの波形データが入力される。また、波形と粒子の同期性を確保するためのカウンタとして、SWPIAカウンタをFPGA内部で生成する。波形処理部では、信号を複数の周波数帯域に分割し、分割された各帯域での信号強度の違いを利用し、ビット長を削減する圧縮手法であるサブバンド圧縮を1,024点ごとに行う。スペクトル処理部では、1/8デシメーションと512点FFTを行い、最終的に対数振幅を算出して1 kHz - 10 kHz, 100 Hz - 1 kHz, 100 Hz以下の3つの帯域を観測する。その後、処理を施したデータは後段のテレメトリ送信処理を行うFPGAに送信される。

現状では、波形の圧縮処理及び、スペクトルの生成処理ともにリアルタイムで処理が行えることが検証済みであり、テレメトリ伝送容量内にデータを収めることにも成功した。FPGA 内部の信号処理モジュールは基本動作の確認を終えているが、ADC からのデータ入力部や処理後のデータ出力など、周辺回路との I/F については今後詳細を詰める必要がある。発表の際にはさらなる詳細な信号処理部と、周辺回路との I/F、観測シーケンスについて説明する。

SS-520-3号機北欧ロケット実験に向けた波形捕捉受信機（WFC）の開発

徳永 祐也 [1]; 頭師 孝拓 [2]; 尾崎 光紀 [3]; 八木谷 聡 [1]; 小嶋 浩嗣 [2]; 山田 航平 [1]
[1] 金沢大; [2] 京大・生存圏; [3] 金沢大・理工・電情

Development of the Wave Form Capture (WFC) receiver for the SS-520-3 rocket experiment

Yuya Tokunaga[1]; Takahiro Zushi[2]; Mitsunori Ozaki[3]; Satoshi Yagitani[1]; Hirotsugu Kojima[2]; Kohei Yamada[1]
[1] Kanazawa Univ.; [2] RISH, Kyoto Univ.; [3] Electrical and Computer Eng., Kanazawa Univ.

The SS-520-3 rocket experiment has proceeded to understand the ion outflow near the polar cusp. This experiment is an important mission to detect in-situ wave-particle interaction causing the ion outflow phenomena. We have been developing Wave Form Capture (WFC) for the SS-520-3 rocket experiment. The WFC consists of four-stage circuit blocks. First stage is a differential input LPF to remove common mode noise. Second stage has main amplifiers to adjust the gain. Third stage is a Switched Capacitor (SC) filter to prevent aliasing. The cut off frequency of the SC filter can be changed with the clock pulse frequency. Final stage is an LPF to remove ringing noise from the clock for the SC filter. Our WFC has been developed by using Application Specific Integrated Circuit (ASIC) technology to reduce resources (size, mass and power) for the rocket experiment. The size of our WFC chip (1 ch) is 2.8 mm^2 , and the power is 26 mW. The equivalent input noises (100 Hz) are $7.4 \text{ uV/Hz}^{1/2}$ (main amplifier gain: 0 dB) and $0.93 \text{ uV/Hz}^{1/2}$ (20 dB gain). The WFC receiver onboard the ERG satellite is assembled with discrete devices. The size of WFC (1 ch) onboard ERG is 9350 mm^2 , the mass is 0.13 kg, and the power is 500 mW. Comparing these WFCs, we can achieve a sufficient reduction in the resources by using the ASIC technology. On the other hand, the WFC requires a high tolerance against the radiation environment for space experiments. We did a radiation test for the WFC chip. Alpha ray of 220 MeV was irradiated onto the WFC chip until the dose rate reached 400 krad. No impulse signals such as Single Event Effects (SEE) were observed during the radiation test. The output noise (100 Hz) of the WFC chip was increased by up to 6 dB in comparison with that before the radiation. This would be caused by degradation of electric performance by the radiation exposure. However, the WFC chip was not broken by the incident alpha ray up to 400 krad. Generally the radiation tolerance required for space experiments is up to 100 krad. Thus the WFC chip is expected to have a high robustness in space radiation environments.

We will present our WFC receiver for the SS-520-3 rocket experiment in detail.

電離大気流出現象を捉えるため、SS-520-3号機による北欧ロケット実験の計画が進められている。この実験は、電離大気流出の原因とされている波動-粒子相互作用をその場で検出し解明するミッションである。我々は、SS-520-3号機に向けて波形捕捉受信機（WFC）を開発中である。WFCは、四段の回路ブロックで構成されている。初段は、コモンモードノイズを除去するため差動入力 LPF となっている。二段目は、ゲイン調整のためのメインアンプであり、三段目はアンチエイリアシングを防ぐため、任意のクロックを与えることでカットオフ周波数を変化させることのできる SC (Switched Capacitor) フィルタである。最終段の四段目は、SC フィルタにクロックを使用することで発生するリングングノイズを除去するための LPF である。我々が開発した WFC チップは、科学搭載機器のリソース（サイズ、質量、電力等）削減のためにアナログ ASIC（特定用途向け集積回路）技術を用いて開発している。そのため、1ch 分のサイズは 2.8 mm^2 で、消費電力は 26 mW となっており、入力換算雑音（100 Hz）はメインアンプが 0 dB の時は $7.4 \text{ uV/Hz}^{1/2}$ で、20 dB の時は $0.93 \text{ uV/Hz}^{1/2}$ である。ディスクリット部品で構成される ERG 衛星に搭載されている 1ch 分の WFC はサイズが約 9350 mm^2 、重量が 0.13 kg、消費電力は約 500 mW である。両者の比較から、ASIC 技術により大幅なリソースの削減が実現できていることがわかる。また、WFC は放射線が飛び交う宇宙空間に暴露されるため、放射線に対しての耐性が必要である。そこで、我々は将来の科学衛星への搭載を見込み WFC チップに対して放射線試験を行った。試験内容は、220 MeV のアルファ線を WFC チップにトータルドーズ量として 400 krad まで照射するというものである。試験を行った結果、WFC チップの出力電圧波形からは、放射線によるシングルイベント効果のような瞬時的な影響は見られなかった。しかし、出力雑音（100 Hz）は放射線暴露前と比較して最大 6 dB 増大することがあった。これは放射線暴露による電氣的諸特性の劣化と考えられる。しかしながら WFC の吸収線量が 400 krad になっても故障に至ることはなかった。一般的に、静止衛星軌道で 10 年分の吸収線量は 100 krad といわれていることから WFC チップは放射線に対して十分な耐性があるといえる。

本発表では、SS-520-3号機に搭載予定である WFC チップについて詳細に説明する。

Specification and Observation plan of the plasma wave experiment (PWE) on board ERG

Yoshiya Kasahara[1]; Yasumasa Kasaba[2]; Hirotsugu Kojima[3]; Satoshi Yagitani[1]; Shoya Matsuda[4]; Fuminori Tsuchiya[5]; Keigo Ishisaka[6]; Mitsunori Ozaki[7]; Tomohiko Imachi[1]; Atsushi Kumamoto[8]; Yoshizumi Miyoshi[4]; Mamoru Ota[1]; Satoshi Kurita[4]; Naoko Takahashi[2]; Kazushi Asamura[9]; Iku Shinohara[10]
[1] Kanazawa Univ.; [2] Tohoku Univ.; [3] RISH, Kyoto Univ.; [4] ISEE, Nagoya Univ.; [5] Planet. Plasma Atmos. Res. Cent., Tohoku Univ.; [6] Toyama Pref. Univ.; [7] Electrical and Computer Eng., Kanazawa Univ.; [8] Dept. Geophys, Tohoku Univ.; [9] ISAS/JAXA; [10] ISAS/JAXA

The ERG (Exploration of energization and Radiation in Geospace) project is a mission to study acceleration and loss mechanisms of relativistic electrons around the Earth. In order to achieve comprehensive observations of the inner magnetosphere, electrons and ion detectors, magnetic field sensors, and electric sensors are equipped on the spacecraft. The Plasma Wave Experiment (PWE) is one of scientific instruments on the ERG satellite. It measures electric field in the frequency range from DC to 10 MHz, and magnetic field in the frequency range from a few Hz to 100 kHz. Three kinds of receivers are implemented in the PWE; EFD (Electric Field Detector), OFA/WFC (Onboard Frequency Analyzer and Waveform Capture), and HFA (High Frequency Analyzer).

The measured data are processed and edited by onboard software implemented in the CPUs in order to realize varieties of operational modes. We produce continuous spectra below ~200 Hz and waveforms below 64 Hz (256 Hz) at L-values larger (less) than 4 as EFD double probe data. Spacecraft potential is also provided by the EFD by single probe measurement. As for the data from OFA and WFC, raw waveforms are once stored in the onboard memory and we calculate wave spectra and spectral matrix using FFT. They are continuously processed and all data are sent to the ground. On the other hand, waveforms are intermittently stored as 'PWE burst' data in the mission data recorder (MDR). Two kinds of PWE-burst mode are implemented; one is 'chorus burst' and another is 'EMIC-burst'. Several seconds of continuous VLF waveforms sampled at 65 kHz are produced after lossy compression in the 'chorus burst' mode, while a few minutes of continuous ELF waveforms down-sampled at 1024 Hz are generated in the 'EMIC burst' mode. These two modes are exclusively operated. Due to the limitation of telemetry resource, the PWE burst data stored in the MDR are partially selected and downloaded to the ground. In addition, a triggering logic is implemented for the PWE-burst to capture significant plasma waveforms such as 'large-amplitude whistlers'. The HFA measures high frequency spectra from 10 kHz to 10 MHz for electric field and 10 kHz to 100 kHz for magnetic field. Electron density along the spacecraft trajectory can be determined from upper-hybrid resonance (UHR) frequency measured by the HFA.

Development of the PWE has finished and passed its product quality review (PQR) in August, 2016. In parallel, we are now constructing a pipeline data processing scheme on the ground to provide excellent science data and to perform smooth and effective data analyses. In the present paper, we introduce a final design of the PWE and its observation plan to meet the scientific objects of the ERG mission.

ERG搭載プラズマ波動観測器PWEにおける受信器特性の機上校正手法の実装

松田 昇也 [1]; 笠原 禎也 [2]; 小嶋 浩嗣 [3]; 笠羽 康正 [4]; 井町 智彦 [2]; 尾崎 光紀 [5]; 八木谷 聡 [2]; 石坂 圭吾 [6]; 櫻井 勢一郎 [2]

[1] 名大 ISEE; [2] 金沢大; [3] 京大・生存圏; [4] 東北大・理; [5] 金沢大・理工・電情; [6] 富山県大・工

Development of the Onboard Calibration System for ERG/PWE

Shoya Matsuda[1]; Yoshiya Kasahara[2]; Hirotsugu Kojima[3]; Yasumasa Kasaba[4]; Tomohiko Imachi[2]; Mitsunori Ozaki[5]; Satoshi Yagitani[2]; Keigo Ishisaka[6]; Seiichiro Sakurai[2]

[1] ISEE, Nagoya Univ.; [2] Kanazawa Univ.; [3] RISH, Kyoto Univ.; [4] Tohoku Univ.; [5] Electrical and Computer Eng., Kanazawa Univ.; [6] Toyama Pref. Univ.

The Plasma Wave Experiment (PWE) is one of the science instruments on board the ERG (Exploration of energization and Radiation in Geospace) satellite to measure electric field and magnetic field in the inner magnetosphere. The sensor part of the PWE consists of a pair of dipole wire-probe antenna (WPT) and tri-axis magnetic search coils (MSC). The receiver part of the PWE consists of three sub-components, EFD (Electric Field Detector), OFA/WFC (Onboard Frequency Analyzer and Wave Form Capture), and HFA (High Frequency Analyzer). Especially, OFA/WFC measures electric and magnetic field spectrum and waveform from a few Hz to 20 kHz. Observed signals are amplified and filtered inside the analogue circuits. Finally, the signals are digitized by the A/D converters.

It is well known that the characteristics of the sensors in space change depending on the plasma parameters (e.g. plasma density, temperature, etc). In order to measure the nature of natural plasma waves, 'calibration procedure' is necessary. In this study, we developed the onboard calibration system for the middle frequency range receiver (OFA/WFC) and implemented as a part of the onboard software of the PWE. The calibration signal generator is contained in the analogue circuit of the PWE. An arbitrary frequency square wave is fed into the receiver or preamplifier by commands. The onboard calibration system controls calibration signal frequency and ON/OFF of the output. The system performs a fast Fourier transform (FFT) on the signal output from the A/D converters, and collects frequency responses of the fundamental and that of odd-numbered harmonics below 32.768 kHz. The transfer function can be derived on the ground by dividing observed responses into the reference square signal in the frequency domain. We successfully derived gain and phase specification of the onboard sensors and receivers (analogue circuit of the PWE) by using arbitrary frequency square waves generated in the receiver. Our software based calibration technic will be useful for future missions.

ERG衛星プラズマ波動観測データの地上データ処理の開発

奥田 拓希 [1]; 松田 昇也 [2]; 太田 守 [1]; 笠原 禎也 [1]; 笠羽 康正 [3]; 土屋 史紀 [4]; 小嶋 浩嗣 [5]; 井町 智彦 [1]; 後藤 由貴 [1]; 三好 由純 [2]

[1] 金沢大; [2] 名大 ISEE; [3] 東北大・理; [4] 東北大・理・惑星プラズマ大気; [5] 京大・生存圏

Development of the ground data processing system for the plasma wave measurements onboard ERG satellite

Hiroki Okuda[1]; Shoya Matsuda[2]; Mamoru Ota[1]; Yoshiya Kasahara[1]; Yasumasa Kasaba[3]; Fuminori Tsuchiya[4]; Hirotsugu Kojima[5]; Tomohiko Imachi[1]; Yoshitaka Goto[1]; Yoshizumi Miyoshi[2]

[1] Kanazawa Univ.; [2] ISEE, Nagoya Univ.; [3] Tohoku Univ.; [4] Planet. Plasma Atmos. Res. Cent., Tohoku Univ.; [5] RISH, Kyoto Univ.

The ERG(Exploration of energization and Radiation in Geospace) satellite is a Japanese small satellite mission to investigate dynamics of the inner magnetosphere. To achieve comprehensive observations of plasma/particles, fields, and waves, the Plasma Wave Experiment (PWE) is installed onboard the ERG satellite to measure electric field in the frequency range from DC to 10 MHz, and magnetic field in the frequency range from a few Hz to 100 kHz. A variety of operational modes are implemented in the PWE, and the raw data consists of several kinds of data such as power spectrum, waveform, spectral matrix and DC E-field.

It is very important to check and analyze the raw data quickly and select valuable data. Therefore, it is essential to standardize data format. CDF (Common Data Format) is known as one of standardized data format developed by NASA Goddard Space Flight Center suitable for solar-terrestrial physics.

In the present paper, we propose a data processing plan for the PWE to realize quick data survey and analyses. We first convert PWE OFA/WFC into CDF files. Those files are called Level 1 and they are non-calibrated data. In actual operation, those files are divided into species of data products. Secondly, we divided CDF files creation program into various common items; common items in the satellite unit and common considerations in the equipment unit, common items in the observation mode unit. Therefore, it will be possible to create the generic CDF program. Finally, we demonstrate that our data processing system is general enough to adopt the other equipment.

今年度打ち上げ予定のジオスペース探査衛星 ERG(Exploration of energization and Radiation in Geospace) は、地球内部磁気圏観測を行い、プラズマ統合観測による放射線帯の粒子加速、輸送、消失過程の解明、および宇宙嵐のダイナミックスの解明を目指している。搭載されるプラズマ波動観測器 PWE(Plasma Wave Experiment) は、DC から 10MHz までの周波数帯の電場と数 Hz から 100kHz までの周波数帯の磁場を計測する。PWE は様々な動作モードが実装され、地上伝送されたテレメトリデータは、電磁界スペクトル、および波形、スペクトルマトリクスなどより構成される。

科学衛星により観測されたデータが衛星の打ち上げ後、迅速に解析できる体制を整えるには、取得データをいくつかの階層に分けて蓄積・公開する必要がある。科学衛星から伝送されるデータは、各観測器毎に独自形式となっているうえに、複数の観測器のデータが入り混じっている。そのため、データ解析者が迅速かつ容易にデータ解析を行えるように、機器別・データ種別毎に分類されたデータを、標準化された共通フォーマットで蓄積することが必要不可欠である。

本研究では、ERG 衛星プラズマ波動データを即時解析するための共通フォーマット CDF(Common Data Format) へのデータ変換・校正、および他機器に転用可能な汎用化 CDF プログラムの作成を目指す。初めに PWE OFA/WFC テレメトリデータのスペクトル、および波形データに校正を加えず蓄積するレベル 1 データの CDF 化を行った。レベル 1 はその後の校正済みデータであるレベル 2 ファイルを生成する元データとなるため、CDF ファイルはデータ構造をシンプルにして容易に取り扱えるように、観測モード単位でファイルを分けることにした。次に CDF 作成の汎用化を目的とし、ERG 衛星以外にも応用可能な共通事項、ERG 搭載機器で共通して利用できる事項、PWE のサブ機器で共通に利用可能な事項など、CDF の関数群や変数類を階層化した CDF 作成機構を設計した。さらに生成した CDF ファイルが Autoplot などの汎用描画ツールで簡単に描画できるよう波形・スペクトルデータ毎に、データフォーマットを工夫した。本講演では、地上試験での PWE OFA/WFC テレメトリデータを用いたスペクトルデータ、および波形データの CDF ファイル構成と、他機器への転用を可能とするプログラム構成について紹介する。

Processing method of wave data in Wave-Particle Interaction Analyzer onboard ERG satellite

Mitsuru Hikishima[1]; Hirotsugu Kojima[2]; Yuto Katoh[3]

[1] ISAS; [2] RISH, Kyoto Univ.; [3] Dept. Geophys., Grad. Sch. Sci., Tohoku Univ.

The Wave-Particle Interaction Analyzer (WPIA) is a software function installed on the Exploration of energization and Radiation in Geospace (ERG) satellite. The WPIA directly measures the quantity of energy transfer between whistler-mode chorus waves and resonant energetic electrons by using plasma wave vectors and velocity vectors of plasma particles. In order to statistically evaluate the significance of the quantity of energy transfer, the WPIA require accurate phase angles of waves with certain frequency and resonant electrons. The waveform data of SWPIA data includes various wave mode except whistler-mode chorus which is main target of WPIA. The waveform data processing is important to obtain SWPIA result with larger S/N. We discuss applicative processing method to suppress the statistical error using wave-particle interaction reproduced in the simulation and application to onboard algorithm.

スペクトルマトリクスを用いる伝搬ベクトル推定手法の性能評価

太田 守 [1]; 笠原 禎也 [1]; 後藤 由貴 [1]
[1] 金沢大

Performance Evaluation of Direction Finding Method using Spectral Matrix

Mamoru Ota[1]; Yoshiya Kasahara[1]; Yoshitaka Goto[1]
[1] Kanazawa Univ.

Investigating characteristics of plasma waves observed by scientific satellites in the Earth's magnetosphere and plasmasphere is the effective key to understand not only generation mechanisms of the waves but also a plasma environment which influences its generation and propagation conditions. In particular, direction finding of plasma waves is most important for understanding these characteristics.

Spectral matrix composed by cross spectra of observed signals is widely used for direction finding of VLF waves in the Earth's magnetosphere/plasmasphere. Many solutions of the direction finding problem using a spectral matrix have been proposed for each analysis target wave. Means method [1] and SVD method [2] are derived by the single plane wave approximation. The wave distribution function (WDF) method [3] can estimate directional distribution of wave energy density, and its theory is based on the assumption that the observed signals follow stationary and ergodic Gaussian random process. In order to obtain a unique solution of the continuous directional distribution, a model of the distribution function expressed with few parameters must be assumed. Although conventional methods for direction finding had often been evaluated by using test data adapted to individual assumptions, however, the performance comparison for each method and the evaluation for plasma waves with frequency drift such as chorus emission are not enough.

In the present study, on the basis of Bayesian inference, we investigated the behavior of estimated solutions of WDF method without arbitrary assumption. The performance of Means method, SVD method, and WDF method were also evaluated by using computer-generated data which imitate chorus emission.

地球磁気圏およびプラズマ圏内の科学衛星で観測されるプラズマ波動の特性調査は、波動の伝搬機構だけではなく、その励起・伝搬条件に影響を与えるプラズマ環境を知るために重要である。特にプラズマ波動の到来方向は、これらの特性の理解のために極めて有用な情報を提供する。

磁気圏およびプラズマ圏内の VLF 波動の到来方向推定には、科学衛星で観測される電磁場成分のクロススペクトルから構成されるスペクトルマトリクスが広く用いられている。スペクトルマトリクスを用いた到来方向推定問題の解法は、解析対象とする波動の性質を考慮したモデリングに応じて数多く提案されている。例えば、Means 法 [1] や、SVD 法 [2] は単一平面波の仮定の元に導かれるものであり、波動のエネルギー密度方向分布を推定する波動分布関数 (WDF) 法 [3] の理論はインコヒーレント波動のガウス性不規則信号としての取り扱いに基づいている。WDF 法の場合、推定対象である連続的な方向分布関数を一意に得るためには、少数のパラメータで規定される分布関数を仮定する必要がある。また、従来の方向推定手法の評価は、各手法の仮定に適合した擬似データによってなされる場合が多く、手法相互の性能比較やコーラスのように周波数変動を伴うコヒーレント波動に対する推定解の評価は少ない。

本研究では、波動分布関数法の評価にあたって、ベイズ推定理論に基づき方向分布関数に対する恣意的な仮定を極力排除した条件下での推定解の挙動を調査した。また、コーラスを模擬した擬似データによる Means 法、SVD 法、WDF 法の性能評価を行った。

参考文献

1. Means, J. D., "Use of the Three-Dimensional Covariance Matrix in Analyzing the Polarization Properties of Plane Waves," *Journal of Geophysical Research*, 77(28), pp. 5551-5559, 1972.
2. Santolik, O., M. Parrot, and F. Lefeuvre, "Singular value decomposition methods for wave propagation analysis," *Radio Science*, 38(1), 2003.
3. Storey, L. R. O., and F. Lefeuvre, "The analysis of 6-component measurements of a random electromagnetic wave field in a magnetoplasma I. The direct problem," *Geophysical Journal International*, 56(2), pp. 255-268, 1979.

音声信号処理による VLF エミッションの雑音除去とオーロラヒスの発生周波数解析

出島 工 [1]; 尾崎 光紀 [2]; 八木谷 聡 [3]; 塩川 和夫 [4]; 三好 由純 [5]
[1] 金沢大・自然研; [2] 金沢大・理工・電情; [3] 金沢大; [4] 名大宇地研; [5] 名大 ISEE

Noise reduction technique for VLF emissions by audio signal processing and generation frequency analysis of auroral hiss

Takumi Dejima[1]; Mitsunori Ozaki[2]; Satoshi Yagitani[3]; Kazuo Shiokawa[4]; Yoshizumi Miyoshi[5]
[1] Kanazawa Univ.; [2] Electrical and Computer Eng., Kanazawa Univ.; [3] Kanazawa Univ.; [4] ISEE, Nagoya Univ.; [5] ISEE, Nagoya Univ.

VLF emissions (right-handed circularly polarized waves) are common phenomena in the magnetosphere. VLF emissions greatly contribute to pitch angle scattering for the generation of pulsating aurora (tens of keV to 100 keV electrons) and acceleration of MeV electrons in the radiation belts. We have been conducting the ground-based observations of VLF emissions (10Hz to tens of kHz) at Athabasca ($L = 4.3$) in Canada. Ground-based observations can continuously observe VLF emissions propagating along the geomagnetic field line from the magnetospheric source region at a fixed L with a high time resolution. However, observation data include stationary noise (white noise and line noise etc.) and a pulse noise (atmospheric noise and artificial clock noise etc.) coming from artificial facilities.

We have studied a noise reduction technique by using audio signal processing techniques. To remove the stationary noises, we use spectral subtraction (SS) method. SS method uses an average noise spectrum in the noisy data to remove background noise components in the frequency domain. In this study, to estimate the average noise spectrum, spectral entropy method is used for distinguishing the signals from the noises. The spectral entropy for the noises becomes larger due to its random behavior. In contrast, the spectral entropy for the signals becomes smaller. Chirp signals (2 to 4 kHz) (simulated chorus waves) with stationary noises were evaluated by using the SS method. The noise reduction result by the SS method showed that the SNR was improved from 0dB to 10dB. We could extract auroral hiss emissions from observation data including strong lighting sferics (5 to 10 kHz) by using the SS method combined with the expected wave polarization. Auroral hiss emissions had a lower cutoff frequency of around 10 kHz and showed a good correlation with auroral activity. The lower cutoff frequency of auroral hiss decreased as the auroral activity moved to lower latitudes. This would be caused by the latitude dependence of the resonance cone angle of auroral hiss.

In this presentation, we will discuss our noise reduction technique for VLF emissions and generation frequency analysis of auroral hiss in detail. We believe that our noise reduction technique can significantly contribute to reduction in the cost and time for a conventional EMC test.

磁気圏で観測される VLF エミッションは、脈動オーロラ (数十 keV~100keV) の発生や放射線帯 MeV 電子など高エネルギー粒子のピッチ角散乱や加速に大きく寄与している。我々は、磁力線で放射線帯とつながるカナダのアサバスカ ($L=4.3$) にて VLF エミッション (10 Hz~数十 kHz) の地上連続観測を行っている。地上観測は、固定の L 値で電磁波動現象を高い時間分解能で連続観測できる利点がある。しかし、VLF エミッションの他に観測機器や伝搬経路で生じた雑音が観測波形に含まれる欠点がある。伝搬経路で生じる雑音は、定常雑音 (白色雑音やライン雑音など) とパルス性雑音 (空電雑音や機器のクロック雑音など) の 2 種類がある。我々は VLF エミッションが可聴周波数帯域であることに着目し、音声信号処理技術を用いて雑音除去の検討を行っている。本研究では、定常雑音を除去するために、音声信号処理で一般に用いられるスペクトルサブトラクション (SS) 法を用いた。SS 法は事前に雑音スペクトルを推定し、周波数領域で雑音成分を除去する手法である。本研究では、事前雑音スペクトルを推定するために、スペクトルエントロピー法を用いた。スペクトルエントロピーは定常雑音の区間はランダム性のため値が大きく、信号区間では小さくなるため、雑音区間と信号区間を区別することができる。コーラス波動を模擬したチャープ信号 (2~4kHz) に定常雑音を付加したテスト信号に SS 法を適用した。雑音除去性能の評価を行った結果、SNR が 0dB から 10dB に改善される結果を得た。

さらに、SS 法による雑音除去に加えて VLF エミッションは右回りの円偏波成分をもつ性質を利用し、VLF エミッションが発生している領域の抽出を行う。その結果、雷空電 (5~15 kHz) に隠れていたオーロラヒスを検出することができた。オーロラヒスは、10 kHz 付近に強度のピークをもち、オーロラの出現とよい相関をもって発生するプラズマ波動現象である。オーロラヒスのスペクトルと撮影したオーロラ画像を比較した結果、オーロラヒスの発生周波数が低くなるほど、オーロラの出現する領域の緯度が低くなっている傾向が見られた。これは、低緯度側でレゾナンスコーンの角度が大きくなり、電離層を突き抜ける低周波の波動が多くなるためと考えられる。

本発表では、VLF エミッションの観測データの雑音除去法、オーロラヒスの発生周波数とオーロラの緯度の相関関係について詳細に報告する。信号処理による雑音除去法は、従来の EMC 試験などのコストを大幅に削減できることに貢献できると考えている。

Propagation Characteristics of Omega Signals with Regard to Plasma Density and Ambient Magnetic Field

Suarjaya I Made Agus Dwi[1]; Yoshiya Kasahara[1]; Yoshitaka Goto[1]
[1] Kanazawa Univ.

Poynting Flux Analyzer (PFX) subsystem on board the Akebono satellite had been received signals at 10.2 kHz from Omega system since 1989 to 1997. Omega was a navigation system which transmitted its signals based on pattern every 10 seconds. Because the global plasmaspheric electron density changes day by day, it is important to see the trend of this change by using statistical study of electromagnetic wave propagation for several years. Observing signal from artificial transmitters is worth analyzing for such purpose because these signals were transmitted with constant power all the time, thus we can analyze how much change happened to the propagation depending on local time, season and solar activity. To analyze these data, we developed a method for automatic detection of Omega signals from the PFX data in a systematic way, it involves identifying a transmission station, calculating the delay time, and estimating the signal intensity.

Based on the PFX data from October 1989 to September 1997, our analysis on high-middle latitude of omega station revealed that signals transmitted from two stations located at Norway and North Dakota, whose geomagnetic latitude are almost the same at 55.9 N, propagated along the Earth's magnetic field through different L-shell. We believe this was caused by different latitude in geographic coordinate, where the Norway station was located at 56.42 N and the North Dakota station was located at 46.37 N. Thus, the different sunlit condition affected the plasmaspheric electron density, that is, the night duration is expected to be longer at the Norway station than the North Dakota station. This finding also clarified by our seasonal analysis, by looking at the shifted high intensity region especially in the electric field because of change in day and night duration between equinox and solstice. We found that the omega signal tends to propagate farther in the night side where the plasmaspheric electron density lower than in day side. Lower intensity level especially near the equator in day side suggested denser plasmaspheric electron density in that region. We also found that solar activity effects the omega signal propagation. In 1991 when the solar activity was maximum, the omega signal propagated lower in intensity level and in 1996 when the solar activity was minimum, the omega signal propagated higher in intensity level and farther from the transmitter station. Both of the seasonal and yearly analyses confirmed that plasmaspheric electron temperatures also affected the propagation of Omega Signal.

Causal Relationship between Relativistic Electron Acceleration and Microbursts depend on Magnetic Latitude of Whistler Chorus

Shinji Saito[1]; Yoshizumi Miyoshi[2]; Satoshi Kurita[2]
[1] Nagoya Univ.; [2] ISEE, Nagoya Univ.

We investigate flux enhancement and atmospheric precipitation of relativistic electrons associated with whistler chorus elements propagating along a magnetic field line, by using GEMSIS-RBW simulation code (RBW). The RBW is a test-particle code solving bounce motion of electrons along a field line, parallel propagating whistler chorus, and wave-particle interactions by using the equation of motion. The RBW simulation can calculate scattering processes, not only diffusion process but also nonlinear scattering processes such as phase bunching and phase trapping in coherent whistler chorus. Especially the phase trapping process accelerates electrons from a few hundred keV to a few MeV in a short time scale which is of the order of a second.

By using the RBW simulations we compare simulation results with observations which have discussed in Kurita et al.(GRL 2015). They found that whistler chorus waves responsible for flux enhancement of relativistic electrons involves relativistic electron microbursts simultaneously. Microbursts are a good proxy to indicate that whistler chorus activity actually causes significant variations of relativistic electrons. Our simulations demonstrate that both the relativistic electron flux and relativistic electron precipitation into the atmosphere are more enhanced as the whistler chorus waves propagate more away from the equator. We will discuss dependency of latitude of the whistler chorus on the flux enhancement and precipitation of relativistic electrons.

[1] Kurita, S., Y. Miyoshi, J. B. Blake, G. D. Reeves, and C. A. Kletzing (2016), Relativistic electron microbursts and variations in trapped MeV electron fluxes during the 8-9 October 2012 storm: SAMPEX and Van Allen Probes observations, *Geophys. Res. Lett.*, 43, 3017-3025, doi:10.1002/2016GL068260.

EMIC ライジングトーンとの相互作用によるプロトンのピッチ角散乱の直接検出

北原理弘 [1]; 加藤 雄人 [1]; 小路 真史 [2]; 三好 由純 [2]
[1] 東北大・理・地球物理; [2] 名大 ISEE

Direct measurement of pitch angle scattering of protons by EMIC rising tones observed by THEMIS satellites

Masahiro Kitahara[1]; Yuto Katoh[1]; Masafumi Shoji[2]; Yoshizumi Miyoshi[2]
[1] Dept. Geophys., Grad. Sch. Sci., Tohoku Univ.; [2] ISEE, Nagoya Univ.

Electromagnetic Ion Cyclotron (EMIC) waves with rising tone have been observed by various satellites in the Earth's inner magnetosphere (Pickett et al., 2010; Sakaguchi et al., 2013; Nakamura et al., 2014; Engebretson et al., 2015). EMIC waves are generated by anisotropic ions and scatter the pitch angle of energetic ions through the cyclotron resonant interactions. Previous simulation studies have reproduced EMIC rising tones using the one dimensional hybrid code. In the simulation, the pitch angle of energetic protons is effectively scattered by EMIC rising tones and velocity distribution function is strongly modulated (Shoji and Omura, 2011; 2013). Furthermore, observation study indicates protons scattered by EMIC rising tones precipitate into the atmosphere and cause proton aurora (Nomura et al., 2016).

Fukuhara et al. (2009) proposed a new type instrument called Wave-Particle Interaction Analyzer (WPIA) as a new means of the study of wave-particle interactions. One of methods of the WPIA is to calculate the energy exchange between waves and particles and the method enables us to evaluate wave-particle interactions directly and quantitatively (Katoh et al., 2013). The method is applied to EMIC rising tones observed by the THEMIS satellite and the feasibility of the method and the adequacy of the nonlinear theory is evaluated (Shoji et al., submitted). In addition to the method to detect the energy exchange, we have proposed a method to directly detect the pitch angle scattering of resonant particles by calculating G (Kitahara and Katoh, 2016), which is defined as the accumulation value of a pitch angular component of the Lorentz force acting on each particle and indicates the lost momentum of waves.

In this study, we apply the proposed WPIA method (Kitahara and Katoh, 2016) to the EMIC rising tone event observed by THEMIS satellite on September 9, 2010. During this event, THEMIS A, D, and E were close to each other (within $0.4 R_E$) in the dayside inner magnetosphere ($R_{GSM} \sim 8.5 R_E$, LT ~ 13 h, LAT ~ 5 deg) and all of those satellites observed the same EMIC rising tone packets almost simultaneously. We calculate the G value from burst-mode data of the Electrostatic Analyzer (ESA), the Electric Field Instrument (EFI), and the Fluxgate Magnetometer (FGM) installed on each THEMIS satellite. In results of analysis, we detect the pitch angle scattering of protons in the energy range from 4 keV to 10 keV in the data of each satellite. We observed multiple enhancements of the amplitude of EMIC waves in the event, and we obtained significant G values at the timing of the enhancements. Using the WPIA analysis, we successfully identify the G values whose sign indicates the direction of the pitch angle scattering as a function of kinetic energy and pitch angle of protons. The results of analysis indicate that energetic protons are scattered toward the loss cone through the interaction at a timing of the wave enhancement. This characteristic depends on the proton energy range, and sometimes we obtained the opposite sign of G . In this presentation, we also discuss details of the calculation method and the statistical significance of G value.

Relativistic electron microbursts during different solar wind drivers

Satoshi Kurita[1]; Yoshizumi Miyoshi[1]

[1] ISEE, Nagoya Univ.

Relativistic electron microbursts are short-lived and bursty precipitations of relativistic electrons due to pitch angle scattering by discrete whistler mode emissions known as chorus [e.g., Lorentzen et al., 2001]. They are frequently observed during storm-time conditions [e.g., O'Brien et al., 2003] and high-speed solar wind stream (HSS) events [e.g., Blum et al., 2015], while important solar wind drivers for the frequent microburst precipitations have not been well understood. Using the data obtained by SAMPEX, we perform a superposed epoch analysis of the microburst occurrence during geomagnetic disturbances caused by two different solar wind drivers: HSS and the coronal mass ejection (CME). The HSS events are further categorized by considering the polarity of interplanetary magnetic field and solar wind speed according to the method used by Miyoshi and Kataoka (2008). In case of the HSS events, we find the most frequent microburst precipitations during the higher-speed solar wind streams with a southward offset of IMF (SBZ-fast HSS events). The microburst activity during the fast SBZ-HSS events is identified at L value range from 4.0 to 6.0 and lasts for several days after the arrival of stream interface. On the other hand, during the CME-driven geomagnetic storms, microbursts are frequently observed at L-value range from 3.5 to 5.0 and its activity continues for about 12 hours after the minimum in the Dst index. This indicates that resonant interaction between chorus and relativistic electrons more frequently and continuously takes place during the SBZ-fast HSS events than during the other HSS events and CME-driven storms. Since fluxes of radiation belt electrons largely increase during the SBZ-fast HSS events [Miyoshi and Kataoka, 2008; Miyoshi et al., 2013] and microburst activity coincides well with local acceleration by chorus [Kurita et al., 2016], the result gives observational support that relativistic electron microbursts are a proxy of acceleration of MeV electrons by chorus as suggested by Kurita et al. [2016]. We propose that highly relativistic electrons are preferentially produced during the SBZ-fast HSS events via resonant interaction with chorus which causes relativistic electron microbursts.

地球磁気圏サブパケットコーラス波によるサイクロトロン共鳴電子加速過程

平賀 涼子 [1]; 大村 善治 [2]
[1] 京大・工; [2] 京大・生存圏

Dynamics of energetic electrons interacting with sub-packet chorus emissions in the magnetosphere

Ryoko Hiraga[1]; Yoshiharu Omura[2]
[1] Engineering, Kyoto Univ.; [2] RISH, Kyoto Univ.

The recent study has revealed RTA and URA processes, the acceleration of relativistic electrons by interaction with chorus emissions. The wave model, however, is found to require some updates based on the recent observations. We develop a new wave model compatible with the observations and study the particle motion under the influence of this new wave model. The most distinctive feature of the new model is its amplitude growth manner. The wave is excited near the equator and grows in amplitude as an absolute instability as a function of time. This amplitude growth is bounded by the optimum and threshold amplitudes. When the amplitude grows to reach the optimum amplitude, it drops down to the threshold value and repeats the growth with a saw-like shape defined as sub-packet wave. The sub-packet wave generated near the equator experiences the convective amplitude growth propagating to the higher latitude region. Since the group velocity of the wave propagation is a function of its frequency, a wave source generated and released from the equator at a certain time and a group velocity could be overtaken by another wave released at a later timing and hence a faster group velocity. Furthermore, the chorus wave propagation is also strongly influenced by the initial frequency of its generation process near the equator. Since the group velocity grows to the maximum when the wave frequency is a quarter of the local gyrofrequency, f_{ce} , a chorus wave generated at a lower initial frequency than one fourth of f_{ce} is compressed during the propagation process. This is because frequency of chorus wave is increased at the equator and consequently a wave generated at a later timing has a closer frequency to one fourth of f_{ce} to propagate faster than those waves released at earlier timings. By the same logic, chorus wave with a higher initial frequency than one fourth of f_{ce} is elongated during the propagation by getting the frequency away from one fourth of f_{ce} and hence slowing down the propagation speed as time passes. In sub-packet case, this frequency value is further affected by the sub-packet amplitude wave form to make the process more complex. Into this new wave form, energetic electrons are inserted and their motions are examined. For example, a resonant electron can be entrapped by the wave, being accelerated and normally detrapped after a certain period of time, but there can be a possibility that the following sub-packet wave in a complex propagation manner coincidentally entraps the electron to provide multiple accelerations. We injected a large number of electrons over a wide energy range from 10keV to 10MeV into the sub-packet wave to simulate the nonlinear dynamics of RTA and URA. The electrons motion or more precisely entrapping and detrapping processes are examined under various conditions.

内部磁気圏における運動論的不安定性の高エネルギー粒子ハイブリッドシミュレーション

天野 孝伸 [1]; 三好 由純 [2]; 関 華奈子 [3]
[1] 東大・理; [2] 名大 ISEE; [3] 東大理・地球惑星科学専攻

Energetic Particle Hybrid Simulations for Kinetic Instabilities in the Inner Magnetosphere

Takanobu Amano[1]; Yoshizumi Miyoshi[2]; Kanako Seki[3]
[1] University of Tokyo; [2] ISEE, Nagoya Univ.; [3] Dept. Earth & Planetary Sci., Science, Univ. Tokyo

The energetic ring current particles dominate the plasma pressure in the inner magnetosphere. Therefore, it is essential to take into account the ring current dynamics in understanding the various inner magnetospheric phenomena. It has been known that the Magnetohydrodynamics (MHD) approximation is not adequate in numerical modeling of the ring current dynamics and the kinetic effect associated with the ring current ions must be taken into account for modeling the global magnetic-field reconfiguration in the inner magnetosphere. In addition, local kinetic instabilities excited by the ring current population may also play important roles. For instance, the so-called drift-bounce resonance has been considered to be a plausible mechanism for internal excitation of Pc5 ULF waves. Also, Electro-Magnetic Ion-Cyclotron (EMIC) waves responsible for pitch-angle scattering for relativistic radiation belt electrons are thought to be excited by the temperature anisotropy of energetic protons.

We have developed a new three-dimensional numerical simulation code that incorporates the self-consistent coupling between the fully kinetic ring current particle dynamics and the cold background plasma. In other words, it is essentially a hybrid code that solves the ring current ions by using the particle-in-cell method, whereas the two-fluid approximation is adopted for the background electron and proton fluids. The coupling between the two populations has been introduced in a systematic manner. By performing kinetic temperature-anisotropy driven instabilities in a homogeneous plasma, we show that the code is indeed capable of describing the kinetic effect associated with the ring current ions. The code is applied for studying the ring-current driven kinetic instabilities with the effect of background magnetic-field inhomogeneity. An initial equilibrium obtained by iteratively solving a Grad-Shafranov-like equation for an anisotropic bounce-averaged ring current pressure distribution is used. We investigate the dependence of the instability on the plasma beta, temperature anisotropy, and the ratio between the Larmor radius and the gradient scale length of the background magnetic field.

Pitch angle dependence of drift resonance and its effects on the formation of pitch angle distributions of relativistic electrons

Kei Kamiya[1]; Kanako Seki[2]; Shinji Saito[3]; Takanobu Amano[4]; Yoshizumi Miyoshi[5]

[1] STEL, Nagoya Univ.; [2] Dept. Earth & Planetary Sci., Science, Univ. Tokyo; [3] Nagoya Univ.; [4] University of Tokyo; [5] ISEE, Nagoya Univ.

Radial transport of relativistic electrons in the inner magnetosphere can be driven by drift resonance with Pc5 Ultra Low Frequency (ULF) waves. Radial transport due to the drift resonance has also been considered as an important acceleration candidate of the outer radiation belt electrons. A key point of the drift resonance is that the energy and equatorial pitch angle of electron changes with the radial transport under conservation of first and second adiabatic invariants. It can affect the drift period of electron and make the resonant electron become longer into the resonant range. Therefore, the transport efficiency of electrons is different from each equatorial pitch angle and it is expected to contribute the formation of pitch angle distribution.

In this study, we focus on the radial transport of relativistic electrons due to the drift resonance with a monochromatic Pc5 wave and investigate dependence of the radial transport on the equatorial pitch angle of electron. For this purpose, we combine two simulation models of the inner magnetosphere: GEMSIS-RC (ring current) and RB (radiation belt) models. The GEMSIS-RC model is a self-consistent and kinetic numerical simulation code solving the five-dimensional Boltzmann equation for the ring-current ions coupled with Maxwell equations. The GEMSIS-RB code conducts test particle trajectory tracings of relativistic electrons in arbitrary magnetic and electric field configurations. We first conduct Pc5 wave simulation with GEMSIS-RC, and then the obtained time variations of the magnetic and electric fields are used as inputs to GEMSIS-RB to trace relativistic electron trajectories under the calculated Pc5 wave. We trace a great number of electrons to sample wide range of 5-D phase space. Simulation results show the pitch angle distribution can be formed butterfly distribution from the initial flat distribution. We also discuss the differences of transport efficiency of electron with each equatorial pitch angle.

Characteristics of Pc5 Wave Observed by two GOES Satellites during MeV Electron Flux Enhancement

Kentarou Kitamura[1]; Satoko Saita[2]; Yoshimasa Tanaka[3]; Akiko Fujimoto[4]
[1] NIT,Tokuyama.; [2] NITkit; [3] NIPR; [4] ICSWSE, Kyushu Univ.

It is well known that MeV electron flux efficiently increases during the recovery phase of magnetic storms. ULF wave propagating in the magnetosphere is recognized as one of the possible candidates which can accelerate the electron in the radiation belt while various acceleration processes have been widely proposed by many investigators.

In this study, total 20 electron flux enhancement events associated with the CIR (Corotating Interaction Region) driven storms in 2008 have been analyzed using the magnetic field vector data obtained by GOES 10 and 11 satellites. The GOES 10 and 11 were located at 60 deg. and 75 deg. West in geographical longitude, respectively, which corresponds to 1 hour separation in local time. We used the bandpass filtered (150-1000 sec) magnetic data in the ENP coordinate system to investigate the oscillation mode of the field line and the propagation characteristics of Pc5 pulsations in the GEO orbit (6.6 Re).

The Pc5 power in the P (northward) component is predominant in the dusk sectors during main phase of the magnetic storms. The time lag of the Pc5 observed by GOES 10 and 11 satellites was analyzed to estimate the azimuthal wave number (m) of Pc5. As the result, both compressional and transverse modes of Pc5 show the anti-sunward propagation on the frank side of the GEO orbit with small m number of ~ 1.5 . On the other hand, the temporal variation of peak frequency of Pc5 shows the obvious local-time dependence during the early recovery phase of the storm. The peak frequency decreases to 2.2-2.5 mHz during the early recovery phase. This feature is predominant at the evening to night sectors in the P component and at the morning and evening sectors in the E (earthward) and N (eastward) components.

The latter result suggests that the Pc5 wave associated with the MeV electron flux enhancement seems to be related to the plasma injection in the night side during the early recovery phase of the storm, whereas the anti-sunward propagation of the Pc5 is also suggested in the former result. Both results imply that the Pc5 wave during the MeV electron flux enhancement seems to be generated simultaneously by several sources associated with the passage of high speed solar wind such as Kelvin Helmholtz Instability, dynamic pressure disturbances in the solar wind and particle injection in the night side magnetosphere related to the substorm.

Ionospheric Alfvén resonator and Pc1 geomagnetic pulsations observed at low-latitude ground station

Masahito Nose[1]; Makoto Uyeshima[2]; Jun Kawai[3]; Hideaki Hase[4]
[1] DACGSM, Kyoto Univ.; [2] ERI, Univ. Tokyo; [3] AEL, KIT; [4] KSVU, Tokyo Tech

We started observations by an induction magnetometer at low-latitude station, Muroto (GMLAT=24.40 degree), in December 2013. Cadence of data is 64 Hz. We find that geomagnetic pulsations below 4 Hz are sometimes active even at low-latitude during nighttime and can be classified into the following three categories according to their features in dynamic power spectrum: (1) broad-band resonance structures with a frequency separation between adjacent bands (Δf) of approximately 0.5-1.0 Hz, (2) narrow-band resonance structures with $\Delta f \sim 0.1-0.3$ Hz, and (3) bursty unstructured enhancements around 0.5-2 Hz. We suppose that the pulsations of categories 1 and 2 are caused by the ionospheric Alfvén resonator, in which the shear Alfvén waves are trapped in the F region ionosphere that is bounded by sharp gradients of the Alfvén velocity. The pulsations in category 3 are considered to be low latitude Pc1 geomagnetic pulsations. We will examine statistical characteristics of these pulsations and discuss possible excitation mechanisms.

モンテカルロ法による磁力線固有振動数推定の並列計算手法についての研究

才田 聡子 [1]; 河野 英昭 [2]; 尾花 由紀 [3]

[1] 北九州高専; [2] 九大・理・地球惑星; [3] 大阪電通大・工・基礎理工

A Parallel computation technique for the Monte Carlo solutions of the field line

Satoko Saita[1]; Hideaki Kawano[2]; Yuki Obana[3]

[1] NITkit; [2] Earth and Planetary Sci., Kyushu Univ.; [3] Engineering Science, Osaka Electro-Communication Univ.

Shear Alfvén waves propagating along a geomagnetic field line can form standing waves along the field line. The magnetic field intensity and the plasma mass density affect the velocity of shear Alfvén waves. Thus temporal and spatial variations in the field-line eigenfrequency are potentially caused by variations in the field-line length, the magnetic field intensity, and the mass density along the field line.

We can estimate the eigenfrequency by numerically solving the standing Alfvén wave equation along the geomagnetic field.

In this paper we propose a parallel computation technique for the Monte Carlo solutions of the standing Alfvén wave equation along the geomagnetic field line.

磁気圏内に発生する磁気流体波動の中でも磁力線沿いに伝搬し定在振動する波動は shear Alfvén wave(以下 Alfvén 波) という名前で知られている [Obayashi and Jacobs, 1958]。Alfvén 波の速度は磁場強度と質量密度に依存するため、定在振動の周波数は磁力線の長さや磁力線沿いの磁場圧・質量密度に依存している [Kitamura and Jacobs., 1968; Troitskaya, 1997]。この弦振動に近似される現象を FLR (Field Line Resonance) と呼ぶ。FLR は地上磁場観測では高緯度で Pc4-5、低緯度で Pc3-4 周波数帯の地磁気脈動として観測される。そして定在振動の周波数を FLR 周波数と呼ぶ。磁力線沿いに定在振動する Alfvén 波の波動方程式の数値解を求めることで任意の時間と空間における FLR 周波数の推定が可能だが、一般的には波動方程式の数値解を求めるには多くの時間計算量が必要である。

本研究では多数のプロセッサを使う並列演算を用いて高速に FLR 周波数を推定する手法を確立することを目的とする。本論文ではモンテカルロ法による解法を検討した。モンテカルロ法による解法の特徴の 1 つは任意の解を他の解とは独立に計算できることである。したがって、演算の並列化が容易である。

本論文では従来の反復法を用いた解法とモンテカルロ法を用いた解法の違いを比較し、並列演算による FLR 周波数推定の有効性について検証する。

Kitamura, T., Jacobs, J. A., 1968. Determination of the magnetospheric plasma density by the use of long-period geomagnetic micropulsations. *J. Geomag. Geo- electr.* 20, 33 – 43.

Obayashi, T., Jacobs, J. A., 1958. Geomagnetic pulsations and the earth ' s outer atmosphere. *Geophys. J. R. astr. Soc.* 1, 53.

Singer, H. J., Southwood, D. J., Walker, R. J., Kivelson, M. G., 1981. Alfvén wave resonances in a realistic magnetospheric magnetic field geometry. *J. Geophys. Res.* 86 (A6), 4589 – 4596.

Troitskaya, V. A., 1997. Early ground based approach to hydromagnetic diagnostics of outer space. In: *Discovery of the Magnetosphere, History of Geophysics.* Vol. 7. AGU, p. 221.

磁気嵐時におけるプラズマシート電子地球側境界に関する研究

大木 研人 [1]; 熊本 篤志 [2]; 加藤 雄人 [3]

[1] 東北大・理・地球物理; [2] 東北大・理・地球物理; [3] 東北大・理・地球物理

Study of the plasma sheet electron inner boundary during the magnetic storm

Kento Ohki[1]; Atsushi Kumamoto[2]; Yuto Katoh[3]

[1] Dept. Geophys., Grad. Sch. Sci., Tohoku Univ.

; [2] Dept. Geophys, Tohoku Univ.; [3] Dept. Geophys., Grad. Sch. Sci., Tohoku Univ.

The locations of the inner boundary of the plasma sheet electrons during magnetic storm have been analyzed by using the dataset from Time History of Events and Macroscale Interactions during Substorms (THEMIS) satellites. The dependence of the location of the inner boundary of the plasma sheet electrons on geomagnetic indices such as Kp and AE was investigated in several previous studies [Korth et al., 1999; Jiang et al., 2011]. As for the convection electric, a simple model such as Volland-Stern model [Volland, 1973; Stern, 1975] is suggested.

In this study, we investigated the locations of the inner boundary of the plasma sheet electrons by using the electron flux data of 9 keV obtained by Electrostatic Analyzer (ESA) onboard the THEMIS satellites during the magnetic storms and compared these with the open/close boundary of the drift path of the electrons with Volland-Stern convection electric field model [Volland, 1973; Stern, 1975] using the test particle simulation to suggest the new electric field model during the magnetic storm.

From the analysis of the inner edge observed by THEMIS-A during the magnetic storm on June 17, 2012 (Case 1) and observed by THEMIS-A during the magnetic storm on October 1, 2012 (Case 2) around 21:00 MLT, we found that the observed inner edge was located nearer to the Earth than that expected based on Volland-Stern electric field due to some additional electric field. The geocentric distance of open/close boundary, R_{model} , is estimated to be 5.46 in Case 1, and 6.41 in Case 2. In Case 1, the geocentric distance of the inner edge in the magnetic equatorial plane, R_{obs} , is 4.01, which is far less than $R_{\text{model}} = 5.46$, while in Case 2 R_{obs} is 6.10, which is as large as $R_{\text{obs}} = 6.41$.

Also from another analysis of the inner edge observed by THEMIS-E during the magnetic storm on June 17, 2012 (Case 3) and observed by THEMIS-D during the magnetic storm on July 9, 2012 (Case 4) around 20:00 MLT, similar results are obtained: $R_{\text{obs}} = 4.30$ and $R_{\text{model}} = 5.50$ in Case 3, while $R_{\text{obs}} = 6.00$ and $R_{\text{model}} = 6.18$ in Case 4. These results suggest that in the sector from 18:00 to 24:00 MLT, some electric field appears in addition to large-scale magnetospheric convection electric field around 4 RE and within 6 RE.

In the future, it will be necessary to suggest the electric field model including the additional electric field during the magnetic storm.

れいめい衛星観測による磁気嵐中の降込電子に関する考察

益岡 葵 [1]; 高田 拓 [2]; 浅村 和史 [3]
[1] 高知高専・機械電気専攻; [2] 高知高専・電気; [3] 宇宙研

The study of precipitating electrons observed by Reimei satellite during magnetic storm

Aoi Masuoka[1]; Taku Takada[2]; Kazushi Asamura[3]
[1] Kochi-CT; [2] Kochi-CT; [3] ISAS/JAXA

Reimei satellite observed the particle precipitation in an auroral zone, with a polar orbit of an altitude of approximately 620km. When a magnetic storm occurs in the magnetosphere, Reimei satellite observed complex structures of precipitating electrons in a wide range of magnetic latitudes. The space-time distribution of these precipitating electrons is not quantitatively examined. We examined structure distributions of precipitating electrons during magnetic storm. We discuss the generation mechanism of such precipitating electrons, based on characteristics of field-aligned currents and acceleration region.

2015年3月17日の磁気嵐発達に対する酸素イオンの寄与の時間変化

桂華 邦裕 [1]; 三好 由純 [1]; 能勢 正仁 [2]; 町田 忍 [3]; 関 華奈子 [4]; Lanzerotti Louis J.[5]; Mitchell Donald[6]; Gkioulidou Matina[6]; Gerrard Andrew[7]; Manweiler Jerry W.[8]; スペンス ハラン [9]; Larsen Brian A.[10]
[1] 名大 ISEE; [2] 京大・理 地磁気センター; [3] 名大・ISEE; [4] 東大理・地球惑星科学専攻; [5] ニュージャージー工科大学; [6] JHU/APL; [7] NJIT; [8] Fundamental Technologies, LLC; [9] ニューハンプシャー大学; [10] LANL

Temporal variations of oxygen contribution to the ring current during the 17 March 2015 storm: Van Allen Probes observations

Kunihiro Keika[1]; Yoshizumi Miyoshi[1]; Masahito Nose[2]; Shinobu Machida[3]; Kanako Seki[4]; Louis J. Lanzerotti[5]; Donald Mitchell[6]; Matina Gkioulidou[6]; Andrew Gerrard[7]; Jerry W. Manweiler[8]; Harlan Spence[9]; Brian A. Larsen[10]
[1] ISEE, Nagoya Univ.; [2] DACGSM, Kyoto Univ.; [3] ISEE, Nagoya Univ.; [4] Dept. Earth & Planetary Sci., Science, Univ. Tokyo; [5] NJIT; [6] JHU/APL; [7] NJIT; [8] Fundamental Technologies, LLC; [9] Univ. New Hampshire; [10] LANL

We examine the contribution from oxygen ions to the development of the ring current during an intense storm that occurred on 17 March 2015, using Van Allen Probes observations. We primarily use data from the RBSPICE and HOPE instruments which cover a wide energy range of ions and determine composition. During the storm event, Van Allen Probes traveled in the pre-midnight sector on the outbound path and around midnight on the inbound path. The geocentric distance of spacecraft perigee and apogee is 1.1 RE and 5.8 RE, respectively; the orbital period is about 9 hours. The spacecraft completed four full orbits during the main phase of the storm, enabling us to examine temporal variations of the radial profile of ion energy density. The Dst index displayed a typical two-step decrease during the main phase.

The proton energy density was enhanced at an L range of 3 to 6 with a peak at $L \sim 4$. The inner edge was displaced earthward to $L \sim 2.5$ during the second Dst decrease. The energy density peaked at $L = 3 - 4$. The energy range that make the dominant contribution to the energy density differed between the two phases. The energy density was primarily dominated by 20-80 keV at $L \sim 3.5$ (0.01-0.1 keV/nT) during the first phase, while it was contributed predominantly from 80-120 keV at $L \sim 4$ (0.1-0.5 keV/nT) during the second phase. It is also noted that higher energetic protons with energies of 100-300 keV at $L \sim 3$ (0.1 - 1.0 keV/nT) made a significant or even dominant contribution near the Dst minimum. The results indicate that the proton energy density increased in three steps.

The oxygen energy density showed different temporal variations and radial profile from the proton energy density. It was enhanced during the first phase up to the proton energy density level in an L range of 3 to 5. However, it decreased by about an order of magnitude around the beginning of the second phase. It was increased again during the second phase, and its inner edge was displaced earthward to $L \sim 3$. It was further increased by a few factors particularly at $L \sim 3$ during the third phase. The radial profile was affected by temporarily impulsive enhancements more significantly than the proton energy density. The oxygen flux suddenly increased by a factor of ~ 3 during the main phase.

This presentation focuses most on such mass-dependent features of ring current ions to identify when and where ionospheric oxygen ions are energized to make a significant contribution to the ring current. We also examine temporal variations and pitch-angle evolution of lower-energy oxygen ions (lower than 10 keV) on a storm time scale to discuss about the significance of cold-to-warm oxygen supply from the ionosphere prior to the storm.

SECS reconstruction of ionospheric flow fluctuations observed by SuperDARN on St. Patrick's day 2015 storm

Tomoaki Hori[1]; Nozomu Nishitani[1]; Kunihiro Keika[1]; Mariko Teramoto[2]; Akimasa Ieda[3]; Shin'ya Nakano[4]; Kanako Seki[5]

[1] ISEE, Nagoya Univ.; [2] JAXA, ISAS; [3] ISEE, Nagoya Univ.; [4] The Institute of Statistical Mathematics; [5] Dept. Earth & Planetary Sci., Science, Univ. Tokyo

Our previous study reported that ULF-like fluctuations of ionospheric flow as seen by Super Dual Auroral Radar Network (SuperDARN) radars appeared in the sub-auroral region and they propagated westward over a wide range of local time during a stagnant period (~10:30-12:30 UT on March 17, 2015) in the main phase of the St. Patrick's day 2015 storm. In the present study, we further analyze the observed flow fluctuations to deduce the two-dimensional (2-D) ionospheric flow field. To reconstruct the 2-D flow distribution from the observed line-of-sight Doppler velocities (LOS_V) of SuperDARN radars, we employ a method of 2-D vector field expansion with the spherical elementary current systems (SECS) [Amm, JGG, 1997, Amm et al., JGR, 2010]. The merits of using this technique are that the analysis region, where a flow map is deduced from the observed LOS_Vs, can have any shape on a sphere and does not need to assume any boundary condition nor wavelength of spatial variation, favorable for SuperDARN observations with highly variable, non-uniform backscatter occurrence. Since we use only a set of divergence-free base functions of SECS for the present analysis, the resultant flow map satisfies by definition the incompressible flow condition ($\text{div } \mathbf{V} = 0$), which is expected to hold often in ionospheric plasma flows. We apply the technique to observations of two neighboring radars, the Christmas Valley East (CVE) and Fort Hays West (FHW) radars, which share a substantial part of their field-of-views (FOV) and actually have obtained LOS_V data in the common FOV for this event. The result of the flow map reconstruction shows that the analysis region between CVE and FHW generally has a slow, irregular flow during the stagnant period, in opposite to a fast eastward flow before and after the period, corresponding to strong sunward convection expected for the sub-auroral region in the morning sector during a storm main phase. The general evolution of the flow pattern is consistent with that deduced by the conventional map potential technique [Ruohoniemi and Greenwald, 1998]. It is also found that some shear/vortex-like flow structures pass over the analysis region during the stagnant period which appear to be moving westward in association with the westward-propagating flow fluctuations examined by the previous study. The existence of the moving flow shear/vortex structures indicates that a field-aligned current flows between the ionospheric flows and their magnetospheric counterpart driving the electric field fluctuations. These ionospheric observations suggest that the driving source for the ULF-like fluctuations is providing a series of shear Alfvén waves toward the ionosphere in the course of its westward drifting motion.

A Comparison of ULF waves in the inner magnetosphere and Kelvin-Helmholtz instability at the magnetopause

Mariko Teramoto[1]; Naritoshi Kitamura[2]; Craig A. Kletzing[3]; C. T. Russell[4]; Robert J. Strangeway[5]

[1] JAXA, ISAS; [2] ISAS/JAXA; [3] Department of Physics and Astronomy, UoI; [4] UCLA; [5] Inst. of Geophys. and Planet. Phys., Univ. of California, Los Angeles

Global ultra low frequency (ULF) pulsations are MHD plasma waves, that are observed in the magnetopause and on the ground. Several authors have shown that conditions in the solar wind are well correlated with ULF pulsations observed in the magnetosphere [Mathie and Mann, 2001]. ULF pulsations could be excited by Kelvin-Helmholtz (K-H) surface waves at the magnetopause, which is driven by the solar wind. Especially, the toroidal ULF wave dominantly occurs on the flankside in the inner magnetosphere, which is likely associated with the KH instability [Liu et al., 2009]. However, few studies examine whether the Kelvin-Helmholtz instability at the magnetopause is the source of ULF pulsations in the inner magnetosphere via in-situ observations.

We compared magnetic disturbances relating to K-H instability at the magnetopause to ULF perturbations in the inner magnetosphere between 09:21-11:27 UT on September 8, 2015, using data observed by MMS and VAPs satellites, when MMS and VAPs were located at the same local time in the dusk side (MLT \sim 15 h). When MMS crossed the low-latitude boundary layer between 09:20-10:07 UT, it observed KHI waves with the dominant frequency of 13 mHz. When MMS were located at the magnetosheath between 10:07-11:27 UT, the magnetic perturbations have broadband frequency range (10-25 mHz). VAPs-A, which was located at L \sim 5.5 at 10:00-11:00 UT, observed monochromatic Pc4 pulsations in both the radial and azimuthal components of the magnetic field at the dominant frequency of 12mHz and of the electric fields at the dominant frequency of 23 and 4 mHz.

We derived Poynting flux from the magnetic and electric field data from MMS. Poynting flux shows that the wave energy of the magnetic disturbances observed by MMS propagate southward at the LLBL and duskward at the magnetosheath. In this presentation, We will discuss relationship between KHI and ULF in the inner magnetosphere.

SuperDARN レーダーを用いた SI に伴う電離圏電場振動の統計解析

飯田 剛平 [1]; 西谷 望 [2]; 堀 智昭 [2]
[1] 名大・宇地研; [2] 名大 ISEE

Statistical analysis of ionospheric electric field oscillation associated with sudden impulse seen by SuperDARN radars

Kouhei Iida[1]; Nozomu Nishitani[2]; Tomoaki Hori[2]
[1] ISEE, Nagoya Univ.; [2] ISEE, Nagoya Univ.

Sudden Impulse (SI) is observed mainly as a sudden increase of the H-component of geomagnetic field at low latitudes. Past studies showed that it is caused by a sudden compression of the magnetosphere associated with rapid increases of the solar wind dynamic pressure. At middle and high latitudes, SIs cause perturbations associated with twin vortex type ionospheric currents. It was reported that the disturbance of the ionospheric current and the electric field associated with SI consists typically of the Preliminary Impulse (PI) and the Main Impulse (MI). Examining SI-associated flow variations observed by SuperDARN radars in the present study, we find that some of them show only the two successive pulses of PI and MI, while some others are accompanied by damped oscillations of the ionospheric electric field lasting for about several tens of minutes to an hour with periods of several minutes. The cause of this difference, however, has not yet been understood well.

We examine the cause of the difference between the two kinds of SI events, using SuperDARN radars in the northern hemisphere covering ~40 to 90 geomagnetic latitudes. For the analyzed period from January 2012 to December 2015, 199 SI events were identified and 38 events out of them were accompanied by the ionospheric electric field oscillations immediately following MIs, as observed by at least one SuperDARN radar. We find that some of the electric field oscillations exhibit phase differences in latitude and longitude, while some others not. These observations indicate that the ionospheric electric field oscillations sometimes have finite-speed two-dimensional propagation properties.

We discuss the frequency and propagation speed / direction estimated from two-dimensional distribution of Line-of-Sight Doppler velocity observed by SuperDARN radars, and also discuss the characteristics of the ionospheric electric field oscillations from the viewpoint of the dependences on the MLT spatial displacement of the magnetopause.

磁気急始 (Sudden Impulse, SI) は、地磁気 SYM-H 指数等にも現れる低緯度地磁気水平 (H) 成分の急激な増大として観測され、それは太陽風動圧の急増によって磁気圏が急激に圧縮されることが原因であると知られている。また、中高緯度においては、電離圏に通常存在するプラズマ対流に重畳して、SI に伴う対流変動を生じることがある。この SI に伴って起こる電離圏の対流変動は、Preliminary Impulse (PI) と Main Impulse (MI) の重ね合わせとして現れるが、この一対のインパルス的な変動のみで終了する場合と、このインパルス的な変動の後に、継続時間が数十分~1 時間程度で周期が数分~十数分の電離圏電場の振動を伴う場合があることが過去の観測からわかっている。しかし、この違いを発生させる原因はまだ完全には特定されていない。そこで、我々の研究では、世界各地に設置された SuperDARN レーダーのうち、北半球のレーダーを用いて、SI の後に続いて起こる電離圏電場の振動について統計的に解析を行うことで、これら 2 つの種類 SI イベントの違いを生み出している原因を探ることを目的としている。

2012 年 1 月から 2015 年 12 月の期間について、地磁気 SYM-H 指数と太陽風動圧の OMNI database を用いて SI を同定し、SI イベント時の SuperDARN レーダーのデータから電離圏電場の振動の有無について定量的に調べた。その結果、199 例の SI イベントが得られ、そのうち、38 例のイベントにおいて、少なくとも 1 箇所の SuperDARN レーダーで電離圏電場の振動が確認された。更に、レーダーの Range-Time-Intensity プロットから、一部の電離圏電場の振動において、1 レーダーの視野内で緯度・経度方向に位相のずれが存在することがわかった。このことは、SI に伴う電場振動が、ある 2 次元的な構造をもって伝搬していることを示唆している。

発表では、レーダーによって得られた 2 次元分布から見積もられた、振動の周波数や伝搬方向に関する解析結果の考察だけでなく、SI に伴う電場振動における磁気地方時への依存性や SI イベント前後の磁気圏境界面の変位量の比較といった観点から統計的に調べた結果についても議論する。

大規模沿磁力線電流を駆動する磁気圏ダイナモ機構

渡辺 正和 [1]; 田中 高史 [2]; 藤田 茂 [3]
[1] 九大・理・地惑; [2] 九大・宙空センター; [3] 気象大

Magnetospheric dynamo driving large-scale field-aligned currents

Masakazu Watanabe[1]; Takashi Tanaka[2]; Shigeru Fujita[3]
[1] Earth & planetary Sci., Kyushu Univ.; [2] SERC, Kyushu Univ.; [3] Meteorological College

Using a magnetohydrodynamic (MHD) description, we develop a general theory of the magnetospheric dynamo driving large-scale field-aligned currents (FACs). The purpose of this study is to provide a physical basis in interpreting various phenomena in the magnetosphere-ionosphere system reproduced by global MHD simulations. Numerical simulations indicate that in the magnetosphere plasma thermal energy is much higher than flow kinetic energy, showing that the energy source of the FACs is mainly plasma thermal energy. From kinematic relations, the plasma gas must expand in order for the thermal energy to be extracted. At the same time, from Maxwell equations with Ohm's law, dynamo conditions are expressed in terms of spatial configurations of the magnetic field. The diverging Poynting flux arises from either the magnetic pressure-dominated configurations or the magnetic curvature-dominated configurations. The former is interpreted to be 'expanding slow mode' disturbances in MHD waves, while the latter to be 'contracting slow mode' disturbances in high beta plasma. As their names indicate, the two disturbance modes are mutually exclusive and do not concur with each other. The expanding slow mode is basically a quasi-stationary process, while the contracting slow mode allows temporal variations. An example of the expanding slow mode is the dynamo of region 1 FACs in the cusp-mantle region, and an example of the contracting slow mode is the dynamo of region 2 FACs on the nightside.

電磁流体力学 (MHD) の枠組みで、われわれは大規模沿磁力線電流を駆動する磁気圏ダイナモの一般論を構築する。本研究の目的は、グローバル MHD シミュレーションによって再現される磁気圏-電離圏結合系の様々な現象を解釈する際の物理的基礎を与えることである。数値シミュレーションによると、磁気圏ではプラズマの熱エネルギーはプラズマ流の運動エネルギーに比べてずっと大きい。これは沿磁力線電流のエネルギー源が主にプラズマの熱エネルギーであることを示している。力学的関係から、プラズマの熱エネルギーを取り出すためには、プラズマ気体は膨張しなければならない。同時に、Maxwell 方程式と Ohm の法則から、ダイナモ条件は磁場の空間形状を用いて表される。発散するポインティングフラックスは、磁気圧が支配的な形状か磁場曲率が支配的な形状かのいずれかによって生じる。前者は MHD 波動の「膨張する磁気遅進波」擾乱で解釈され、後者は高ベータプラズマにおける「収縮する磁気遅進波」擾乱で解釈される。各々の名称が示すように、両モードはお互いに排他的で同時には起こらない。膨張する磁気遅進波擾乱は基本的には準定常過程であるのに対し、収縮する磁気遅進波擾乱は時間変化を許す。膨張する磁気遅進波の例はカusp・マントル領域における region 1 沿磁力線電流のダイナモであり、収縮する磁気遅進波の例は夜側 region 2 沿磁力線電流のダイナモである。

昼側低緯度磁気圏境界面における磁気リコネクションジェットの統計解析による磁気リコネクションラインの位置の推定

星 康人 [1]; 長谷川 洋 [2]; 北村 成寿 [3]; 齋藤 義文 [4]
[1] 東大・理・地惑; [2] JAXA・宇宙研; [3] JAXA 宇宙研; [4] 宇宙研

Location of magnetic reconnection lines at the low-latitude dayside magnetopause estimated from 8 years of THEMIS observations

Yasuto Hoshi[1]; Hiroshi Hasegawa[2]; Naritoshi Kitamura[3]; Yoshifumi Saito[4]
[1] Earth and Planetary Sci., Univ. of Tokyo; [2] ISAS/JAXA; [3] ISAS/JAXA; [4] ISAS

Magnetic reconnection at the Earth's dayside magnetopause is the most important physical process by which solar wind plasma enters the magnetosphere. This process connects the interplanetary magnetic field (IMF) with the geomagnetic field at an X-line formed in the magnetopause current layer. The occurrence of magnetic reconnection at the dayside magnetopause and location of X-lines affect the efficiency of the solar wind transfer. It has long been studied, however, the actual location of X-lines and its tilt angle have not been made clear. We report the statistically investigated occurrence pattern and velocities of the reconnection jets observed at the dayside magnetopause, based on plasma and magnetic field data from the THEMIS spacecraft and also estimated the location of X-lines.

The five identical THEMIS spacecraft have observed Earth's magnetosphere since launched in 2007, although two spacecraft observed the region only until 2010. We used low energy ions and magnetic field data taken in the dayside magnetopause region within the magnetic local time range of 6 to 18 hours. Among full magnetopause crossing events, flows with a speed tangential to the magnetopause significantly higher than the magnetosheath flow are chosen as candidates of reconnection jets. The Walen relation is used to test whether it is generated by reconnection. The events that have the following characteristics were excluded: fluctuations in the solar wind dynamic pressure or IMF were extreme, or the jets came from drifted multiple X-lines that involve flow reversals and an enhancement of the total pressure of order a few nPa. We also estimated the location of X-lines based on the occurrence pattern and directions of reconnection jets. We discuss effects of the IMF clock angle and geomagnetic dipole tilt angle on the location of X-lines and its tilt angle.

太陽風の質量、運動量、エネルギーが地球磁気圏内へ流入する最も重要な過程の一つとして、昼側磁気圏境界面の電流層内で惑星間空間磁場と地球磁場がつながり変わる磁気リコネクションがある。この現象が起こる領域は磁気圏境界面上にライン状に広がる事が知られており、Xラインと呼ばれる。磁気リコネクションの発生条件やXラインの存在する位置は、太陽風流入の効率を変化させうるものの、これらについて統計的な描像は未だに明らかになっていない。そこで、THEMIS 衛星観測データを用いて、昼側低緯度の磁気圏境界面において、磁気リコネクションに伴うジェットの統計解析を行い、Xラインの存在位置とXラインの傾きを調べた結果を報告する。

THEMIS 衛星は 2007 年の打ち上げ以来、2010 年まで同一構成の 5 機、2010 年以降は 2016 年現在まで、月周回衛星となった 2 機を除いた 3 機で地球磁気圏の編隊観測を行っている。この期間のうち、磁気地方時が 6 時から 18 時までの範囲で観測された低エネルギーイオン、及び磁場データを用いた。さらにこのうち、衛星が磁気圏側からシース側へ、又はその反対向きに完全に境界領域を通過し、かつ磁気圏境界面付近でシースの流れに比べ境界面に沿って高速のイオン流を観測したイベントを選び、ワレンの関係式を満たすイベントを磁気リコネクションに伴うジェットと同定した。ただし、イベントの前後で太陽風動圧、太陽風磁場が安定しないもの、またイオン流速の反転に伴って全圧が数 nPa 上昇するなど、複数 X ラインが運動していると思われるイベントは除いた。発表では、磁気リコネクションジェットの発生位置と向きから示唆された X ラインの存在位置と X ラインの傾きに対する、惑星間空間磁場の向きや地磁気双極子の傾きの影響について議論する。

GEOTAIL 衛星による地球磁気圏前面での磁気リコネクションの観測

坂口 達哉 [1]; 近藤 光志 [2]

[1] 愛大・理工・数物; [2] 愛媛大・宇宙センター

Satellite observation of magnetic reconnection in the dayside geomagnetosphere

Tatsuya Sakaguchi[1]; Koji Kondoh[2]

[1] Science, Ehime Univ.; [2] RCSCE, Ehime Univ.

The magnetic reconnection is frequently observed in the dayside magnetopause. In the magnetic reconnection process, the reconnection jet and contact discontinuity play a important role. It is important to understand about them in order to understand physics around the magnetosphere. In addition, S. Nitta et al.,(2016) revealed that following new results using the numerical computation of the asymmetry reconnection.

1. Contact discontinuity separating the plasma of magnetic sheath and magnetosphere crawl into the magnetosphere side of the plasmoid.
2. Reconnection jet strongly blows in magnetosphere side of the plasmoid.

The followings are the purposes of this study.

1. Identification of the reconnection jet in the dayside magnetopause from the GEOTAIL observation data.
2. Identification of the contact discontinuity from GEOTAIL observation data.

T. D. Phan et al.,(2001) identified the reconnection jet from satellite data. Plasma in the sheath is accerlated by the magnetic field tension force. They calculated the theoretical velocity from magnetic field change. In this study, we employ the same method. We identified the reconnection jet by comparing the observed plasma velocity with the theoretical velocity. Furthermore, we identify whether reconnection jet flows in the sheath side or magnetosphere side of the plsmoid from orientation of the magnetic field.

Across the contact discontinuity, plasma pressure does not change, but plasma density changes, so we identify the contact discontinuity from the observation data using this characteristic. Then, we discuss the contact discontinuity statistically.

More than 80% of the plasma jet velocities agreed with the estimated velocites, and the directions of the magnetic field of these all jets were northward. So, we conclude that these reconnection jets are in the magnetosphere side of the plasmid. Across the contact discontinuity, a phase gap of the plasma pressure and plasma density is found in a reconnection jet.

reference

S. Nitta, et al., Critical differences of asymmetric magnetic reconnection from standard models, the Astrophysical Journal, accepted

T. D. Phan, et al., Evidence for an extended reconnection line at the dayside magnetopause, Earth Planets Space, 53, 619-625, 2001

地球磁気圏前面では、磁気リコネクションは頻繁に起こっていることが知られている。磁気リコネクション過程において、リコネクションジェットや接触不連続面の存在が示唆されている。この磁気リコネクションのメカニズムについて理解する上で上記の2つの理解を深めることは磁気圏周辺の物理を理解する上で重要である。また、S. Nitta et al.,(2016)において、太陽風と地球磁気圏のような非対称磁気リコネクションの数値計算の結果により、磁気シースと磁気圏のプラズマを分けている接触不連続面が磁気圏側に潜り込むこと、リコネクションジェットが磁気圏側で強く吹くことが示された。

本研究の目的は以下の通りである。

1. GEOTAIL 衛星による地球磁気圏前面の観測データからリコネクションジェットを同定する。
2. シミュレーションの結果で示唆されている密度と圧力の関係を用いて、接触不連続面を観測データから見つける

リコネクションジェットの同定に関しては、磁気圏境界をまたぐ際の磁気エネルギーの変化量によりプラズマが Alfvén 速度まで加速されることから速度を推定する方法がある [T.D. Phan et al., 2001]。この方法を用いて速度成分を推定し、観測された速度成分と比較することでリコネクションジェットの同定を行った。また、リコネクションジェット観測時の磁場の成分からジェットが磁気圏側で測定されているのか磁気シース側で測定されているのかを特定する。接触不連続面に関しては、通過時に圧力は変化しないが、密度が変化するため、リコネクションジェット観測時の観測データの密度と圧力の位相のずれから接触不連続面を探し、この接触不連続面の存在を統計的に議論する。

リコネクションジェットの同定では、ほとんどのジェットに関して推定値の 80%以上の一致が得られ、またこの際の磁場が磁気圏の北向き磁場と同じ方向を向いていることが分かった。これによりこれらのリコネクションジェットは磁

気圏側に存在していることが分かり、シミュレーションの結果を裏付ける結果が得られた。接触不連続面に関してはリコネクションジェット内で密度と圧力の位相がずれるようなデータを得た。またこれがジェットの磁気圏側で観測されていることが分かり、これも非対称リコネクションの数値計算を裏付ける観測結果となった。

参考文献

S.Nitta, et al., Critical differences of asymmetric magnetic reconnection from standard models, the *Astrophysical Journal*, accepted

T.D.Phan, et al., Evidence for an extended reconnection line at the dayside magnetopause, *Earth Planets Space*, 53, 619-625, 2001

昼側磁気圏界面リコネクションの最地球側開放境界層におけるプラズマ波動

内野 宏俊 [1]; 栗田 怜 [2]; 原田 裕己 [3]; 町田 忍 [4]; Angelopoulos Vassilis[5]
[1] 京大・理・地惑; [2] 名大 ISEE; [3] 京大・理・地球惑星; [4] 名大・ISEE; [5] UCLA

Waves in the innermost open boundary layer formed by dayside magnetopause reconnection

Hirotochi Uchino[1]; Satoshi Kurita[2]; Yuki Harada[3]; Shinobu Machida[4]; Vassilis Angelopoulos[5]
[1] SPEL, Kyoto Univ.; [2] ISEE, Nagoya Univ.; [3] Dept. of Geophys., Kyoto Univ.; [4] ISEE, Nagoya Univ.; [5] UCLA

We present two THEMIS observations of whistler-mode and electrostatic wave events in the innermost open boundary layer (IOBL), formed by dayside magnetopause reconnection. The IOBL is identified by high-speed electron flow on the magnetospheric side of the ion outflow from the reconnection site. Quasi-parallel whistler-mode waves propagating toward the reconnection region are observed in association with a partial shortage of magnetospheric electrons moving away from the reconnection region at small pitch angles. We interpret the partial shortage of magnetospheric electrons as caused by a change in the magnetic field geometry due to reconnection, which suddenly opens the magnetosphere to the magnetosheath. Calculation of wave linear growth rates shows that the waves can be excited by the perpendicular electron temperature anisotropy that develops due to the partial shortage of field-aligned magnetospheric electrons. Electrostatic waves close to the lower hybrid resonance frequency are observed in the IOBL in the second case, during the main phase of a magnetospheric storm. Magnetospheric electrons are almost completely lost in the event, except at pitch angles close to 90 degrees, yet whistler-mode waves are not observed. An electron beam from the magnetosheath and cold ions originating from the plasmaspheric plume are observed in association with the electrostatic waves. Growth rate calculation shows that the waves can be excited via couplings between the electron beam and cold ions. We suggest that the duration of magnetopause reconnection is one factor controlling the properties of waves excited in the IOBL.

非対称磁気リコネクションにおける接触不連続面の発達の数値シミュレーション

近藤 光志 [1]; #丸山 翔矢 [2]
[1] 愛媛大・宇宙センター; [2] 愛媛大・理工・数物

Numerical simulation of the contact discontinuities evolution in the asymmetric magnetic reconnection

Koji Kondoh[1]; # Shoya Maruyama[2]
[1] RCSCE, Ehime Univ.; [2] Science, Ehime Univ.

Magnetic reconnection is generally accepted as an important elementary process of mass, momentum and energy transport in the geomagnetosphere and Sun. Especially, the asymmetric magnetic reconnection is more general than the symmetric magnetic reconnection, such as Anemone type flares and flux transfer events at the dayside magnetopause. However, asymmetric magnetic reconnection have many unsolved problems. We examine the asymmetric magnetic reconnection using MHD simulation by HLLD code.

In the previous work by Nitta et al.(2016), the differences between symmetric magnetic reconnection and asymmetric magnetic reconnection were studied. In the symmetric magnetic reconnection, the contact discontinuity is located in the center of the current sheet to separate the plasma in the higher beta side and the lower beta side. However, in the asymmetric magnetic reconnection, according to the difference of Alfvén speed in both sides of the current sheet, the higher beta side plasma is caught into the lower beta side plasma. As a result, contact discontinuity is formed in the lower beta side. Thus, in this study, we examined about the time evolution of the contact discontinuity.

磁気リコネクションは、地球磁気圏や太陽における質量・運動量・エネルギー移送に関する重要な素過程の一つとして受け入れられている。特に非対称な磁気リコネクションは対称なものよりも一般的であり、太陽表面に

おけるアネモネ型フレアや、地球前面で起こる FTE の解明に重要である。しかし、未解決な問題の多い現象でもある。そこで、我々は HLLD code を用いて MHD シミュレーションを行い、非対称磁気リコネクションについて理解する。

Nitta et al.(2016) の先行研究では、対称磁気リコネクションと非対称磁気リコネクションの違いについて調べられている。対称磁気リコネクションの場合、接触不連続面は高ベータ側と低ベータ側のプラズマを分離するように電流シートの中心に位置する。しかし、非対称磁気リコネクションの場合、電流シートの両側での Alfvén 速度の違いにより、高ベータ側のプラズマが低ベータ側のプラズマへ巻き込まれる。その結果、低ベータ側に接触不連続面が作られる。本研究では、その接触不連続面の時間発展と非対称度依存について調べた。

Reconstruction of the electron diffusion region of magnetic reconnection observed by Magnetospheric MultiScale

Hiroshi Hasegawa[1]; Bengt Sonnerup[2]; Naritoshi Kitamura[3]; Yoshifumi Saito[4]
[1] ISAS/JAXA; [2] Dartmouth Coll.; [3] ISAS/JAXA; [4] ISAS

We present first results of the electron magnetohydrodynamic (EMHD) reconstruction applied to the electron diffusion region encountered by the Magnetospheric Multiscale (MMS) spacecraft on 16 October 2016, 1307 UT [Burch et al., Science, 2016]. The reconstruction is based on a two-dimensional, incompressible, and inertia-less version of the EMHD equations [Sonnerup et al., JGR, 2016] and uses, as the initial conditions, magnetic fields and electron moments observed along the path of a single spacecraft and the coordinate system estimated from four-spacecraft magnetic field measurements [Denton et al., GRL, 2016]. An X-type magnetic field configuration and quadrupolar Hall field pattern, consistent with the electron inflow and outflow, were successfully recovered. The results show that although MMS encountered the dissipation region of near antiparallel magnetopause reconnection, the X-point was not inside the MMS tetrahedron but at a few km from the MMS4 spacecraft at the closest approach. The electron flow stagnation point was shifted toward the magnetosphere from the X-point. The estimated reconnection electric field is 0.3-0.9 mV/m, equivalent to the dimensionless reconnection rate of 0.1-0.3. Comparison between the reconstruction results from individual MMS data and multi-spacecraft measurements suggests that there were significant spatial structures along the X-line direction.

一様抵抗 MHD モデルにおける間欠的で自発的な 2 次元高速磁気再結合過程の可能性

清水 徹 [1]; 近藤 光志 [2]
[1] RCSCE, 愛媛大; [2] 愛媛大・宇宙センター

Intermittent plasmoid instability is possible in uniform resistivity MHD model ?

Tohru Shimizu[1]; Koji Kondoh[2]
[1] RCSCE, Ehime Univ.; [2] RCSCE, Ehime Univ.

In many resistive numerical MHD studies, the Petschek model (1st possibility) is considered to be plausible in explosive phenomena such as solar flares and substorms, rather than Sweet-Parker model (2nd), in high magnetic Reynolds number (MRe). However, the 3rd possibility was recently proposed, where intermittent plasmoid instability under the uniform and extremely low resistivity can generate large scale plasmoids (Bhattacharjee, Cassak, Loureiro, Shibayama, etc.). With numerical studies, we invoke that the 3rd possibility essentially may return back to a controversy where the Petschek model may be impossible in the uniform resistivity leading to Sweet-Parker model (Biskamp, Kulsrud, Uzdensky vs Priest).

高速磁気再結合過程の MHD モデルとしては、古くから Petschek モデル（第一の可能性）と Sweet-Parker モデル（第二）があり、太陽フレアや磁気嵐に関する宇宙プラズマ爆発現象を説明するためには前者が有力視されてきた。しかし、近年になって、第三の可能性として、「高磁気レイノルズ数におけるプラズモイド不安定性が間欠的で自発的に大規模なプラズモイド形成を起すこと」が、理論的に予想され、数値的に検証されたとする、多数の研究報告がなされている (Bhattacharjee, Cassak, Loureiro, Shibayama, etc.)。これらの報告では「一様抵抗」が仮定されているが、一方で、それまでの多くの研究において、一様抵抗では Petschek モデルは起こらず、Sweet-Parker モデルが起こると示唆されており、この矛盾が第三の可能性として注目を集める一つの理由となっている。本講演では、この第三の可能性を否定し、これが、「一様抵抗で Petschek モデルは起こらず、Sweet-Parker モデルが起こるか否か（第一と第二の可能性の議論）」という古くから続く論争 (Biskamp vs Priest) の延長線にある一つの研究テーマにすぎないことを独自の数値的研究により主張する。

Direct evidence of energy exchange between EMIC waves and ions observed by the MMS spacecraft at the off-equator magnetosphere

Naritoshi Kitamura[1]; Masahiro Kitahara[2]; Masafumi Shoji[3]; Satoko Nakamura[4]; Yoshizumi Miyoshi[3]; Yuto Katoh[2]; Yoshifumi Saito[5]; Hiroshi Hasegawa[6]; Shoichiro Yokota[5]; Barbara L. Giles[7]; C. T. Russell[8]; Robert J. Strangeway[9]

[1] ISAS/JAXA; [2] Dept. Geophys., Grad. Sch. Sci., Tohoku Univ.; [3] ISEE, Nagoya Univ.; [4] Dept. of Geophys., Kyoto Univ.; [5] ISAS; [6] ISAS/JAXA; [7] NASA/GSFC; [8] UCLA; [9] Inst. of Geophys. and Planet. Phys., Univ. of California, Los Angeles

Wave particle interactions, which cause particle acceleration and pitch-angle scattering, are a fundamental energy exchange process in collisionless space plasma. The four MMS (Magnetospheric Multiscale) spacecraft traversing the duskside magnetosphere measured electromagnetic ion cyclotron (EMIC) waves around 3.6, 8.7, and $-5.2 R_E$ in X, Y, and Z GSM from $\sim 12:18$ to 12:22 UT on 1 September 2015. In this period, the burst ion data (150 ms resolution) are available, and cold ions (below 300 eV) are detected due to a large magnitude of the electric field drift by the wave electric fields under weak background magnetic fields (~ 22 -40 nT). Since the frequency of the EMIC waves were lower than $\sim 1/5$ of the proton gyro frequency, perpendicular electric fields were derived from the cross product of the negative cold ion velocity and the magnetic field. Using these data, we investigate energy exchange between EMIC waves and ions. Thirty second averages of the dot product of the perpendicular components of the wave electric fields (0.05-0.1 Hz) and ion resonant currents reached -0.2 pW/m^3 in the energy range of 14-30 keV in the pitch angle range from 33.75 to 67.5 degrees near the beginning of the wave ($\sim 12:18:30$ UT). The negative value in this pitch angle range indicates that the perpendicular energy of ions was being transferred to the EMIC waves propagating toward higher latitudes at the MMS location. This initial result indicates that EMIC wave growth due to wave particle interactions can occur far from the equator, although it has been thought that the source region of EMIC waves is near the equator.

Magnetotail structures reproduced by a magnetosphere MHD model

Aoi Nakamizo[1]

[1] NICT

The development of global magnetosphere MHD models started about thirty years ago [e.g., Ogino., 1986; Fedder and Lyon, 1987]. Now there are several major models [e.g., Lyon, Fedder, and Mobarry, 2004; Tóth et al., 2005; Raeder et al., 2008; Tanaka et al., 2010; Janhunen et al., 2012] used widely in the community. In recent years in the U.S., in parallel with the model utilization, the efforts of the validation and verification of models have been actively pursued, for example, targeting global structures during storm events [e.g., Honkonen et al., 2013], bursty bulk flows in the near-earth plasma sheet [Wiltberger et al., 2015], and global evolution of FACs [Merkin et al., 2013]. If the calculated results are far from the reality, it would be hard to rely on its dynamics. Therefore, these examinations are indispensable in order to conduct the true science with magnetosphere simulations. However, it seems that the similar efforts have been missing in Japan. Recognizing the current situation, we test the calculation results of a magnetosphere MHD model in NICT by using observation data. In this talk the focus will be placed on the mid-tail structure, including cross-sections (both in the X_{GSM} - Y_{GSM} and Y_{GSM} - Z_{GSM} planes), lobe-plasma sheet structure dynamically changed by the solar wind/IMF input.

サブストームに伴う尾部磁気圏境界面の变形

城谷 一真 [1]; 河野 英昭 [2]

[1] 九大・理・地球惑星; [2] 九大・理・地球惑星

Substorm-associated deformation of the tail magnetopause

Kazuma Shirotani[1]; Hideaki Kawano[2]

[1] Earth and Planetary Sciences, Kyushu Univ.; [2] Earth and Planetary Sci., Kyushu Univ.

The magnetopause is the boundary where the solar wind pressure balances with the magnetospheric pressure. The purpose of this study is to statistically analyze the deformation of the tail magnetopause associated with substorms. In a preceding study by Kawano et al. [2000], a case was reported in which the GEOTAIL spacecraft was located near the mid-tail equatorial magnetopause and three substorms took place in a consecutive manner; from the GEOTAIL observations during that interval, they suggested a temporary shrinkage of the mid-tail equatorial magnetosphere after each expansion onset.

We intend to extend their study by performing a statistical analysis, toward a better understanding of the substorm and the magnetospheric structure.

To select events for the statistical analysis, we use the following two conditions:

- (1) GEOTAIL must be moving relatively parallel to the model magnetopause; and
- (2) GEOTAIL must make an in-then-out or an out-then-in motion across the magnetopause in a relatively short interval.

We are currently creating lists of events satisfying the above two conditions, and at the meeting we expect to report the analysis results of thus identified events.

磁気圏は地球起源磁場が支配的である領域で、太陽風動圧と磁気圏磁気圧が釣り合う境界面はマグネトポーズ (magnetopause) と呼ばれている。磁気圏の前面は太陽風によって圧縮され、夜側では太陽風によって引き伸ばされて磁気圏尾部を形成している。

本研究では、サブストームが発生した時の尾部マグネトポーズの短期間の变形について研究する。先行研究である Kawano et al. (2000) では、サブストーム発生時に GEOTAIL 衛星が尾部赤道域マグネトポーズ付近に滞在していたイベント 1 例の解析が行われ、サブストームに同期した尾部赤道域マグネトポーズの短期間の内向き移動 (磁気圏尾部中心軸に向かって移動して GEOTAIL を通過し、~30 分後に再度 GEOTAIL を通過して元の位置に戻っていった) が報告されている。

本研究では先行研究を更に進めて統計解析を行う。尾部マグネトポーズが移動して GEOTAIL を通過したイベントを全て同定し、その統計解析を行ってそれらのイベントへのサブストームの影響について研究することで、サブストームや磁気圏構造の理解へとつなげることを最終的な目的としている。

統計解析のためのイベントリストの作成においては、まずはサブストームの有無とは無関係に、

- (1) GEOTAIL の軌道運動の方向がモデルマグネトポーズと比較的平行であった
- (2) GEOTAIL がマグネトポーズ通過を実測した

という 2 つの条件を同時に満たすイベントを同定する。客観性を確保するため、目視と自動同定プログラムでそれぞれ独立にイベント同定し、それらの結果を比較してイベントを最終的に同定する。

上記条件 (1) は、GEOTAIL がマグネトポーズを出入りしたことが、GEOTAIL 自体の軌道によるものではないということ担保する為のものである。Shue et al. (1998) のマグネトポーズモデルと GEOTAIL の位置データを用いて、マグネトポーズモデルに対する GEOTAIL の距離と、その時間変化率を計算している。

条件 (2) については、観測データから、GEOTAIL がマグネトポーズを通過したイベントを自動同定するプログラムを作成した。GEOTAIL が磁気圏内にいたか外にいたかを判断する条件は、Nakamura et al. (1997) におけるマグネトシースの判別条件をもとにしている。一方で、プログラム自動同定とは独立に、GEOTAIL の観測データのプロットから、衛星がマグネトポーズを通過したイベントを目視で同定する。自動同定結果と目視同定結果の比較によりマグネトポーズ通過イベントの客観性を確保し、その結果最終的に同定したイベントについて更に、Kawano et al. (2000) で見られたような、磁気圏内外の出入り (in → out あるいは out → in) がペアになっているものを同定する。そして、それらとサブストームとの時間関係、太陽風パラメタとの関係、観測位置の空間分布、等を調査する。

現在、上記の手順でイベントリスト作成を行っており、本発表においてはその経過および統計解析結果について報告する予定である。

地球磁気圏尾部領域における電子の異方性分布生成

幅良太 [1]; 羽田亨 [2]; 松清修一 [3]
[1] 九大・総理工・大海; [2] 九大総理工; [3] 九大・総理工

Generation of electron anisotropies at earth's magnetotail

Ryota Haba[1]; Tohru Hada[2]; Shuichi Matsukiyo[3]
[1] ESST, Kyushu Univ.; [2] ESST, Kyushu Univ.; [3] ESST Kyushu Univ.

Anisotropic electron distributions are often found in the night-side region of the earth's magnetosphere in the energy range from about 10eV to 10keV, in particular, in association with the so-called dipolarization events where the stretched magnetic field recovers to be closer to the earth's dipolar field. Theoretical models are proposed to explain the appearance of these distributions, using the first and the second adiabatic invariants. While the first invariant (magnetic moment) is almost always conserved, the second invariant (action associated with the mirroring motion along the field lines) can be violated depending on the time scale of the external perturbations and the electron energy. Recently, Wang et al (JGR, 2014) made a statistical analysis on variation of the electron anisotropies during geomagnetic depolarization events using THEMIS data. They found that, after the dipolarization, the pancake type (perpendicular temperature > parallel temperature) anisotropy increases when the electron energy is < 1keV, while the cigar type (perp < parallel) anisotropy dominates for higher electron energies.

In this presentation we show our results of test particle simulations to discuss what types of pitch-angle anisotropies would emerge for various field line configurations, and also by varying the strength and time scales of the external electric field. Electron trajectories are computed by directly time integrating the equation of motion and also by integrating the guiding center equation of motion. After showing that the observed dependence of the types of anisotropies on the electron energy can roughly be explained by the present model, we will discuss evolution of anisotropies at distant magnetotail. Application of the present model to other planetary magnetospheres will also be discussed.

地球磁気圏尾部領域では、太陽風起源の電磁場が地球磁気圏内に侵入することにより地球磁場が変形し、これに伴い温度異方性を持った電子分布が出現することが知られている。異方性生成には様々な要因が考えられるが、ここでは電子の断熱不変量の保存・非保存による生成モデルを考える。周知のように、地球磁場中での荷電粒子の運動は3種の周期運動(サイクロトロン、ミラー、ドリフト)の重ね合わせとして近似的に表現できる。これらの運動はそれぞれオーダーが大きく異なる周期を持ち、第1不変量(磁気モーメント)はどのような状況でもほぼ保存されるが、第2不変量(沿磁力線ミラー運動の伴う作用)の断熱性は、外力のタイムスケールと電子のエネルギーに依存して決まる。

最近、THEMIS衛星により dipolarization に伴う異なるエネルギーでの電子ピッチ角分布の変動が観測されている(Wang et al, 2014)。Dipolarization とは外部電場によって地球の磁力線が、地磁気ダイポールによるものに近づくことである。この観測結果から、粒子のエネルギー、また地球からの距離、磁力線の形状により異方性の出現の傾向に違いがあることが判明している。

本研究では、地球磁気圏における電子の異方性生成をテスト粒子計算により解析する。磁場は地球磁場(ダイポール磁場)と尾部電流等によりつくられる磁場の重ね合わせとし、この中での電子運動を、運動方程式の直接積分および旋回中心の運動方程式の積分により求めた。外部電場により地球磁気圏が圧縮され、dipolarization が起きたときの異方性の生成を議論した。生じる異方性の外部電場パラメータ依存性、背景磁場への依存性、また旋回中心方程式の妥当性などについて議論する。地球以外の惑星磁気圏における同様のプロセスについても言及する。

A statistical study of severe magnetic fluctuations effective for ion gyration in the near-earth magnetotail observed by THEMIS-E

Heqiucen Xu[1]; Kazuo Shiokawa[1]
[1] ISEE, Nagoya Univ.

Additional Coauthor: Dennis Fruehauff (Institute of Geophysics and extraterrestrial Physics, Braunschweig University of Technology, Braunschweig, Germany)

We have statistically studied severe magnetic fluctuations which can modify ion gyro-motion to cause kinetic effect in the magnetotail dynamics which can be a cause of current disruption in the inside-out substorm model. We used magnetic field data from 2013 and 2014 obtained by the THEMIS-E satellite with a sampling rate is 4 Hz in the nightside near-Earth plasma sheet at $|X|= 6 - 12$ Re. A total of 1283 severe fluctuation events were identified that satisfy the criteria $\text{Sigma}_B/B_{\text{bar}}$ larger than 0.5, where Sigma_B and B_{bar} are the standard deviation and the average of magnetic field intensity during the time interval of local ion gyro-periods. The occurrence rates of severe fluctuation events are 0.00118%, 0.00899% and 0.0238% at $|X|= 6-8$ Re, 8-10 Re and 10-12 Re, respectively. Most events last for no more than 15 s. By using the Tsyganenko magnetic field model (T01), we found that almost all the severe fluctuation events occurred at the Zgsm close to the model neutral sheet within 1.0 Re. The superposed epoch analyses indicated that the fluctuation events occurred in association with a sudden decrease in AL index and magnetic field depolarization, suggesting their association with substorms. Sixty-two percent of events were accompanied by ion flow with v larger than 100 km/s. The superposed epoch analysis also indicated that flow speed increased before the severe magnetic fluctuations, suggesting that the magnetic fluctuations are caused by these ion flows. This contradicts the assumption of the inside-out model which suggests that the fluctuations cause earthward ion flow by reducing the tailward pressure-gradient force. These results indicate that the inside-out substorm onset caused by severe magnetic fluctuations can only be suitable for a relatively small number of substorm cases. These results also indicates that the violation of ion gyro-motion is mainly caused by high-speed ion flow in the near-earth tail. In the presentation, we will also show the result based on modified criteria ($\text{Sigma}_B / B_{\text{bar}}$ larger than 0.2) for a comparison.

Correlated temporal variations of SCW, AKR and global Pi 2

Teiji Uozumi[1]; Akimasa Yoshikawa[2]; Shinichi Ohtani[3]; Shun Imajo[4]; Dmitry Baishev[5]; Alexey Moiseev[5]; Boris Shevtsov[6]

[1] ICSWSE, Kyushu Univ.; [2] ICSWSE/Kyushu Univ.; [3] The Johns Hopkins University Applied Physics Laboratory; [4] Earth and Planetary Sci., Kyushu Univ.; [5] IKFIA, SB, RAS; [6] IKIR

A transient geomagnetic pulsation Pi 2 is well known to occur at every auroral breakup [e.g. *Sakurai and Saito*, 1976], and is accepted as an onset indicator of the magnetospheric substorm [e.g. *Saito*, 1969; *Rostoker et al.*, 1980]. The formation of the substorm current wedge (SCW) [e.g. *McPherron et al.*, 1973; *Nagai*, 1982] and the breakup of the auroral kilometric radiation (AKR) [e.g. *Gurnett*, 1974, *Morioka et al.*, 2008] are also enumerated as other essential manifestations of the substorm expansion onset. Past studies addressed the timing relations among the onsets of these phenomena [e.g., *Sakurai and McPherron*, 1983; *Liou et al.*, 2000a, 2000b; *Morioka et al.*, 2008]. However, the relation of temporal variations between Pi 2 and other phenomena have not yet been clarified. In this study we investigate a temporal relationship between AKR / SCW modulation and global Pi 2 oscillations. We present some typical events, which revealed highly correlated modulations/oscillations of AKR, SCW and global Pi 2. It is confirmed that the height-integrated AKR power (P_{AKR}) tended to increase/decrease during the interval when the D component Pi 2 (dB_D) deviated in the same/opposite sense as the D-component bay of the SCW. This result suggests that the time derivative of the height-integrated AKR power was modulated coherently with the D component Pi 2 oscillation. This result is consistent with the finding of *Uozumi et al.* [2011]. We reexamined Pi 2 oscillations by applying the Hilbert transform method. The Hilbert transform is the integral transform in the time domain, and shifts the original phase 90deg behind for all the frequency components. We found that the Hilbert-transformed Pi 2 period range oscillations in the D component, $HT(dB_D)$, shows temporal variation similar to $d\log_{10}P_{AKR}$ without lag time. This result supports the aforementioned time-derivative relation between Pi 2 oscillation and AKR modulation. We also analyzed global Pi 2s, which were observed from low- to high-latitude region with highly correlated waveforms (global high-correlation Pi 2 [*Uozumi et al.*, 2009, 2011, 2016]). The result shows that the middle- and high-latitude D component Pi 2 oscillated without any significant time lag, whereas the middle- and high-latitude Pi 2 in the H component oscillations revealed some time lags due to the propagation delay of the Pi 2 waves. The azimuth of the initial deflection of the middle- and high-latitude duskward Pi 2s are consistently explained by the development of an upward field-aligned current that is assumed to be located at the center of the auroral breakup region. These results suggest that the middle- and high-latitude D component Pi 2 oscillations can be treated as a proxy of the modulation of the SCW ($dB_D \sim dB_{SCW}$), and therefore, the time derivative of the height-integrated AKR power was modulated coherently with the SCW oscillations. It is also found that the H component of the low-latitude Pi 2, which is a manifestation of the fast wave propagated from nightside magnetosphere (dB_{FW}), and dB_{SCW} are highly correlated without any significant time lags ($|dT| < \sim 10$ s). The high-correlation signature between dB_{FW} and dB_{SCW} suggests that the driving sources of these wave elements in global high-correlation Pi 2 are closely coupled with each other.

THEMIS 衛星による磁気圏尾部観測と地上全天観測との比較

川嶋 貴大 [1]; 家田 章正 [1]; 三浦 翼 [2]
[1] 名大宇宙地球研; [2] 名大 ISEE

THEMIS satellite observations of magnetotail signatures for auroral brightenings observed in all-sky images

Takahiro Kawashima[1]; Akimasa Ieda[1]; Tsubasa Miura[2]
[1] ISEE, Nagoya Univ.; [2] ISEE, Nagoya Univ.

In this study, we compared THEMIS-3 satellite observations of the magnetotail and ground all-sky images. THEMIS-3 satellite was located near midnight 11 Re down the tail, and observed earthward high-speed flow at 0800 and 0858 UT on 14 November 2015.

The THEMIS-3 footpoint was located near Whitehorse (WHIT, magnetic latitude: 63.6 degree) in Alaska. Looking WHIT all-sky images, aurora brightened at 0830 UT, 0838 UT, and 0858 UT. For the first and the third brightenings, THEMIS-3 observed earthward high-speed flows and decreases in the total pressure at 0830 UT and 0858 UT. On the other hand, for the second brightening THEMIS-3 did not observe these characteristics. This may be because THEMIS-3 was located deep inside the plasma sheet with observed high plasma beta.

本研究では、THEMIS-3 衛星の磁気圏尾部観測と地上全天画像との比較を行った。THEMIS-3 衛星は真夜中付近の尾部側 11 地球半径に位置しており、地球向き高速流を 2015 年 12 月 14 日 08:30 UT 及び 08:58 UT に観測した。THEMIS-3 衛星の footpoint はアラスカの Whitehorse(WHIT) 付近 (磁気緯度 63.6 度) にあった。WHIT の全天画像を見ると、08:30 , 08:38 , 08:58 UT にオーロラが増光していた。このうち 1 番目と 3 番目の増光に対応して、THEMIS-3 衛星では 08:30 , 08:58 UT に、地球向き高速流と全圧の減少が観測された。一方で、2 番目の増光では、これらの特徴は観測されず、また、プラズマ β は高くなっていた。したがって、2 番目の増光で地球向き高速流が観測されなかった原因は、プラズマシートの奥深くに衛星がいたことと関係があると考えられる。

オーロラオーバルの分岐現象の空間分布特性

宮本 正輝 [1]; 田口 聡 [1]
[1] 京大理

Characteristics of the spatial distribution of the auroral oval bifurcation

Masaki Miyamoto[1]; Satoshi Taguchi[1]
[1] Grad school of Science, Kyoto Univ.

We report on the statistical characteristics of the spatial distribution of the auroral oval bifurcation on the basis of remote-sensing measurements made by TIMED/GUVI. We analyzed the TIMED/GUVI data obtained during 5 years (2002-2006). IMF By-dependent dawn-dusk asymmetry is clear for northward IMF. For southward IMF, many bifurcation events are seen during non-substorm intervals as well as during substorm intervals. We will discuss the field-line geometry for the auroral oval bifurcation.

オーロラオーバルの内側の境界は、北向き IMF 時でポーラーアークが現れている場合やサブストームの場合に特徴的な構造を見せることが知られている。IMF が北向きで東向きの成分をもつ時、北半球の夕方側のオーロラオーバル付近でポーラーアークが現れる。また、IMF が北向きで西向きの成分をもつと、ポーラーアークは朝側のオーロラオーバルの近くで現れる。一方、サブストームの際には、真夜中付近のオーロラオーバルが2つに割れたようになることがある。いずれの場合も、夜側のオーロラオーバルから切れること無く極側に向けて延びていけば、その部分は、オーバル部分と同様にプラズマシート起源であると考えられる。本研究では、オーロラオーバルから極側への分岐が明確なオーロラ構造に注目して、その空間分布特性を明らかにする。

我々は、2002年から2006年の5年間にTIMED衛星のGUVI装置によって取得されたオーロラのグローバルイメージの大量のデータに対して定量的な基準を導入して、オーロラ分岐現象の多数の事例を同定した。北向きIMFに対しては、過去の研究で示されているように、分岐現象にはIMFの東西成分に依存する朝夕の非対称性が見られた。我々の解析では、IMFが南向き時についても、多くの分岐現象が同定された。最も顕著な事例は、IMF B_z が -50nT にも及ぶような巨大磁気嵐が発生した際に見出された。夜側で分岐して昼間側へと延びる分岐オーバルの長さは 3000km にも及んでいる。同時観測されたDMSP衛星のデータからも、このような分岐が間違いなく起こっていることがわかる。DMSP衛星との同時観測のいくつかの事例研究を含めて、オーロラオーバルの分岐現象の空間分布の統計的性質を報告する。また、その性質に基づいて、プラズマシートの状態や磁力線のジオメトリーを議論する。

Sun-aligned arc の運動メカニズム再考: 3 台の全天カメラと短波レーダーによる同時観測

木村 洋太 [1]; 細川 敬祐 [2]; 塩川 和夫 [3]; 田口 聡 [4]; 大塚 雄一 [3]; 小川 泰信 [5]
[1] 電通大・情報理工・情報・通信工; [2] 電通大; [3] 名大宇地研; [4] 京大理; [5] 極地研

Motion of sun-aligned arc revisited: Simultaneous observations with three ASIs and HF radars

Yota Kimura[1]; Keisuke Hosokawa[2]; Kazuo Shiokawa[3]; Satoshi Taguchi[4]; Yuichi Otsuka[3]; Yasunobu Ogawa[5]
[1] Information and communication engineering, sec; [2] UEC; [3] ISEE, Nagoya Univ.; [4] Grad school of Science, Kyoto Univ.; [5] NIPR

Polar cap arcs have frequently been observed in the high-latitude ionosphere during northward interplanetary magnetic field (IMF) conditions. Polar cap arcs extending along the Sun-Earth line are sometimes called Sun-aligned arcs (SAA). It was statistically indicated that SAA move either duskward or dawnward depending on the sign of the IMF By. Milan et al. (2005) reasonably explained the motion of SAA as viewed from the IMAGE satellite, especially its dependence on the IMF By, by using a model based on magnetic flux transport by the ionospheric convection during northward IMF conditions. However, the spatial resolution and sensitivity of the space-based FUV images were insufficient for evaluating the model in detail. To further test the model, it is necessary to combine highly sensitive ground-based all-sky optical observations from more than two stations.

In this study, we evaluate and/or modify the model of Milan et al. (2005) by investigating large-scale imaging of SAA with three ASIs, respectively at Resolute Bay (RSB; 74.7 N, 265.0 E, 82.9MLAT) and Eureka (EUR; 88.5 N, 273.6 E, 88.5 MLAT) in Canada, and at Longyearbyen (LYR; 78.1 N, 15.5 E, 75.3 MLAT) in Norway. On January 9, 2016, a transpolar SAA was observed to move duskward during a 190 min interval from 1930 to 2240 UT (Interval A), and the arc moved dawnward during a subsequent 50 min interval from 2240 to 2330 UT (Interval B). This arc was extending across the fields-of-view of LYR and EUR ASIs and its sunward end was clearly connected to the auroral oval on the dayside near the cusp region. Since the model of Milan et al. (2005) assumes that there is a gap between the dayside oval and the sunward end of SAA, the model is not able to explain the current observations of fully-connected SAA. Moreover, as a result of comparison between the direction of the SAA motion and the IMF data from the OMNI data set, it was found that the dawnward motion of SAA during Interval B was not consistent with the sign of the upstream IMF By. To further analyze this event, the ionospheric convection data from HF radars of SuperDARN were employed. Based on the simultaneous optical and radar measurements, we propose a model which employs magnetic reconnection between closed magnetic field and northward IMF, which can only take place either in the northern or southern hemisphere during non-zero IMF Bx conditions. The transport of open magnetic flux in the polar cap driven by this type of reconnection pushes the SAA either dawnward or duskward depending on the sign of IMF Bx (not By). This new model is able to account for the motion of fully-connected SAA which is sometimes independent of the polarity of the IMF By.

極冠オーロラは、惑星間空間磁場 (IMF) が北向きのとき、磁気緯度 75 度以上の高緯度地域で頻りに観測される現象である。極冠オーロラの中でも太陽方向に伸びた構造を持つものを特に Sun-aligned arc (SAA) と呼び、IMF By 成分の正負に依存して朝夕方向に運動することが統計的に示されている。その運動メカニズムは、北向き IMF 時に生じるロープセル対流に伴う開いた磁力線の輸送モデルによって説明されてきたが (Milan et al., 2005), モデル考案の際に用いられたデータは人工衛星からの極端紫外光観測によるものであり、空間分解能や感度に限界があった。このため、地上からの高感度光学観測によって、モデルの妥当性や適用限界を検証することが求められている。

Milan らのモデルで提案されている運動メカニズムは SAA の構造的特徴と密接に関連するため、地上からの光学観測を行う際にも、アークの大規模な空間構造を把握することが重要となる。これまでの研究では、単一地点からの全天光学観測が用いられてきたため、観測視野の制限により SAA の全体像を把握することが困難であった。この問題点を克服するために、本研究では、カナダのレゾリュートベイ (RSB) とイウレカ (EUR), ノルウェーのロングイヤービエン (LYR) に設置されている 3 台の高感度全天イメージャを用いる。3 地点からの、波長 630.0 nm の広域オーロラ観測を用いて、Milan らによる SAA 運動モデルと実際の観測データとの整合性を検証することを目的とする。

2016 年 1 月 9 日の 1930 Ó 2400 UT の時間帯において、朝夕方向に往復運動する SAA が 3 台の全天カメラによって同時に観測された。このアークは、EUR と LYR の全天カメラの視野にまたがる巨大な構造を持ち、さらに昼側カスプ域近傍においてオーロラオーバルと接続されていることが確認された。Milan らの運動モデルは、SAA が昼側でオーロラオーバルと接続されていない場合に磁気フラックスの輸送が生じることを前提としているため、今回観測されたような SAA の朝夕方向の運動を説明することができない。さらに、この時間帯の後半部分における SAA の朝方向への運動は、IMF By 成分に依存していないことが明らかになった。

この結果を受け、SuperDARN によって得られた高緯度領域の対流と、SAA の運動、IMF の極性の対応関係の解析を行った。その結果、IMF Bx がある程度の大きさを持つ場合に、昼間側磁気圏に存在する閉じた磁力線と北向き IMF が片側半球のみで磁気リコネクションを起こし、それに伴う磁気フラックスの輸送が SAA の朝夕方向の運動を駆動するというモデルを提案するに至った。この新しいモデルにより、昼間側カスプ近傍でオーロラオーバルと接続している SAA の朝夕方向の運動を IMF Bx, By の極性変化によって矛盾無く説明することが可能となった。

MHD シミュレーションによって生成された極冠域アークの衛星データを用いた 検証

三村 恭子 [1]; 小原 隆博 [2]; 藤田 茂 [3]; 田中 高史 [4]
[1] 東北大・理・地球物理; [2] 東北大・惑星プラズマセンター; [3] 気象大; [4] 九大・宙空センター

Assessment of the MHD simulation results by the satellite observations for the case of transpolar arc

Kyoko Mimura[1]; Takahiro Obara[2]; Shigeru Fujita[3]; Takashi Tanaka[4]
[1] Geophysics, Tohoku Univ; [2] PPARC, Tohoku University; [3] Meteorological College; [4] SERC, Kyushu Univ.

According to the results of the MHD simulation by Tanaka et al. [2004], plasma sheet was inclined very much when the IMF By has a large value during northward IMF condition. Change of IMF By polarity causes a dynamical change of the shape of plasma sheet and the transpolar arc has been detached from the morning (evening) side oval and moved dusk ward (dawn ward), corresponding to IMF By change from negative to positive (positive to negative). Tanaka et al. [2004] insisted that, due to the change of IMF By polarity, a rotation of plasma sheet to opposite inclination as well as a reformation of ionospheric convection could be made. In the midst of these reconfigurations, the growth of new lobe results in the blocking of the return path of closed field lines generated in the old merging cell and leads to form the kink structure in the plasma sheet. Losing their return path, these closed field lines generated from old lobes accumulate on the night side.

In order to assess the MHD simulation results, we have examined observations by the IMAGE satellite and DMSP satellites by paying a particular attention to the formation and movement of the transpolar aurora. IMAGE satellite observed 40 transpolar cap arc events. It was found there have been 4 events, in which the arc was moving. We examined the variation of IMF By component and found that the IMF By changed its polarity for these cases. Most cases of IMAGE observations show the stagnant transpolar arcs which illuminated at the poleward edge of the dawn or dusk side of expanded main oval. We examined the variation of IMF By components and found that the IMF By was almost constant.

In the presentation, we demonstrate the results of assessment by accommodating DMSP observations and consider the stagnant transpolar arcs based on the MHD simulation for strongly constant IMF By.

[Tanaka et al., 2004] による極冠域アークの MHD シミュレーションでは、北向き IMF 下で強い By がある時、プラズマシートが大きく張り出していたが、これに IMF の By の符号反転が加わるとアークがオーロラオーバルから分離し、極冠域を移動する事が示されていた。具体的には、IMF の By 成分の反転がプラズマシートの傾斜を逆転させ、その結果折れ曲がり構造が作られた。そしてこの過程で、古いマーキングセルの閉じた磁力線が昼側に戻ろうとする運動がブロックされ、夜側のプラズマシート部分に蓄積されていく様子が示されていた。

本研究では MHD シミュレーションで提唱された極冠域オーロラ生成のモデルを検証する目的で IMAGE 衛星、DMSP 衛星などによる撮像データを調べ、その結果を以下に報告する。IMAGE 衛星では、40 例の極冠域アークが観測されたが、その中で 4 例のみ朝夕方向に運動していた。これら移動する極冠域アークは、4 例すべてにおいて IMF の By 成分の符号の変化をもなっていた。また、移動しない極冠域アークについて詳細に見ていくと、アークとオーバルの間の領域に sun-aligned の細かい構造がいくつも観測されるものも多くあり、その高緯度側のエッジが輝くことで、極冠域アークとして観測されているように見えた。

発表では DMSP 衛星観測データを加え、より多くの例について解析した結果を報告する。また、[Tanaka et al., 2004] がこれまで扱っていなかった朝・夕のオーバルから張り出して輝いている sun-aligned-arc に関しても、MHD シミュレーション結果も踏まえつつ解析し、極冠域におけるオーロラの発生について総合的に考察する。

地磁気共役点観測を目指したプロトンオーロラスペクトログラフの開発

高橋 優希 [1]; 田口 真 [2]; 門倉 昭 [3]

[1] 立教大・理・物理; [2] 立教大・理・物理; [3] 極地研

Development of a proton aurora spectrograph for geomagnetic conjugate aurora observation

Yuki Takahashi[1]; Makoto Taguchi[2]; Akira Kadokura[3]

[1] Rikkyo Univ.; [2] Rikkyo Univ.; [3] NIPR

Electron auroras have been mainly studied by optical methods, because they are bright. However, proton auroras can also be a target of optical observation as the technology in optical measurement of a faint object has progressed. For example, A. V. Roldugin et al. (2014) showed that the H-alpha (656.3nm) emission of January 22, 2012 was caused by solar wind protons. The emission was determined with a spectrometer, which obtained the meridian arc spectrum image. However, when the brightest proton aurora H-beta (486.1nm) is observed, emissions from nitrogen molecular ions by an electronic origin may be a contamination. They cannot be completely eliminated even using a bandpass filter. For the observation of H-beta it is necessary to evaluate the contamination due to the emission of electron auroras. Two all-sky monochromatic imagers (PAI1 and PAI2) have been operated at Showa Station for observation of proton aurora. They have passbands of H-beta and the background, respectively. Use of these data enables us to extract proton aurora from the observed image which depicts mixture of proton and electron auroras. In this study proton aurora has been extracted using the data obtained by PAI1 and PAI2, and they have been evaluated in the point of view whether the features characterized by proton auroras are seen or not.

The data analyzed in this study was obtained from February 25 to July 11, 2013 and from February 26 to October 15, 2014. The size of images is 512 * 512 pixels, and pixel counts are increased by 8 * 8 pixel binning. Since the cameras and optical systems of PAI1 and PAI2 are identical, we have only corrected shift and rotation of the field of views of the two imagers using stars identified in the images. Sensitivities of the two imagers have been calibrated taking the difference between the transmittances of the two filters into account. As a result of subtracting the background we obtained a proton aurora image. However, the images show no characteristic features of proton aurora except for the all-sky proton aurora similar to those observed by Takahashi et al. [1995]. In addition, in this way of analysis of all-sky image data, it is difficult to quantitatively discuss contamination of electron aurora in the proton aurora image. It is concluded that precise evaluation of proton aurora using only all-sky images is impossible and that we should obtain a spectrum in the wavelength range that includes the wavelength of proton aurora in order to precisely eliminate the background.

According to the results of analysis we developed a proton aurora spectrograph (PAS), which will be installed it at the optical observation site at Tjornes in Iceland in early September 2016. PAS has a narrow field-of-view along the geomagnetic meridian and disperses light into the field-of-view by a diffraction grating. An image of space vs wavelength is obtained. An example of the obtained data will be introduced. In the future a long-term observation will be conducted and geomagnetic conjugate proton aurora will be investigated using the data obtained by PAS.

オーロラ光学観測はこれまで明るい電子起源のオーロラを主な観測対象としてきた。しかし、観測技術の向上により、暗い陽子起源のオーロラ（プロトンオーロラ）も観測されるようになってきた。例えば A. V. Roldugin et al. (2014) によれば、2012年1月22日のH-アルファ（656.3nm）の発光を地磁気子午線に沿った視野で分光観測した結果から、この発光が太陽風の陽子により生じたことを示している。しかし、陽子起源のオーロラで最も明るいH-ベータ（486.1nm）の発光を観測する場合、電子起源の窒素分子イオンの発光が混入する。これはバンドパスフィルターを使用しても完全には除去できない。H-ベータの観測を行う上ではこの電子起源の発光の寄与を見積もる必要がある。昭和基地で稼働しているプロトンオーロラ観測用の二台の全天単色イメージャー PAI1、PAI2 は、それぞれ H-ベータとそのバックグラウンドの観測を行っており、これらのデータを用いることで H-ベータの発光強度を抽出可能となっている。そこで、本研究ではまずこれらの装置で得られたデータを用いて、プロトンオーロラの抽出を試み、その特徴が見られるかどうかを調査した。

使用したデータは2013年2月25日から7月11日まで、2014年2月26日から10月15日までの期間の観測データである。画像は512pixel*512pixelのサイズで得られ、弱い発光のプロトンオーロラを短時間に十分なカウント数で観測するため、8*8のビニングを行っている。解析では、PAI1、PAI2の光学系と使用しているカメラが一致していたことから、星を用いて二つの装置の視野のずれを補正する視野補正と、使用するフィルターの透過率の違いを用いて装置の得られる光量を一致させる感度補正を行った。これらの補正を行ったうえでバックグラウンドを除去した結果、プロトンオーロラらしきオーロラ画像を得られた。しかし目的としていたプロトンオーロラ特有の特徴は見られず、例えば (Takahashi et al., 1995) といった過去の全天観測結果と同じような特徴のオーロラが見られるのみであった。また、全天観測のみの場合、プロトンオーロラに対してどの程度電子オーロラが含まれていたかといった定量的な議論が困難である。最終的に全天観測のみでのプロトンオーロラの厳密な抽出は難しく、プロトンオーロラを含む波長領域のスペクトルを取得して、バックグラウンドを除去する方法を採用すべきであると結論付けた。

この結果を受けて、スペクトル取得のための分光観測装置 (Proton Aurora Spectrograph: PAS) を2016年9月初めにア

イスランド・チョルネスにある観測拠点に設置した。PAS は地磁気子午線に沿った細長い視野を持ち、視野内の発光を透過型回折格子で分光して、空間 1 次元、波長 1 次元の 2 次元画像を得る。ここで得られたデータについても可能であれば一部紹介する。今後は長期間の観測を行い、プロトンオーロラのイベントを抽出、調査していく予定である。

無人オーロラ観測装置の開発：昭和基地における試験運用

門倉 昭 [1]; 山岸 久雄 [2]; 岡田 雅樹 [1]; 小川 泰信 [1]; 田中 良昌 [1]
[1] 極地研; [2] 極地研

Development of unmanned auroral observation system: Test operation at Syowa Station

Akira Kadokura[1]; Hisao Yamagishi[2]; Masaki Okada[1]; Yasunobu Ogawa[1]; Yoshimasa Tanaka[1]
[1] NIPR; [2] National Inst. Polar Res.

Space and upper atmospheric sciences group in the National Institute of Polar Research (NIPR) is now developing a new unmanned auroral observation system, which is equipped with 3-axis fluxgate magnetometer, all-sky auroral imager, and GNSS/TEC receiver, in the current 9th term Japanese Antarctic Research Expedition (JARE) programme. Electric power of the system is supplied by a hybrid natural energy electric generation system which consists of three sets of wind generators and 8 sets of solar panels. Observation data are stored in a memory card in the system box and also are transmitted via the Inmarsat satellite data communication system to a server in Japan by FTP.

The 57th JARE, who left Japan in December, 2015, had installed one set of the unmanned system at Syowa Station in January, 2016 to do a test operation. All the instruments have been working normally until now, even during the polar night period in Antarctica. The 58th JARE, who will leave Japan in November, 2016, will install this system at Amundsen Bay area, which is located about 500 km eastward from Syowa Station. In our presentation, we will talk about the abstract of the unmanned system and the test operation at Syowa Station.

国立極地研究所（極地研）の宙空圏研究グループは、現在実施中の第57期南極観測計画において、3成分磁力計、オーロラ全天カメラ、GNSS/TEC観測機を備えた「無人オーロラ観測装置」の開発を行っている。電源系は、3式の風力発電機と8枚の太陽電池パネルからなるハイブリッド自然エネルギー発電システムで、取得されたデータは観測器内のメモリーカードに記録されると共に、インマルサット衛星回線を利用した通信システムにより、国内の外部サーバーにFTP伝送される。

2015年12月に出発した第57次観測隊は、一式を試験運用のため昭和基地に持ち込み、2016年1月に設置した。これまで全ての観測機器が正常に動作し、極夜期にも観測中断することなく、観測とデータ伝送を継続することが出来ている。この実績を踏まえ、2016年11月出発の第58次観測隊では、この一式を昭和基地から東に約500km離れた沿岸域のアムンゼン湾に移設する予定である。講演では、昭和基地に設置したシステムの概要と運用結果について報告する。

全天画像によるオーロラ爆発の事例研究

三浦 翼 [1]; 家田 章正 [2]; 川嶋 貴大 [2]
[1] 名大 ISEE; [2] 名大宇宙地球研

A Case Study of the Aurora explosion due to all-sky image.

Tsubasa Miura[1]; Akimasa Ieda[2]; Takahiro Kawashima[2]
[1] ISEE, Nagoya Univ.; [2] ISEE, Nagoya Univ.

Aurora is a luminous phenomenon of the atmosphere, which is observed in the polar region. Auroral breakup is believed to occur typically in 1 hour after the southward turning of the Interplanetary Magnetic Field (IMF).

In this study, we investigated developments of auroras in response to the southward turning of IMF that occurred at 10:30 UT, 15 December 2015. All-sky images in Inuvik, Canada near the midnight were used.

As a result, auroral breakups were observed at 10:15, 10:30, 11:39 UT. In particular, the auroral breakup at 10:30 UT included a westward traveling surge, revealing that a full auroral breakup can occur during the northward IMF interval.

オーロラは極域で観測される大気の発光現象である。オーロラの爆発的な増光（オーロラ爆発）は、典型的には惑星空間磁場（IMF）が南向きになった約1時間後に生じると考えられている。

本研究では、2015年12月15日10:30 UTに生じたIMFの北向きから南向きへの変化に対応するオーロラの変化を、真夜中付近に位置していた、カナダのイヌビクにおける全天画像を用いて調べた。

その結果、オーロラ爆発は10:15, 10:30, 11:39 UTに開始していた。特に10:30 UTのオーロラ爆発について、IMFが北向きの場合でもサージ構造を持つオーロラ爆発が発生しうることが明らかになった。

北極圏におけるオーロラ観測と画像解析による分類

菅原 正伍 [1]; Dennis van Dijk [2]; 新 浩一 [1]; 西 正博 [1]; 山内 正敏 [3]
[1] 広島市大; [2] Hague Univ., IRF-Kiruna; [3] IRF-Kiruna

Image Classification and Observations of the Aurora in the Arctic Circle

Shogo Sugahara [1]; Dennis van Dijk [2]; Koichi Shin [1]; Masahiro Nishi [1]; Masatoshi Yamauchi [3]
[1] Hiroshima City Univ.; [2] Hague Univ., IRF-Kiruna; [3] IRF-Kiruna

Using digital camera images since March 2014 for monitoring the auroral activities, we classified the auroral morphology in both manual and automatic methods to evaluate the auroral activities. In this study, we defined five states of the aurora, classified aurora images depending on the visual judgement, and evaluated the occurrence range and the max brightness of the aurora.

Our aurora observation system was placed STF tourist station (lat. 68 20' 56.9" N, long. 18 49' 58.8" E) of Abisko in Sweden. Auroras were photographed by a digital camera with an equisolid angle-type fisheye lens (90 degree angle of view, 180 degree field of view) at 30 second intervals during night-time in aperture priority mode. ISO speed and image size of the digital camera was 800, 2464*1632 pixels, respectively. A period of observation time in a day was altered with respect to the seasons.

In analyses of the aurora activities, we used jpeg image data obtained from March 2014. The images were manually classified into an invisible, a pale aurora, an auroral arc, an active aurora and an expansive aurora by an aurora activity level depend on the brightness and the visible size of auroras. As well as, states of weather conditions were defined into cloudy/rainy and sunny based on the amounts of clouds. As a result, it was found that occurrences of pale auroras and active auroras increase from November to December, 2014.

In order to quantify an area and a maximum brightness of the auroras, RGB values of pixels in a photo image are converted HLS values. In the HLS values, the maximum brightness (seen in L) increased associated with the occurrence range of the aurora, while the RGB values are used for identification. The criterion values are compared between different cameras. We also tried to extract auroral substorm activity by combining the variation in the geomagnetic field. After comparing between the above classification and the visual inspection we reproduced the well-known relation that the area and the maximum brightness of an aurora simultaneously increased in the occurrences of active aurora.

我々は、オーロラの出現頻度、出現傾向を評価するため、2014年3月より北極圏にてデジタルカメラを用いたオーロラ撮影による観測を行っている。オーロラの状態による分類ならびに特徴量の抽出を本研究では行った。

オーロラ観測システムのカメらは、晴天率の高い場所である北極圏におけるスウェーデン・アビスコの STF ツーリストステーション (北緯 68 度 20 分 56.9 秒, 東経 18 度 49 分 58.8 秒) に設置した。オーロラの撮影には、広範囲におよぶオーロラ活動の鮮明な写真を撮影する必要があるため、等立体角射影方式を採用した画角 180 度、視界 360 度の円周魚眼レンズを搭載したデジタルカメラを用いた。デジタルカメラの設定は、ISO 感度 800、絞り優先モード、画像サイズ 2464*1632 ピクセルとした。また、オーロラの撮影可能な夕方から朝方にかけて 30 秒のインターバル撮影を行った。また、スウェーデンでは 5 月から 8 月にかけては白夜の期間にあたるため、時期により撮影時間は適宜変更している。

解析対象は、観測を開始した 2014 年 3 月以降に取得した画像データとした。目視により、画像内におけるオーロラの状態をオーロラの明るさと出現領域をもとに、オーロラ不可視、薄いオーロラ、オーロラアーク、活発なオーロラ、爆発したオーロラと判断した。また、デジタルカメラの上空を雲が覆っていることによりオーロラを視認できない場合もあるため、画像内における雲の出現領域をもとに、くもり・雨、晴れと天気の状態もあわせて分類し、オーロラ画像とは区別した。目視による解析からオーロラ活動度の評価を行った結果、2014 年の 11 月から 12 月にかけて薄いオーロラや活発なオーロラの出現頻度が高くなっていったことが分かった。

さらに、オーロラの定量的な特徴量の抽出・解析を行うため、画像内における 1 ピクセルごとの RGB 値とそれを HLS に変換した値により、オーロラの出現範囲・最高輝度を求めた。この解析結果から、オーロラの出現範囲が拡大するにつれて最高輝度が増加する傾向を確認した。また判定値が 2 つのカメラでどのように変わるかも調べた。更に地磁気の変動を組み合わせることでサブストーム時のオーロラを自動判定することも試みた。加えて目視による分類と画像解析結果から本手法の評価を行ったところ、爆発したオーロラが出現している時は、出現範囲、最高輝度がともに高い値であり、本手法を用いて、爆発したオーロラの出現を評価可能であることが分かった。

Analyses of time series of auroral images for deducing properties of diffuse and pulsating aurorae

Shin'ya Nakano[1]; Yasunobu Ogawa[2]

[1] The Institute of Statistical Mathematics; [2] NIPR

Auroral images provide much information on the motion and variation of aurorae which are attributed to physical processes in the magnetosphere-ionosphere system. We are developing a technique for quantifying various auroral properties by analyzing time series of auroral images. In our technique, the translational motion of diffuse aurorae is described by a state space model. In principle, estimation for a state space model can be achieved by using the Kalman filter algorithm. However, since a high dimensional vector is required to represent each auroral image, the use of the Kalman filter is computationally expensive. In order to reduce the computational cost, we introduce a reduced-rank approximation of the Kalman filter and apply it to the estimation of the translational motion. Properties of pulsating aurora are also analyzed by using a sparse analysis technique, which enables us to extract structures varying differently from ambient aurorae. Some results of pilot analyses will be demonstrated.

全天カメラで取得された脈動オーロラの画像に対する主成分分析を用いた変調解析

浅野 貴紀 [1]; 三好 由純 [1]; 栗田 怜 [1]; 町田 忍 [2]; 西山 尚典 [3]; 片岡 龍峰 [3]; 福田 陽子 [4]; 内田 ヘルベルト陽仁 [5]; 大山 伸一郎 [6]; 塩川 和夫 [7]; 細川 敬祐 [8]; 小川 泰信 [3]
[1] 名大 ISEE; [2] 名大・ISEE; [3] 極地研; [4] 東大・理・地惑; [5] 総研大; [6] 名大・宇地研; [7] 名大宇地研; [8] 電通大

The application of Principal component analysis to pulsating aurora image data obtained from ground-based all-sky cameras

Takaki Asano[1]; Yoshizumi Miyoshi[1]; Satoshi Kurita[1]; Shinobu Machida[2]; Takanori Nishiyama[3]; Ryuho Kataoka[3]; Yoko Fukuda[4]; Herbert Akihito Uchida[5]; Shin-ichiro Oyama[6]; Kazuo Shiokawa[7]; Keisuke Hosokawa[8]; Yasunobu Ogawa[3]
[1] ISEE, Nagoya Univ.; [2] ISEE, Nagoya Univ.; [3] NIPR; [4] Dept. Earth & Planet. Sci, Univ. Tokyo; [5] SOKENDAI; [6] ISEE, Nagoya Univ.; [7] ISEE, Nagoya Univ.; [8] UEC

Pulsating aurora (PsA) is a kind of diffuse aurora and shows quasi-periodic intensity modulation with a 2-3 s to 30 s intervals. PsA is mainly observed from the post-midnight to the morning sectors during the recovery phase of substorms. PsA consists of not only main modulations but also internal modulation with a few Hz. In order to investigate spatial and temporal variations of PsA, we apply Principal Component Analysis (PCA) to a time series of PsA image data considering difference between the main modulations and the internal modulations. PCA is a method of orthogonal transformation and can be used to decompose into the main modulation and the internal modulations. By applying PCA to the time series of PsA data, it is expected that an image with the largest variance and coherence will be extracted as the first principal component that corresponds to the main modulation, while the second and third principal components that may correspond to the internal modulations. In this study, we applied PCA presented in Nishiyama et al. [2016] to all-sky PsA images from EMCCD cameras (Athabasca, Canada), and s-CMOS camera (Fairbanks, USA) will be shown. Furthermore, we may report an initial result of auroral images taken with EMCCD cameras to be installed in Tromso, Norway and Sodankyla, Finland this year.

脈動オーロラは、2-3~30 秒の間隔で発光する、準周期的なオーロラであり、主にサブストームの回復相に、深夜から明け方にかけて観測され、形状的な特徴としてパッチ構造などを取り、南北への振動を見せることがある。また、脈動オーロラは、主脈動と呼ばれる上記の数秒周期の変調に加え、内部変調と呼ばれる数 Hz での輝度変調を内在していることが知られている。脈動オーロラの時間変動特性である主脈動と内部変調、および空間構造特性であるパッチ構造との関係を調べるために、本研究では主成分分析を用いた脈動オーロラの解析を行った。主成分分析においては、異なる時間で取得された画像間でコヒーレントかつ分散の大きな領域から順に、第一、第二主成分として抽出され、主脈動と内部変調とが分離されることが期待される。そこで、本発表では、本研究グループがこれまでアサバスカ（カナダ）、フェアバンクス（米国）に設置した EMCCD、s-CMOS カメラデータによって取得された脈動オーロラの全天画像に対して、Nishiyama et al. [2016] で報告された主成分分析のアルゴリズムを適用し、脈動オーロラの時空間変動特性について解析を行った結果を報告する。また、今秋、新たに北欧に設置される予定の EMCCD カメラによる脈動オーロラの観測結果についても報告する予定である。

脈動オーロラ主脈動の周期性に関する統計解析

川村 勇貴 [1]; 細川 敬祐 [1]; 小川 泰信 [2]
[1] 電通大; [2] 極地研

Periodicity of main pulsation of pulsating aurora: a statistical analysis

Yuki Kawamura[1]; Keisuke Hosokawa[1]; Yasunobu Ogawa[2]
[1] UEC; [2] NIPR

Pulsating auroras (PsA) are known to switch on and off with a period ranging from a few seconds to a few tens of second by quasi-periodic electron precipitations. PsA almost always appear in the morning side during the recovery phase of auroral substorm. Previous studies have suggested that pitch angle

scattering by chorus waves near the equatorial plane of the magnetosphere causes quasi periodic precipitation of PsA electrons. Especially, it has been indicated that there is one to one correspondence between chorus wave amplitude and the luminosity variation of PsA. This means that the analysis of the periodicity of PsA may enable us to clarify the origin of the modulation of chorus wave amplitude.

However, there have been no recent studies that analyzed the periodicity of PsA by using long term optical observations; thus, we still do not know the average/typical periodicity of the main pulsation of PsA.

The purpose of this study is to provide fundamental characteristics of the main pulsation of PsA (i.e., modulation of chorus wave amplitude). For this purpose, we make use of All-sky Watec Imagers (AWI) operative in Tromsø, Norway (69N, 19E). This system is composed of small cameras (WAT-910HX), fish-eye lens, and optical filters which have different transparent wavelengths. All-sky auroral images are taken with a temporal resolution of 1-2 Hz. In this study, we checked the existence of PsA every 5 min window in almost 3 years of data from November 2010 to March 2013 and extracted

528 events of PsA (2640 minutes in total). Most of the events occurred at 03-05 MLT sector, which is in good agreement with the well-known MLT distribution of PsA occurrence seen from the ground and that of chorus waves in the magnetosphere. We derived the average period of the main optical pulsation and it was estimated to be 17 sec. By analyzing the dependence of the average period on MLT, it was found that the average period was about 12 sec near midnight and that in the morning sector was about 18 sec, for example at ~06 MLT. Namely, the period of the main pulsation of PsA

tends to be longer. In the presentation, we discuss the possible mechanisms creating the MLT dependence of the period of PsA by considering the MLT dependence of the characteristics of chorus waves

脈動オーロラは磁気圏から高エネルギーの電子が準周期的に降り込むことによって、数秒から数十秒の周期で高度 100 km 付近の超高層大気が明滅する現象である。オーロラサブストームの回復相において、真夜中過ぎから朝方にかけての地方時で頻繁に発生することが知られている。過去の研究から、脈動オーロラを作り出す準周期的電子降下は、磁気圏に存在するコーラス波動によるピッチ角散乱によって起こっていると考えられている。特に、コーラス波動強度と脈動オーロラ発光強度の時間変動に 1 対 1 の対応関係がある事例が報告されている。この事実は、脈動オーロラの周期性を解析することで、コーラス波動の強度変調に関する知見を得ることが

できるということを意味する。しかし、これまでに脈動オーロラの周期性を長期間のデータに基づいて調べた研究はなく、平均周期について定量的な数値が導出されていない。本研究では、脈動オーロラの明滅に見られる周期性について統計的かつ定量的な解析を行うことで、コーラス波の強度変調の周期性に関する基礎的な情報を得ることを目的とする。本研究で用いる観測装置はノルウェー・トロムソ（緯度:69 度）経度:19 度 磁気緯度:66 度）に設置されている全天 WATEC 並列イメージャである。このシステムは共通の小型カメラと魚眼レンズ、及び透過波長の異なる複数のフィルターで構成されており、微弱なオーロラ発光を 1 秒という高い時間分解能で撮像している。本研究では、この全天 WATEC 並列イメージャによって 2010 年 11 月-2013 年 3 月の期間に取得された 557.7 nm の撮像データから、5 分間の解析ウィンドウごとに脈動オーロライベントの有無を確認し、計 528 例（総観測時間 2640 分）の事例を抽出した。これらのイベントは 03-05MLT の間に多く発生しており、磁気圏におけるコーラス波動の空間分布と概ね一致していた。これらの事例についてフーリエ解析を用いて周期スペクトルを導出し、ピークを与える周期（ピーク周期）を求めた。脈動オーロラは数秒から数十秒の周期で明滅することが知ら

れているため、30 秒以下のピーク周期について全イベントの平均を求めた結果、平均周期は 17 秒であった。また、平均周期の磁気地方時に対する依存性を調べたところ、真夜中付近では平均周期は 12 秒程度、朝側（06MLT）では平均周期は 18 秒程度であることが分かり、朝側に行くほど脈動周期が長くなる傾向があることが分かった。発表では、脈動周期の磁気地方時依存性がどのようなメカニズムによって作られているのかを、コーラス波動の変調メカニズムを踏まえて議論する。

オメガバンド型脈動オーロラと電離圏D領域電離現象の地上EISCATレーダー-光学多点観測

近藤 裕菜 [1]; 坂野井 健 [2]; 小川 泰信 [3]; 田中 良昌 [3]; 鍵谷 将人 [4]

[1] 東北大・理・地物; [2] 東北大・理; [3] 極地研; [4] 東北大・理・惑星プラズマ大気研究センター

EISCAT radar and optical observation of omega-band pulsating aurora and electron density enhancement in the D-region ionosphere

Hirona Kondo[1]; Takeshi Sakanoi[2]; Yasunobu Ogawa[3]; Yoshimasa Tanaka[3]; Masato Kagitani[4]

[1] Geophysics, Tohoku Univ.; [2] Grad. School of Science, Tohoku Univ.; [3] NIPR; [4] PPARC, Tohoku Univ

We report the coordinated EISCAT and optical observations for small-scale auroral events.

Omega band aurora has large-scale wavy structures at the poleward boundary of a diffuse aurora, and pulsating auroral patches are often observed inside the structure. Past studies revealed that pulsating aurora is caused by relatively high-energy (greater than 10 keV) electrons and occasionally shows emission below 100km. However, the precise characteristics of precipitating electrons producing omega-band pulsating aurora have not been understood well.

We carried out coordinated observation of aurora by the EISCAT Tromso UHF radar and all-sky imagers at Kilpisjarvi, Abisko and Tromso during the period of 5-15 January, 2016. A few omega band aurora associated with low-altitude ionization event (down to ~80 km) occurred during this observation.

We focused on the omega bands at 01:00-03:00UT on 6 January, 2016. All-sky images at 427.8 nm were used to identify the auroral morphology and were compared with the height profile of electron density obtained with the EISCAT radar. We also estimated the energy distribution of precipitating electrons from the EISCAT radar data with the CARD method [Fujii et al., 1994, J. Geomag. Geoelectr.]. The results are summarized as follows:

(1) Before 01:00UT, an east-west auroral arc appeared. The lower altitude limit of electron density enhancement was about 110km. Electron energy flux with energies greater than 10 keV was small (The flux values were 9.73×10^4 [$\text{eV cm e}^{-2} \text{s e}^{-1} \text{str e}^{-1} \text{eV e}^{-1}$] and 1.39×10^2 [$\text{eV cm e}^{-2} \text{s e}^{-1} \text{str e}^{-1} \text{eV e}^{-1}$] at 10keV and 100keV respectively).

(2) 01:03-01:15UT, three omega bands traveled in the eastward direction. Simultaneously, the electron density in the altitude range of 80-200km increased greatly. Electron flux in the energy range of 1-170 keV up to two or three orders of magnitude (The flux value increased to 1.33×10^7 [$\text{eV cm e}^{-2} \text{s e}^{-1} \text{str e}^{-1} \text{eV e}^{-1}$] and 1.95×10^4 [$\text{eV cm e}^{-2} \text{s e}^{-1} \text{str e}^{-1} \text{eV e}^{-1}$] at 10keV and 100keV respectively).

(3) After 01:15UT, omega band auroras were followed by pulsating auroral patches. Electron density was enhanced in the altitude range of 90-110km altitude, and low-energy electrons less than 10keV decreased.

In addition to the above results, now, we start the estimation of 427.8nm auroral emission of omega band pulsating aurora and pulsating patch after omega bands using the triangulation from the data of another 2 stations (Kilpisjarvi, Abisko). In this presentation, we are going to discuss the characteristics of precipitating electrons producing omega-band pulsating aurora.

今回我々は、地上多点光学観測ならびにEISCATレーダーにより2016年1月6日に観測されたオメガバンド脈動オーロラに伴う低高度電離現象について報告する。

オメガバンド・トーチは夜半過ぎにしばしば現れる大規模な波状構造を持つオーロラであり、その中にパッチ状脈動オーロラを有する複雑な構造をしている。過去の地上観測から、脈動オーロラは10keV以上の比較的高エネルギー降下電子により生成され、100km以下の低高度で発光する場合があることが指摘されている。しかしながら、オメガバンド型脈動オーロラの発生機構や降下電子のエネルギー特性は依然として理解されていない。

2016年1月5日から15日にかけてスカンジナビア半島北部の3地点(Kilpisjarvi, Abisko, Tromso)の全天イメージャとTromsoのEISCAT UHFレーダーを用いた同時観測を実施した。観測期間中には複数回オメガバンドオーロラが見られ、同時に高度80km付近の低高度まで電子密度の増加が確認された。

本研究では、2016年1月6日00:00UT-03:00UT頃に見られたオメガバンド型脈動オーロラに伴う低高度電離現象の解析結果について報告する。まず、Tromsoにおける427.8nmオーロラ発光の画像(4秒間隔)からオーロラの動きと形状を確認し、これをEISCAT UHFレーダーを用いて得た電子密度分布と比較した。次にCARD法[藤井他、1994、J. Geomag. Geoelectr.]を用い、電子密度分布から各エネルギー値(1-170keV)での降下電子フラックスを導出した。これらの解析から、以下3点の結果を得た。

(1) 01:00UT以前にはアーク状のオーロラが現れ、それに伴う電離密度増加の下限は高度110km程度にとどまった。降下電子フラックスのエネルギー分布からも高エネルギー(10keV以上)のフラックスが小さいことが分かった。(フラックスの値はそれぞれ10keVで 9.73×10^4 [$\text{eV cm e}^{-2} \text{s e}^{-1} \text{str e}^{-1} \text{eV e}^{-1}$]、100keVで 1.39×10^2 [$\text{eV cm e}^{-2} \text{s e}^{-1} \text{str e}^{-1} \text{eV e}^{-1}$]であった。)

(2) 01:03UT-01:15UTにかけてオメガバンドオーロラが3度Tromso上空を通過した。いずれも西側の空で発生し東へと伝搬していった。オメガバンド型脈動オーロラがEISCATレーダー上を通過する際には高度80-200kmの広い範囲で電子密度は急激に増加した。降下電子フラックスも解析範囲の1-170keVの全てのエネルギー帯で大きくなったことが確

認された。(フラックスの値はそれぞれ 10keV で 1.33×10^7 [$\text{eV cm e}^{-2} \text{s e}^{-1} \text{str e}^{-1} \text{eV e}^{-1}$]、100keV で 1.95×10^4 [$\text{eV cm e}^{-2} \text{s e}^{-1} \text{str e}^{-1} \text{eV e}^{-1}$] まで増加した。)

(3) 01:15UT 以降、オメガバンド型脈動オーロラが通過した後は全天にパッチ状の激しい脈動オーロラが見られた。電離密度増加は高度 90-110km の間で起こり、低エネルギー (10keV 以下) の電子フラックスは減少した。

以上の結果に加え、現在、Kilpisjarvi、Abisko の 2 点での同時観測結果から、オメガバンド型脈動オーロラ及びオメガバンド通過後のパッチ状脈動オーロラについて 427.8nm 発光高度の推定を行っている。今回の発表では、レーダーデータと光学データを対応させ、オメガバンド型脈動オーロラのエネルギー特性について議論する。

脈動プロトンオーロラ非等方的発光空間分布

井上 智寛 [1]; 尾崎 光紀 [2]; 八木谷 聡 [1]; 塩川 和夫 [3]; 三好 由純 [4]; 片岡 龍峰 [5]; 海老原 祐輔 [6]; 野村 麗子 [7]; 坂口 歌織 [8]; 大塚 雄一 [3]; Connors Martin [9]
[1] 金沢大; [2] 金沢大・理工・電情; [3] 名大宇地研; [4] 名大 ISEE; [5] 極地研; [6] 京大生存圏; [7] ISAS; [8] 情報通信研究機構; [9] Centre for Science, Athabasca Univ.

Anisotropic spatial distribution of pulsating proton aurora

Tomohiro Inoue[1]; Mitsunori Ozaki[2]; Satoshi Yagitani[1]; Kazuo Shiokawa[3]; Yoshizumi Miyoshi[4]; Ryuho Kataoka[5]; Yusuke Ebihara[6]; Reiko Nomura[7]; Kaori Sakaguchi[8]; Yuichi Otsuka[3]; Martin Connors[9]
[1] Kanazawa Univ.; [2] Electrical and Computer Eng., Kanazawa Univ.; [3] ISEE, Nagoya Univ.; [4] ISEE, Nagoya Univ.; [5] NIPR; [6] RISH, Kyoto Univ.; [7] ISAS; [8] NICT; [9] Centre for Science, Athabasca Univ.

Pulsating proton aurora (PPA) is caused by pitch angle scattering of high-energy (several keV to 100 keV) ions with the electromagnetic ion cyclotron (EMIC) waves at the magnetic equator. A part of precipitated ions travels to the ionospheric altitude along the magnetic field lines. Then, PPA is observed. The EMIC waves propagate along the magnetic field line from the source region and are observed as Pc1 geomagnetic pulsations on the ground. In order to explain the generation mechanism of PPA, we have been studying the effects of luminous spatial distribution of PPA. We have been observing PPA using an all-sky EMCCD camera with a high time resolution (110 Hz sampling), and the geomagnetic pulsations by an induction magnetometer (64 Hz sampling) on the ground at Athabasca, Canada (L value=4.3). PPA and related Pc1 geomagnetic pulsations were simultaneously observed on the ground during 7:40-8:40 UT on 12 November 2015. The Pc1 geomagnetic pulsations showed rising tone structures in the frequency domain and left-hand circular polarization. The observed Pc1 geomagnetic pulsations had a clear period of 100 seconds and subpacket structures, which were observed as amplitude modulation with a few tens of seconds. The PPA intensity showed the same repetition period of 100 seconds and a fast luminous modulation of approximately 10 seconds. The results showed that the PPA was generated by pitch angle scattering by the EMIC waves at the magnetic equator. Next, to examine the effects of the magnetosphere and ionosphere on the spatial distribution of PPA, we did a correlation analysis between the PPA intensity and the luminous area. The correlation result showed that the luminous area had a high correlation (0.83) with the PPA intensity. This could be explained by the effects of charge exchange for energetic protons (below 200 keV) in the ionosphere. However, it was found that the luminous area was not spread isotropically, but to southward. If the effect of charge exchange was dominant, PPA should be spread to northward. Therefore, the result showing the southward spread would be caused by the effects of variations of the magnetospheric source region.

In the presentation, we will discuss the analysis results of PPA and the Pc1 geomagnetic pulsations observed at Athabasca in detail.

脈動プロトンオーロラの発生メカニズムとして、磁気赤道域での電磁イオンサイクロトロン (EMIC) 波動による高エネルギー (数 keV-数十 keV) イオンのピッチ角散乱が示唆されている。散乱されたイオンの一部は磁力線に沿って電離層高度まで降り込み、脈動プロトンオーロラが発生する。EMIC 波動も磁力線に沿って伝搬し、その一部は地上で Pc1 地磁気脈動として観測される。しかし、脈動プロトンオーロラと Pc1 地磁気脈動が同時に観測されたデータは少なく、その発生メカニズムは十分に解析されていない。そこで、我々は脈動プロトンオーロラの発生メカニズムを明らかにするために、Pc1 地磁気脈動と脈動プロトンオーロラの発光空間分布の影響を調査している。観測データは、サブオーロラ帯に位置するカナダのアサバスカ (L 値: 4.3) において、脈動プロトンオーロラを高時間分解能 (110 Hz サンプリング) の全天 EMCCD カメラ、地磁気脈動をインダクション磁力計 (64 Hz サンプリング) により地上同時観測を行っている。2015 年 11 月 12 日 7:40 UT から 1 時間にわたって左旋円偏波を示し周波数上昇を伴う Pc1 地磁気脈動と脈動プロトンオーロラが観測された。観測された Pc1 地磁気脈動は 100 秒の周期をもっており、十秒程度のサブパケット構造に似た振幅変調も含まれていた。脈動プロトンオーロラの発光強度も 100 秒の発光周期とその周期の中に十秒程度の内部変調に似た輝度値変化が観測された。この結果は、EMIC 波動が高エネルギーイオンのピッチ角散乱を引き起こし、脈動プロトンオーロラを発光させていることを強く示唆する。次に磁気圏と電離圏による空間分布の影響を調べるため、発光強度とその領域の相関解析を行なった。その結果、発光面積とその強度には高い相関 (0.83) があるということがわかった。この要因として電離圏での電荷交換反応に伴う発光領域の拡大が考えられる。しかし、発光分布が非等方に広がり、磁南側に向かって広がっていることがわかった。電離圏での電荷交換反応の影響であれば磁北側に向かって広がるため、この空間変動は磁気圏での発生領域の変動による影響であると考えられる。

本研究ではアサバスカで Pc1 地磁気脈動と同時に観測された脈動プロトンオーロラの解析結果について詳細に報告を行う予定である。

2015年6月磁気嵐中に昼-夕方側で観測された脈動オーロラの特徴: 昭和基地と Van Allen Probes 観測に基づく事例報告

西山 尚典 [1]; 門倉 昭 [1]; 三好 由純 [2]; 栗田 怜 [2]; 田中 良昌 [1]; 岡田 雅樹 [1]
[1] 極地研; [2] 名大 ISEE

Event study on pulsating aurora in the noon to dusk side during Summer Solstice Storm 2015 based on Syowa and Van Allen Probes

Takanori Nishiyama[1]; Akira Kadokura[1]; Yoshizumi Miyoshi[2]; Satoshi Kurita[2]; Yoshimasa Tanaka[1]; Masaki Okada[1]
[1] NIPR; [2] ISEE, Nagoya Univ.

Pulsating aurora (PsA) is known as a quasiperiodic variation of auroral emission with a typical period that ranges from 2-3 s to 30 s [Oguti *et al.*, 1981; Yamamoto, 1988]. In the recovery phase of a substorm, PsA is commonly observed in the low-latitude region of the auroral oval. It is also well-known that PsA is widely distributed between the midnight and dawn sectors [Royrvik and Davis, 1977; Jones *et al.*, 2011]. Recently, ground-based optical observations in the south pole, which is located close to the high latitude edge of the aurora oval, revealed that PsA often appeared even in the dawn to noon side [Nishimura *et al.*, 2013]. However, a global distribution of PsA including noon to dusk side and its relation to generation mechanism are still poorly investigated due to difficulty in ground-based optical monitoring during sunlit time.

In this presentation, we report an event study on PsA, which was continuously observed in the magnetic noon to dusk side at Syowa station (69.0°S, 39.6°E), during Summer Solstice Storm 2015. PsA with patchy structures and westward propagations were identified by a panchromatic imager with 1-Hz sampling from 1330 to 1930 MLT on 23 June, 2015. In addition, Van Allen Probes-A (VAP-A) was likely to observe at an inner-edge of the outer radiation belt ($L = 5\sim 6$) during this period. An apogee of VAP-A was located in the dusk and the ionospheric footprint of VAP-A was moving close to Syowa. The VAP-A observations demonstrated the important plasma features as follows: Enhancement of energetic electrons from a few tens of keV to 1 MeV were observed. Cold plasma density was higher than usual (~ 20 /cc) despite outside the plasmasphere and f_{pe}/f_{ce} ranged from 7 to 9. Whistler mode waves in a quite wide frequency range from 100 Hz to a few kHz including hiss emissions and lower-band chorus were also observed continuously around the apogee.

These observational evidences imply that PsA can be driven by anisotropy of energetic electrons and subsequent excitations of whistler mode waves even in the noon to dusk side, as well as PsA in the post-midnight to dawn side. Pitch angle diffusion coefficients considering spectrum of the observed whistler mode waves is consistent with electron precipitations in an energy range above 20 keV. One more important point is that this PsA event was associated with the major storm ($Dst \sim -200$ nT). The storm may lead to injections of a large amount of energetic electrons and transportation of the electrons in the noon to dusk side.

脈動オーロラは数秒から30秒程度の準周期的な発光を示すオーロラで [Oguti *et al.*, 1981; Yamamoto, 1988]、サブストームの回復相にオーロラオーバルの低緯度側で普遍的に観測される。また、磁気地方時の深夜過ぎから明け方に広く分布することも知られている [Royrvik and Davis, 1977; Jones *et al.*, 2011]。近年では、オーロラオーバルの高緯度境界に位置する南極点において、地上光学観測から脈動オーロラがしばしば明け方から正午にかけて出現することが報告されている。しかしながら、正午付近から夕方における脈動オーロラの分布と生成機構との関連については、日照条件下における地上光学観測が難しいことから、ほとんど明らかになっていない。

本発表では、2015年6月に起こった巨大磁気嵐に関連して昭和基地 (69.0°S, 39.6°E) で地磁気地方時正午過ぎから夕方まで観測された脈動オーロラの実例について報告する。2015年6月23日の磁気地方時1330から1930の間、昭和基地の全天白色オーロライメージャー (1Hz サンプリング) によって斑点状かつ西側に伝搬する脈動オーロラが連続的に観測された。加えて、この時間帯において Van Allen Probes-A (VAP-A) は放射線帯外帯の内部境界 ($L = 5\sim 6$) を観測していた。この時の VAP-A は遠地点が夕方であり、衛星の電離圏フットプリントは昭和基地付近を通過していた。VAP-A によるプラズマ観測は以下のようにまとめられる。数10keVから1MeV付近までの高エネルギー帯の電子フラックスの上昇が観測された。プラズマ圏の外にも関わらず電子密度は通常より高く (~ 20 /cc)、 f_{pe}/f_{ce} も7から9と非常に高かった。100Hzから数kHzの幅広い周波数帯でホイッスラー波動 (hiss emission, lower-band chorus) が遠地点付近で観測された。

これらの観測結果は、深夜過ぎから明け方付近同様に、高エネルギー電子のピッチ角異方性とそれに伴うホイッスラー波動の励起によって、正午過ぎから夕方にかけても脈動オーロラが発生されうることを示唆している。観測されたホイッスラー波動のスペクトルから見積もられたピッチ角散乱係数は、20keV以上の電子の散乱を十分説明できる値となった。さらに重要な点は、この脈動オーロラが大規模磁気嵐 ($Dst \sim -200$ nT) の回復相に出現しており、この磁気嵐による大量の電子注入と夕方付近までに及ぶ輸送が重要な役割を果たしている可能性がある。